



This work is protected by copyright and other intellectual property rights and duplication or sale of all or part is not permitted, except that material may be duplicated by you for research, private study, criticism/review or educational purposes. Electronic or print copies are for your own personal, non-commercial use and shall not be passed to any other individual. No quotation may be published without proper acknowledgement. For any other use, or to quote extensively from the work, permission must be obtained from the copyright holder/s.



**Keele  
University**

# **The function of sodium/calcium ion exchanger in human platelets and megakaryocytes**

**Peterson Anand**

**Institute for Science and Technology in Medicine, Keele University**

**Thesis submitted to Keele University for the degree of Master of**

**Philosophy**

**June 2017**

## **Table of Contents**

<b>Abbreviations .....</b>	<b>11</b>
<b>Acknowledgements .....</b>	<b>14</b>
<b>Abstract .....</b>	<b>15</b>
<b>1. Introduction .....</b>	<b>17</b>
<b>1.1 Principles of thrombosis and haemostasis .....</b>	<b>17</b>
1.1.1 Platelets and the hemostatic systems of the body.....	17
1.1.2 Too much or too little platelet activation causes pathological outcomes.....	20
<b>1.2 The cellular biology of human platelets .....</b>	<b>22</b>
1.2.1 Platelet Structure .....	22
1.2.2 The platelet plasma membrane .....	22
1.2.3 Open Canalicular System .....	24
1.2.4 The dense tubular system .....	25
1.2.5 The membrane complex.....	26
1.2.6 Platelet Cytoskeleton .....	28
1.2.7 Secretory Granules.....	29
<b>1.3 Thrombus formation requires an agonist-dependent rise in cytosolic Ca<sup>2+</sup> concentration in platelets .....</b>	<b>30</b>
1.3.1 Resting platelets keep cytosolic Ca <sup>2+</sup> concentration low .....	35
1.3.2 Ca <sup>2+</sup> Removal .....	35
1.3.3 Ca <sup>2+</sup> Sequestration.....	37
1.3.4 A rise in cytosolic Ca <sup>2+</sup> concentration is required to trigger platelet activation.....	39
1.3.5 Ca <sup>2+</sup> Release.....	40

1.3.6	Ca <sup>2+</sup> Entry .....	42
1.3.7	Ca <sup>2+</sup> Effectors.....	44
1.3.8	Platelets can selectively respond to cytosolic Ca <sup>2+</sup> signals .....	46
1.3.9	Platelets can create localised Ca <sup>2+</sup> signals .....	48
1.3.10	Nanojunctions permit the creation of isolated cytosolic Ca <sup>2+</sup> nanodomains.....	49
<b>1.4</b>	<b>Megakaryocytes as a model system for studying the platelet membrane complex.....</b>	<b>50</b>
<b>1.5</b>	<b>Aims of the current project.....</b>	<b>53</b>
<b>2.</b>	<b>Materials and Methods.....</b>	<b>54</b>
<b>2.1</b>	<b>Materials .....</b>	<b>54</b>
<b>2.2</b>	<b>Methods for human platelet studies.....</b>	<b>54</b>
2.2.1	Human Platelet Preparation .....	54
2.2.2	Monitoring Cytosolic Ca <sup>2+</sup> concentration [Ca <sup>2+</sup> ] <sub>cyt</sub> in washed platelet suspensions .....	55
2.2.3	Monitoring cytosolic Na <sup>+</sup> concentration ([Na <sup>+</sup> ] <sub>cyt</sub> ) in washed platelet suspensions .....	56
2.2.4	Monitoring extracellular Ca <sup>2+</sup> concentration ([Ca <sup>2+</sup> ] <sub>ext</sub> ) in washed platelet suspensions .....	57
2.2.5	Imaging of agonist-evoked changes in [Ca <sup>2+</sup> ] <sub>ext</sub> in single human platelets .....	57
2.2.6	Immunofluorescent imaging of NCX3 in single platelets .....	58
2.2.7	Monitoring platelet shape change using light transmission aggregometry .....	59

<b>2.3</b>	<b>Methods for human megakaryocyte studies.....</b>	<b>59</b>
2.3.1	Culturing human megakaryocytes from human CD34 <sup>+</sup> cells from bone marrow .....	59
2.3.2	Single cell imaging of morphological changes in CD34 <sup>+</sup> -cultured human megakaryocytes ..	60
2.3.3	Monitoring [Ca <sup>2+</sup> ] <sub>cyt</sub> from CD34 <sup>+</sup> -cultured human megakaryocytes .....	60
2.3.4	Monitoring [Na <sup>+</sup> ] <sub>cyt</sub> from CD34 <sup>+</sup> -cultured human megakaryocytes.....	61
2.3.5	Fixed Cell Imaging of NCX3 antibody in single Megakaryocyte demarcation membrane system.....	62
<b>2.4</b>	<b>Statistical Comparison.....</b>	<b>63</b>
<b>3.</b>	<b>Results.....</b>	<b>64</b>
3.1	Identification and characterisation of a cytosolic nanodomain in DM-BAPTA-loaded human platelets .....	64
3.1.1	Thrombin-evoked rises in [Ca <sup>2+</sup> ] <sub>ext</sub> can be observed in the absence of any detectable rise in cytosolic Ca <sup>2+</sup> concentration in human platelets .....	64
3.2	Nicergoline-induced disruption of the subcellular localisation of the DTS inhibits thrombin -evoked rises in [Ca <sup>2+</sup> ] <sub>ext</sub> and [Na <sup>+</sup> ] <sub>cyt</sub> in DM-BAPTA-loaded platelets.....	70
3.3	Disruption of the actin cytoskeleton does not prevent Ca <sup>2+</sup> removal from the cytosolic nanodomain, but instead significantly potentiates it .....	73
3.4	Disrupting lipid rafts inhibits thrombin-evoked rises in [Ca <sup>2+</sup> ] <sub>ext</sub> in DM-BAPTA-loaded platelets .....	75
3.5	Disruption of lipid rafts with MBCD appears to interfere with platelet Ca <sup>2+</sup> signalling by dissipating the Na <sup>+</sup> gradient across the plasma membrane.....	78

3.6	DM-BAPTA-loading does not prevent the production of pericellular Ca <sup>2+</sup> hotspots in thrombin-stimulated human platelets.....	81
3.7	Subcellular localisation of NCX 3 isoform in fixed human platelets.....	83
3.8	Nicergoline-induced reorganization of the DTS affects the subcellular localization and distribution of NCX3 in human platelets .....	86
<b>4.</b>	<b>Investigating the functional effects of a cytosolic nanodomain in platelets .....</b>	<b>88</b>
4.1	Blockade of NCX activity induces shape change in unstimulated DM-BAPTA-loaded human platelets, and maintains the thrombin-evoked response .....	89
4.2	Preatment of DM-BAPTA-loaded platelets with the myosin light chain kinase.....	92
	inhibitor, ML-7, prevents KB-R7943- and thrombin-evoked shape change	
4.3	Pre-treatment with the Rho-kinase inhibitor, Y-27632, has no significant effect on KB-R7943- and thrombin-evoked shape change in DM-BAPTA-loaded platelets.....	94
4.4	The IP <sub>3</sub> R inhibitor, 2-APB, inhibits KB-R7943- and thrombin-induced shape change in DM-BAPTA loaded cells .....	96
4.5	Nicergoline pre-treatment prevents thrombin-induced shape change in DM-BAPTA-loaded cells.....	99
4.6	ML-7 and Y-27632 inhibit thrombin-evoked rises in [Ca <sup>2+</sup> ] <sub>ext</sub> in DM-BAPTA-loaded platelets .....	101

<b>5.</b>	<b>Investigating the role of the Na<sup>+</sup>/Ca<sup>2+</sup> exchanger in regulating agonist-evoked Ca<sup>2+</sup> signalling in CD34<sup>+</sup>-derived human megakaryocytes.....</b>	<b>105</b>
5.1	Cultured CD34 <sup>+</sup> cells exhibit development of features of mature megakaryocytes and an extensive intracellular Ca <sup>2+</sup> stores. These morphological features are not affected by culturing with calcitriol.....	105
5.2	Pre-treatment with NCX inhibitor, KB-R7943, alters thrombin-evoked Ca <sup>2+</sup> signalling in CD34 <sup>+</sup> -derived megakaryocytic cells.....	109
5.3	KB-R7943 inhibits thrombin-evoked rises in [Na <sup>+</sup> ] <sub>cyt</sub> in CD34 <sup>+</sup> -derived megakaryocytic cells .....	111
5.4	Replacement of extracellular sodium with NMDG alters thrombin-evoked Ca <sup>2+</sup> signalling in megakaryocytes.....	114
5.5	Calcitriol differentially affects thrombin-evoked Ca <sup>2+</sup> signalling elicited in the presence and absence of extracellular Ca <sup>2+</sup> in CD34 <sup>+</sup> -derived megakaryocytic cells .....	116
5.6	Calcitriol has no significant effect on NCX3 expression and localisation in Megakaryocytes.....	118
<b>6.</b>	<b>Discussion .....</b>	<b>121</b>
6.1	Human platelets contain a functionally-isolated cytosolic nanodomain which links intracellular Ca <sup>2+</sup> release with the Na <sup>+</sup> /Ca <sup>2+</sup> exchanger.....	121
6.2	A role for the cytosolic nanodomain in controlling platelet shape change.....	124

6.3	To what extent are culture-derived megakaryocytes a model for human platelet Ca <sup>2+</sup> signalling? .....	125
6.4	Future Plans .....	126
6.5	Conclusions.....	128
<b>7.</b>	<b>References.....</b>	<b>129</b>

## **Table of Figures**

<b>Figure 1.1</b>	Basics of Haemostasis and Platelet plug formation .....	19
<b>Figure 1.2</b>	A summary of key molecular defects found in the platelets of patients with inherited bleeding disorders .....	21
<b>Figure 1.3</b>	Ultrastructure of resting platelet .....	23
<b>Figure 1.4</b>	3D reconstruction of the platelet membrane complex from an electron tomography study of human platelet ultrastructure .....	27
<b>Figure 1.5</b>	Mechanisms of platelet adhesion to the subendothelial matrix .....	33
<b>Figure 1.6</b>	The Pericellular $\text{Ca}^{2+}$ recycling hypothesis.....	52
<b>Figure 3.1</b>	A model of how DM-BAPTA- regulates spatial spread of $\text{Ca}^{2+}$ from microdomain .....	65
<b>Figure 3.2</b>	Thrombin-evoked rises in $[\text{Ca}^{2+}]_{\text{ext}}$ can be observed in the absence of any detectable rise in $[\text{Ca}^{2+}]_{\text{cyt}}$ in human platelets .....	66
<b>Figure 3.3</b>	Thrombin-evoked rises in $[\text{Na}^+]_{\text{cyt}}$ are inhibited by pre-treatment with KB- R7943 in DM-BAPTA-loaded human platelets .....	69
<b>Figure 3.4</b>	Nicergoline-induced disruption of the subcellular localisation of the DTS inhibits thrombin-evoked rises in $[\text{Ca}^{2+}]_{\text{ext}}$ in DM-BAPTA-loaded platelets .....	71
<b>Figure 3.5</b>	Thrombin-evoked rises in $[\text{Na}^+]_{\text{cyt}}$ are inhibited by pre-treatment with nicergoline in DM-BAPTA-loaded human platelets .....	72
<b>Figure 3.6</b>	Cytochalasin D significantly potentiates thrombin-evoked rises in $[\text{Ca}^{2+}]_{\text{ext}}$ in DM-BAPTA-loaded human platelets .....	74
<b>Figure 3.7</b>	MBCD significantly inhibits thrombin-evoked rises in $[\text{Ca}^{2+}]_{\text{ext}}$ in DM-BAPTA-loaded human platelets .....	77

<b>Figure 3.8</b>	Pre-treatment with MBCD dissipates the Na <sup>+</sup> gradient across the plasma membrane in DM-BAPTA-loaded human platelets .....	80
<b>Figure 3.9</b>	Thrombin-evoked pericellular signals are resistant to DM-BAPTA loading .....	82
<b>Figure 3.10</b>	NCX3 appears to be localised in a manner consistent with its presence within the open canalicular system .....	84
<b>Figure 3.11</b>	Nicergoline disrupts the normal localisation of NCX3 within resting platelets .....	87
<b>Figure 4.1</b>	Blockade of NCX activity induces shape change in unstimulated DM-BAPTA-loaded human platelets, and maintains the thrombin-evoked response. ....	90
<b>Figure 4.2</b>	Pre-treatment with ML-7 inhibits KB-R7943- and thrombin-induced shape change in DM-BAPTA-loaded platelets.....	93
<b>Figure 4.3</b>	Pre-treatment with Y-27632 has no significant effect on KB-R7943- and thrombin-induced shape change in DM-BAPTA-loaded platelets .....	95
<b>Figure 4.4</b>	Pre-treatment with 2-APB has no significant effect on KB-R7943- and thrombin-induced shape change in DM-BAPTA-loaded platelets.....	98
<b>Figure 4.5</b>	Pre-treatment with nicergoline inhibits thrombin-induced shape change in DM-BAPTA-loaded platelets.....	100
<b>Figure 4.6</b>	ML-7 pre-treatment inhibits thrombin-evoked rises in [Ca <sup>2+</sup> ] <sub>ext</sub> in DM-BAPTA-loaded platelets .....	102

<b>Figure 4.7</b>	Y-27632 pre-treatment inhibits thrombin-evoked rises in $[Ca^{2+}]_{ext}$ in DM-BAPTA-loaded platelets .....	104
<b>Figure 5.1</b>	Treatment with calcitriol has no significant effect on the morphology of CD34 <sup>+</sup> -cultured human megakaryocytes.....	108
<b>Figure 5.2</b>	Pre-treatment with KB-R7943 alters thrombin-evoked rises in $[Ca^{2+}]_{cyt}$ in CD34 <sup>+</sup> -cultured human megakaryocytes in a maturation-dependent Manner .....	110
<b>Figure 5.3</b>	Pre-treatment with KB-R7943 inhibits thrombin-evoked rises in $[Na^+]_{cyt}$ CD34 <sup>+</sup> -in cultured human megakaryocytes .....	112
<b>Figure 5.4</b>	Na <sup>+</sup> replacement affects thrombin-evoked Ca <sup>2+</sup> signalling in CD34 <sup>+</sup> -cultured megakaryocytes .....	115
<b>Figure 5.5</b>	Calcitriol alters thrombin-evoked Ca <sup>2+</sup> signals both in the presence and absence of extracellular Ca <sup>2+</sup> in CD34 <sup>+</sup> -derived megakaryocytic cells .....	117
<b>Figure 5.6</b>	NCX3 appears to be localised within the demarcation membrane system of CD34 <sup>+</sup> derived megakaryocytes .....	119
<b>Figure 6.1</b>	A model of how DM-BAPTA-loading affects human platelet Ca <sup>2+</sup> signalling .....	122

## **Abbreviation list**

ACD	Acid citrate dextrose
ADP	Adenosine diphosphate
ATP	Adenosine triphosphate
BSA	Bovine serum albumin
$[Ca^{2+}]_{\text{cyt}}$	Cytosolic Calcium concentration
$[Ca^{2+}]_{\text{ext}}$	Extracellular Calcium concentration
DAG	Diacylglycerol
DTS	Dense Tubular System
DM-BAPTA	Dimethyl 1,2-bis(o-aminophenoxy) ethane-N,N,N',N'-tetraacetic acid (BAPTA)
DMS	Demarcation membrane system
ECM	Extracellular matrix
EM	Electron microscopy
GPIb-V-IX	Glycoprotein Ib-V-IX complex
GPVI	Glycoprotein VI
HBS	Hepes-buffered saline
IL-6	Interleukin 6
IL-9	Interleukin 9

IP <sub>3</sub>	Inositol 1,4,5-trisphosphate
IP <sub>3</sub> R	Inositol 1,4,5-trisphosphate receptor
MC	Membrane Complex
MLC	Myosin light chain
MLCK	Myosin light chain kinase
[Na <sup>+</sup> ] <sub>cyt</sub>	Cytosolic Na <sup>+</sup> concentration
NCX	Na <sup>+</sup> /Ca <sup>2+</sup> exchanger
OCS	Open Canalicular System
Orai1	Calcium release activated calcium channel protein 1
PDGF	Platelet-derived growth factor
PGI <sub>2</sub>	Prostacyclin
PIP <sub>2</sub>	Phosphatidylinositol 4,5-bisphosphate
PLA <sub>2</sub>	Phospholipase A <sub>2</sub>
PKC	Protein Kinase C
PLC	Phospholipase C
PRP	Platelet rich plasma
PS	Phosphatidylserine
STIM1	Stromal interaction molecule 1

ROC	Receptor operated channels
ROCK	Rho associated coiled coil containing protein kinase
SCF	Stem cell factor
SEM	Standard error of the mean
SERCA	Sarco/endoplasmic reticulum Ca <sup>2+</sup> -ATPase
SOCE	Store operated Ca <sup>2+</sup> entry
5-HT	Serotonin
TF	Tissue factor
TPO	Thrombopoietin
TXA <sub>2</sub>	Thromboxane A <sub>2</sub>
vWF	von Willebrand factor

## **Acknowledgements**

First and foremost, I would like to thank GOD for giving me the opportunity to pursue this course at ISTM, Keele University. Next I am grateful to my mother for supporting me financially and sponsoring this study at Keele University. I would like to extend my heartfelt gratitude to my supervisor Dr Alan Harper for accepting me to work on this project and for providing excellent supervision throughout. I would like to acknowledge and thank Dr Carmen Coxon for lending the Light Transmission Chronolog Aggregometer. I also acknowledge colleagues Dr Abdullah Al-Ghannam, Faiza Musa for rendering their support and assistance during the project. Last but not least I would like to thank all the blood donors without whom this work would not have been possible.

## Abstract

Previously work from our lab has predicted that  $\text{Ca}^{2+}$  release from intracellular  $\text{Ca}^{2+}$  stores occurs into a  $\text{Na}^+/\text{Ca}^{2+}$  exchanger (NCX)-associated cytosolic nanodomain enclosed within the membrane complex. In this study, we aimed to test the hypothesis that  $\text{Ca}^{2+}$  release initially accumulates into an NCX-associated cytosolic nanodomain. We further aimed to examine whether  $\text{Ca}^{2+}$  accumulation within this nanodomain could be responsible for triggering the first stage of platelet activation - the platelet shape change. Experiments were also performed to assess whether  $\text{CD34}^+$ -cultured megakaryocytes might utilize the NCX in a similar manner to platelets to start to establish this as a model system in which the structures of the cytosolic nanodomain could be assessed in the future.

In this study, we investigated whether removal of  $\text{Ca}^{2+}$  by the NCX is affected by DM-BAPTA loading. Experiments demonstrated that DM-BAPTA slowed but did not prevent NCX-mediated  $\text{Ca}^{2+}$  removal from  $\text{Ca}^{2+}$  released from intracellular stores. This effect could also be observed at the single-cell level. The NCX-mediated removal from DM-BAPTA-loaded cells was disrupted by disorganization of the dense tubular system by nicergoline, suggesting its presence within the membrane complex. Examination of the subcellular distribution of the NCX3 protein in human platelets demonstrated the presence of the NCX3 in a location consistent with being at the membrane complex. These data therefore provided the first demonstration of an NCX-associated cytosolic nanodomain in line with our hypothesis.

Additional experiments demonstrated that NCX inhibition triggers a  $\text{Ca}^{2+}$ -dependent shape change in DM-BAPTA-loaded platelets. Furthermore, this appeared to be dependent upon the function of the  $\text{IP}_3$  receptor. These data therefore provide functional evidence for the close association of these two  $\text{Ca}^{2+}$ -transporting proteins

in a nanodomain of platelets. In addition, these data suggested that  $\text{Ca}^{2+}$  accumulation within the cytosolic nanodomain might be responsible for the rapid activation of the platelet shape in human platelets.

Investigations into the applicability of  $\text{CD34}^+$ -cultured megakaryocytes as a model system in which to study platelet  $\text{Ca}^{2+}$  signalling demonstrated that megakaryocytes utilise NCX to regulate their thrombin-evoked  $\text{Ca}^{2+}$  signals. This effect was altered by changes in the cytokine level concentrations as well as the addition of calciferol to the platelet. These results demonstrate that whilst megakaryocytes also use NCX to critically control their signalling, this effect is modulated by the developmental condition of the megakaryocytes.

These data therefore are consistent with our previous hypothesis that the NCX3 is principally localised at the membrane complex, where it forms a close association with the  $\text{IP}_3$  receptor. The experiments on shape change suggests that localising different  $\text{Ca}^{2+}$ -effectors in the membrane complex or in other subregions of the cell may play a key role in controlling the latency of activation of these process in platelets. These data support the possibility that the membrane complex is a key regulator of  $\text{Ca}^{2+}$  signalling in platelets, and may provide a useful target for future anti-platelet agents.

## **1. Introduction**

### **1.1. Principles of thrombosis and haemostasis**

#### **1.1.1 Platelets and the haemostatic systems of the body**

Platelets are small disc-shaped anucleate cell fragments that play a key role in maintaining the integrity of the blood circulation. Platelets are present at a high-density of  $1.5-4 \times 10^8$  cells.mL<sup>-1</sup> in the blood of healthy adults. They circulate in the bloodstream for around 10 days before being removed by the reticuloendothelial system of the liver and spleen (Broos *et al.*, 2011; Gale, 2011). In this time, the platelets circulate in a resting, quiescent form which prevents platelet interaction with other platelets, blood cells or the endothelial lining. However, when a blood vessel becomes damaged, nearby platelets become activated where they can then coordinate the controlled clotting of the blood, thus preventing excessive blood loss from the damaged vessel (Broos *et al.*, 2011; Kumar & Abbas, 2015).

The formation of a blood clot at the site of damage in an injured blood vessel is called haemostasis (Fig 1.1). Haemostasis is a highly-regulated physiological process that requires the coordinated action of platelets, clotting factors, and endothelial cells leading to a creation of a thrombus. The thrombus prevents excessive bleeding at the injured site, whilst also maintaining normal blood flow in circulation (Broos *et al.*, 2011; Gale, 2011). This process is normally prevented by the endothelium, which produces a number of substances such as nitric oxide, prostacyclin, anti-thrombin III, thrombomodulin, and Tissue Factor Pathway Inhibitor, which inhibits platelet activation and prevents aberrant activation of the blood coagulation cascade (Ignarro *et al.*, 1987; Palmer *et al.*, 1987; Furie & Furie, 2008).

Upon vascular injury, the sub-endothelial extracellular matrix becomes exposed to the blood, which contains several adhesive ligands such as collagen, laminin, fibronectin, and thrombospondin which platelets can adhere to through cell surface receptors (Farndale *et al.*, 2003; Kumar & Abbas, 2015). In addition to cell arrest, platelet adhesion via these receptors triggers platelet activation through the stimulation of signal transduction pathways through G-protein coupled receptors and tyrosine kinase cascades (Broos *et al.*, 2011). This activation triggers platelet spreading upon the surface of the injured vessel, where they can then recruit further platelets via production of thromboxane A<sub>2</sub> (TxA<sub>2</sub>) and secretion of autocrine signalling molecules from their dense granules. These soluble ligands activate other circulating platelets, recruiting them to the developing thrombus through binding to the adherent platelets. This leads to the formation of a platelet plug, which blocks the damaged blood vessel and prevents further blood loss (Varga-Szabo *et al.*, 2008). Finally, the platelet aggregate also presents a catalytic surface for the activation of the blood coagulation cascade, which facilitates the deposition of an insoluble fibrin mesh around the aggregate which helps strengthen the clot and prevents it been washed away by the flowing blood (Walker, 1980; Esmon & Owen, 1981; Fulcher *et al.*, 1984; Guinto & Esmon, 1984; Mann *et al.*, 1990; Shen & Dahlback, 1994; Cramer *et al.*, 2010).

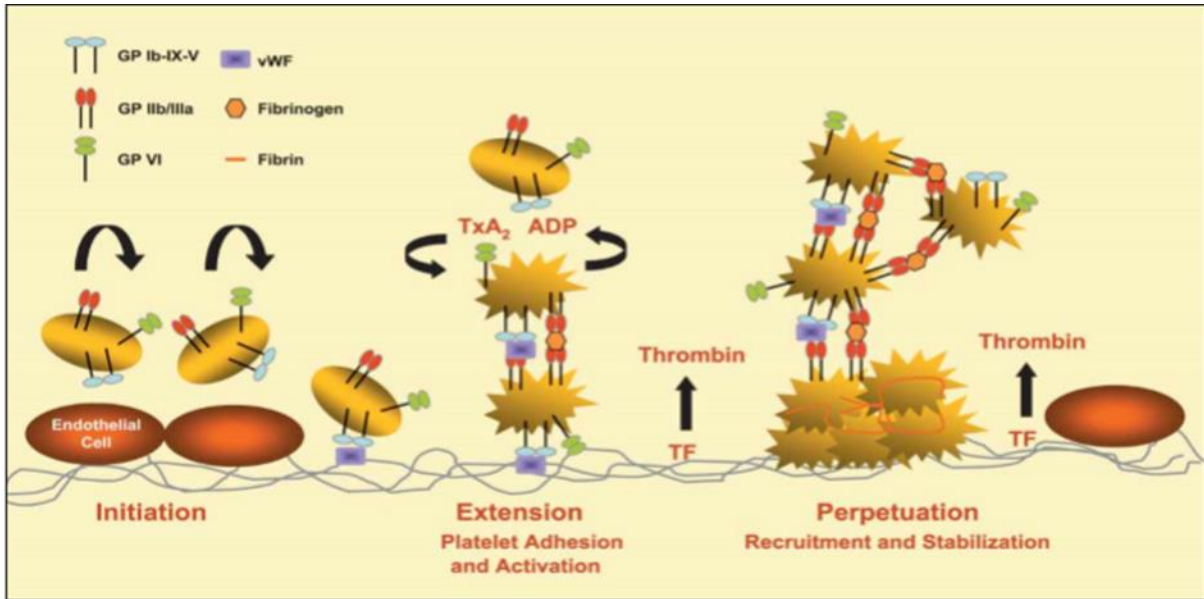


**Figure 1.1: Basics of Haemostasis and Platelet Plug Formation.** Upon vascular injury, the sub-endothelial matrix is exposed to the plasma. This allows platelets to bind to collagen either directly, or indirectly via von Willebrand Factor (vWF), forming a monolayer of activated platelets on the surface of the damaged wall. These activated cells can then release adenosine diphosphate (ADP), adenosine triphosphate (ATP), serotonin (5-HT) and TxA<sub>2</sub> – which can help activate other circulating platelets helping to recruit them to the developing thrombus, via activation of integrin  $\alpha$ IIb $\beta$ 3 and crosslinking of platelet via this fibrinogen receptor. After formation of the thrombus, thrombin can be generated via activation of the extrinsic blood coagulation cascade through the release of tissue factor from the subendothelial wall. A sub-population of activated platelets in the thrombus help target this thrombin generation to the surface of the clot by facilitating a catalytic surface for the assembly of the prothrombinase and tenase complex on the surface of the platelets. This activation of the blood coagulation cascade results in further platelet recruitment and stabilisation of the clot via the production of fibrin, which helps to provide mechanical strength to the blood clot. Reproduced from (Jennings, L.K 2009 and Brass et al 2003).

### ***1.1.2 Too much or too little platelet activation causes pathological outcomes.***

Appropriate control of the platelet activation process is key to ensure appropriate localisation and extent of activation of the haemostatic process. However, if it is activated inappropriately then this can lead to serious haematological disorders. A bleeding diathesis (excessive bleeding) ensues when platelets fail to react sufficiently at the sites of vascular injury leading to a failure to rapidly prevent further blood loss. As outlined in figure 1, there are a number of known inherited platelet disorders which are related to either the platelet's inability to bind to adhesive ligands in the sub-endothelial matrix, to other platelets or coagulation factors (Fig 1.2), or to trigger effective intracellular signalling cascades which lead to their activation and ability to coordinate thrombus formation (Fig 1.2).

In contrast, unwanted platelet activation in undamaged blood vessels is called thrombosis. This uncontrolled platelet activation is a principal event in many cardiovascular diseases such as myocardial infarction, stroke, and venous thromboembolic disorders. In the last two decades, these cardiovascular diseases have been the most common cause of death in the world (World Health Organization, 2002). Thus understanding how platelets change from a quiescent to an active form upon exposure to damaged blood vessels, and how platelets work together to form a thrombus could help us to identify and treat causes of abnormal blood clotting events.

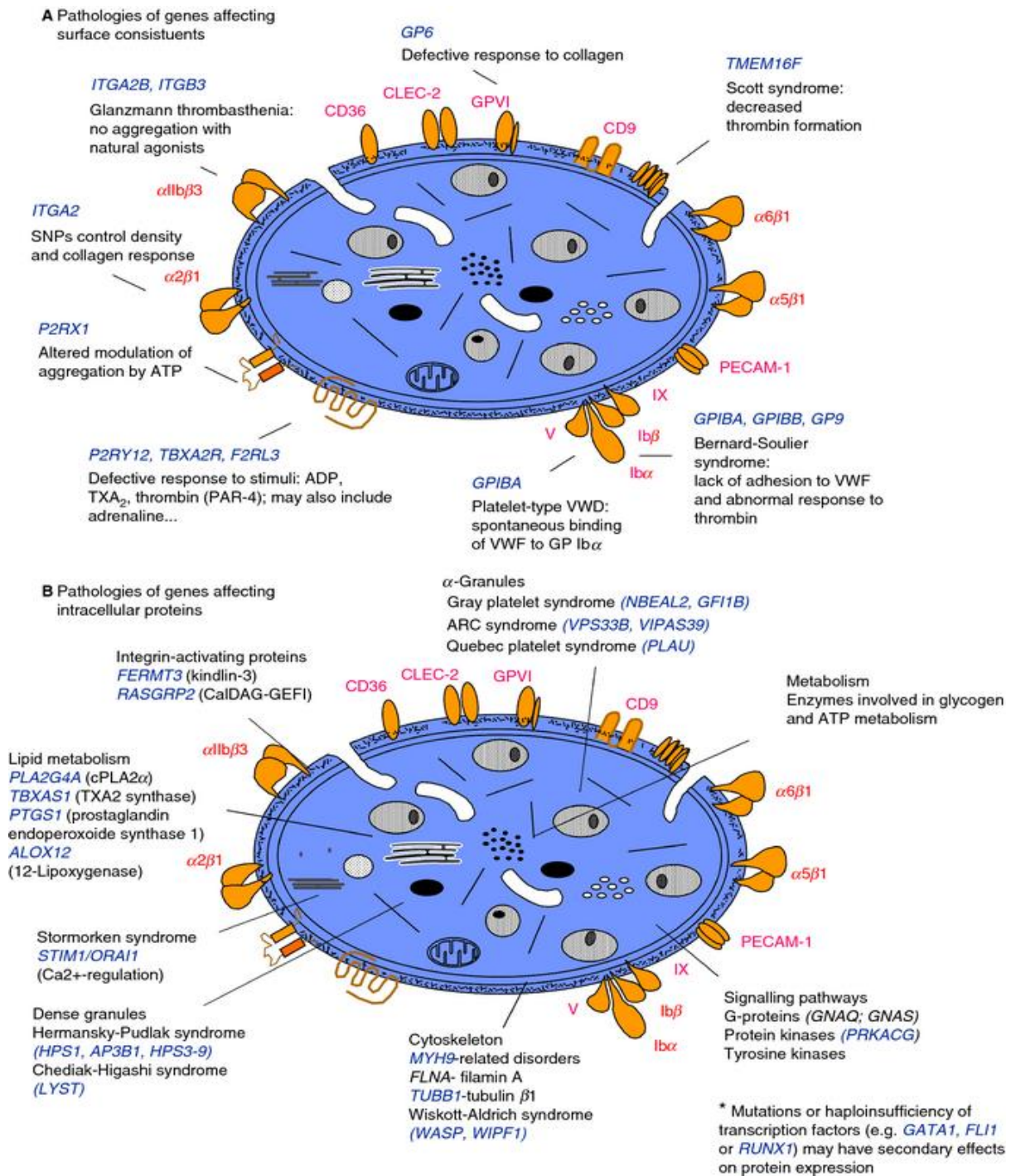


**Figure 1.2:** A summary of key molecular defects found in the platelets of patients with inherited bleeding disorders. Reproduced from Nurden & Nurden (2015).

## **1.2 The cellular biology of human platelets**

### **1.2.1 Platelet structure**

As shown in Figure 1.3, the structure of a resting platelet is mainly composed of three important structural components; the platelet plasma membrane, a highly-regulated cytoskeleton and a range of intracellular organelles and secretory granules. Each of these systems plays a key role in platelet structure and function.

#### **1.2.2 *The platelet plasma membrane***

The plasma membrane is composed of a phospholipid bilayer in which cholesterol, glycolipids, and glycoproteins are firmly embedded (van Joost *et al.*, 1990; White, 1993). The membrane also contains a large number of proteins such as ion channels, transporters and G-protein coupled receptors that are key to platelet activation (see section 2). However, the plasma membrane is not a homogenous structure but also contain lipid rafts rich in cholesterol and sphingolipid which play an important role in portioning platelet signalling pathways, as well as controlling intracellular trafficking of proteins (Bodin *et al.*, 2003; Kaushansky *et al.*, 2010).

The platelet plasma membrane can be seen to be covered in a dense external glycocalyx of around 20-30 nm in thickness. This structure is composed of membrane glycoproteins, glycolipids, mucopolysaccharides, and adsorbed plasma proteins (White, 1993). In resting platelets, the heavy negative charge of glycosaminoglycans and lipids provides an electrostatic repulsive force that prevents platelets from adhering to one another, as well as to endothelial cells (Coller, 1983). However, this lining also provides the first point contact of platelets with the Sub-endothelial matrix, so the presence of a number of glycoproteins in this structure is also crucial for the ability of platelets to bind and trigger platelet aggregation at the site of injury in a blood vessel (see section 2).

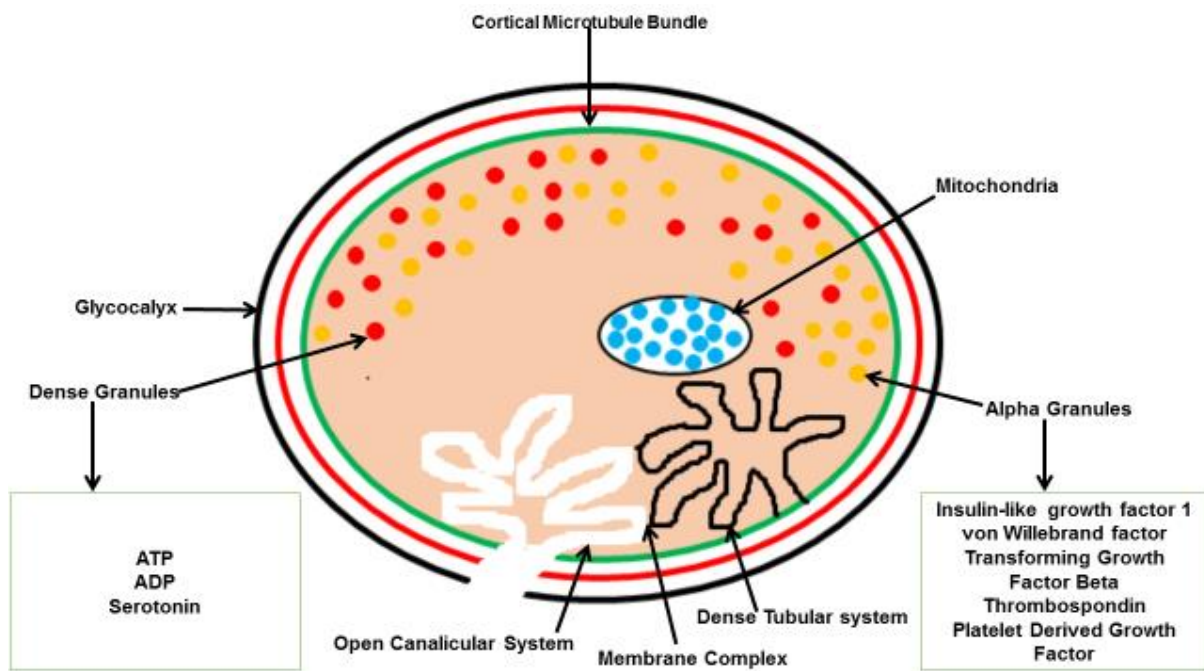


**Figure 1.3: Ultrastructure of the resting platelet.** The cortical microtubule bundle maintains the discoid shape of resting platelets. The platelet plasma membrane has a dense glycocalyx, which is made up of a number of glycoproteins including some which are essential for normal platelet adhesion and activation. The plasma membrane also becomes invaginated forming the structure called the open canalicular system (OCS). Platelets also contain the dense tubular system (DTS), which is the platelet equivalent of the smooth endoplasmic reticulum and is the major intracellular store of  $Ca^{2+}$ . The OCS and DTS are found closely apposed to one another in an eccentric cellular location known as the membrane complex. Platelets also contain secretory granules ( $\alpha$  granules and Dense granules) that contain platelet agonists, growth factors, and components of the coagulation cascade. These granules can be secreted upon platelet activation influencing the cells around them.

### 1.2.3 Open Canalicular System

In addition to the surface membrane, the platelet plasma membrane also invaginates into the interior of the cell, creating an internal space which is continuous with the extracellular fluid. Electron microscopy studies have previously shown that this membrane network displays numerous branching points and extends from one side of the platelet to the other (van Nispen tot Pannerden *et al.*, 2010). This invaginated membrane system is referred to as the open canalicular system (OCS) (Behnke, 1970; White, 1972;). This structure is similar to the t-tubule system of striated muscle cells (White, 1968), and therefore provides a volume of isolated extracellular fluid which can communicate with the external area of the platelet. As individual channels of the OCS have a diameter on the order of magnitude of tens of nanometres (van Nispen tot Pannerden *et al.*, 2010) it has been very difficult to study and so this has limited study, however the OCS is thought to play a number of roles in platelet.

Following adhesion, the surface plasma membrane of resting platelets increases in size rapidly due to filopodia formation and platelet spreading, leading to a rapid increase in the area of the surface membrane of platelets. This rapid increase in size of plasma membrane happens faster than would be possible by independent synthesis of new plasma membrane. Therefore the OCS is thought to act as a membrane reservoir which can be rapidly externalised, alongside that of exocytosed secretory granules, to allow platelet spreading upon activation (Ruggeri, 2002).

The OCS has also been shown to be the principal point of exocytosis of the granules from the platelet – however there is still some controversy over whether this is the sole route of exocytosis or whether there is also a role for release across the surface membrane (Mark *et al.*, 1980; White, 1972). This exocytosis of autocooids into the OCS

may help facilitate autocrine activation of platelets by their own granule contents by allowing adenosine nucleotides to accumulate within this small, isolated pericellular volume (Fogelson & Wang, 1996).

The OCS has also been shown to be a site of clearance of platelet glycoproteins after platelets stimulation. Electron microscopy studies indicate that the open canalicular system membrane may sequester the glycoprotein Ib-V-IX (GPIb-V-IX) complex from the platelet surface upon platelet activation with thrombin (George *et al.*, 1986; Michelson, 1992; Nurden *et al.*, 1994). Similar results have also been shown for glycoprotein VI (GPVI), the P<sub>2Y1</sub> purinergic receptor as well as integrin  $\alpha_{IIb}\beta_3$  (Suzuki *et al.*, 1992; Nurden *et al.*, 1994; Nurden *et al.*, 2003; Suzuki *et al.*, 2003). These data suggest that control of receptor transport into and out of the OCS may play a role in altering platelet reactivity to agonists.

#### **1.2.4 Dense Tubular System**

The dense tubular system (DTS) is a closed network of residual smooth endoplasmic reticulum from the megakaryocyte parent cell. In resting platelets the DTS appears as thin elongated membranes, but it has been shown to be rapidly reorganised upon agonist stimulation leading to it taking on a rounded, vesicular form (Ebbeling *et al.*, 1992) suggesting that it is responsive to platelet activation. The DTS in platelets is known to be the major site for synthesis of thromboxane's and prostaglandins, as well as the principal site of intracellular Ca<sup>2+</sup> release upon agonist-evoked stimulation (Sage *et al.*, 2011; see section 1.3.5). From these finding it is clear that the DTS plays a crucial role in mediating platelet activation (Gerrard *et al.*, 1976; Carey *et al.*, 1982; Ebbeling *et al.*, 1992).

### 1.2.5 Membrane Complex

Although the OCS and DTS are independent membrane systems involved in regulating platelet functions in different ways, previous electron microscopy studies of platelets have also found that these two membrane structures can also be found to lie in direct opposition to one other in a single eccentric location within the cell. This area of close association of the OCS and DTS is known as the membrane complex (Fig 1.4). This interaction between an invaginated membrane system and the intracellular  $\text{Ca}^{2+}$  stores is an analogous structure to the diad and triad made up of t-tubule system and sarcoplasmic reticulum of cardiac and skeletal muscle (Ezerman & Ishikawa, 1967; Hagopian & Spiro, 1967). More recently, it has become clear that tight interactions between the surface membrane and cortical endoplasmic reticulum can also be observed in smooth muscle cells, where these composite membrane systems have been termed as nanojunctions (van Breemen *et al.*, 2013). In all of these cell types, the close interaction between the intracellular  $\text{Ca}^{2+}$  stores and the plasma membrane has been shown to play a key role in regulating  $\text{Ca}^{2+}$  signalling by allowing the creation of highly-localised  $\text{Ca}^{2+}$  signals within subregions of the cells (van Breemen *et al.*, 2013). These localised  $\text{Ca}^{2+}$  signals can create activation of specific  $\text{Ca}^{2+}$  dependent pathways in isolation from other  $\text{Ca}^{2+}$ -regulated processes in these cells (van Breemen *et al.*, 2013). Recently evidence for a similar role for the membrane complex in controlling human platelet activation through regulating cytosolic  $\text{Ca}^{2+}$  signalling in these cells has also been recently presented (Sage *et al.*, 2013; Walford *et al.*, 2016; See Section 1.3.7).

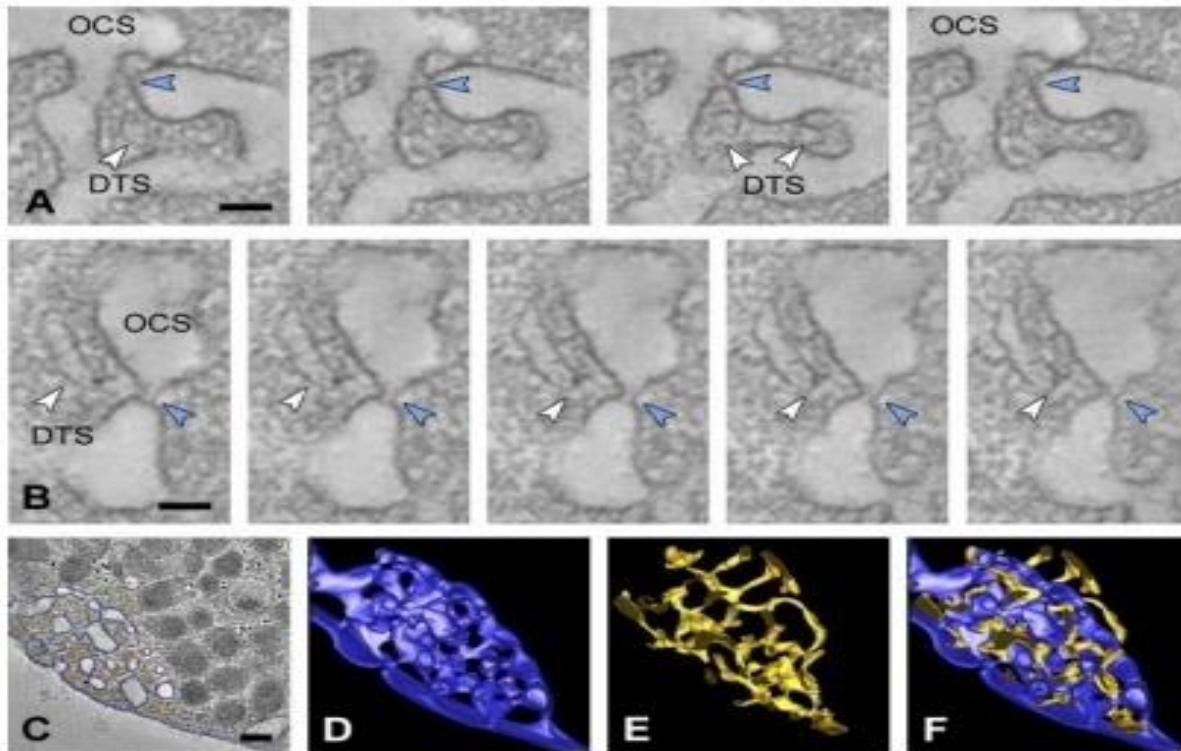


**Figure 1.4. 3D reconstruction of the platelet membrane complex from an electron tomography study of human platelet ultrastructure.** (A,B) series of images showing the close interaction between the open canalicular system and dense tubule system. (C) From each EM slice the DTS (yellow) and OCS (blue) can be traced, leading to the 3D reconstruction compiled from all the slices taken through the platelet of the OCS (D), DTS and the membrane complex (F). Figure reproduced from (van Nispen tot Pannerden et al., 2010)

### 1.2.6 Platelet cytoskeleton

The platelet cytoskeleton in the resting platelet is highly-organised and plays a key role in mediating both the resting discoid state of the cell, as well as the extensive change in morphology upon platelet activation to allow it to spread over the damaged sub endothelial matrix. The system is principally made up of both microtubules and actin-based cytoskeleton.

Microtubules are comprised of hollow cylindrical polarized polymers made up of  $\alpha\beta$  tubulin dimers which are in constant dynamic equilibrium of assembled and disassembled microtubules. Four different tubulin isoforms ( $\beta_1$ ,  $\beta_2$ ,  $\beta_4$ ,  $\beta_5$ ) are found in platelets out of which the  $\beta_1$  tubulin isoform is the most dominant type and specific for megakaryocytes and platelets (Crawford, 1994; Hartwig, 2007; Italiano & Hartwig, 2007). In the resting platelet, much of the tubulin present within the cell can be seen to be found tightly associated with the intracellular face of the platelet plasma membrane. This cortical microtubule polymer is rolled up into a number of coils to give the appearance of a thick ring of microtubules which circumnavigates the cortical region of the platelet. Previous work has demonstrated that this cortical microtubule bundle appears as closely knitted filaments when observed in cross-section (White, 1968; White & Rao, 1998; Italiano *et al.*, 1999). The diameter of the coiling of the cortical microtubule bundle has been shown to be maintained by the antagonistic interaction of kinesin and dynein molecular motors in the resting platelet, whereas upon platelet activation microtubules start to coil due to a net force from the movement of dynein (Diagouraga *et al.*, 2014). This is thought to contribute to the change of platelets from their resting discoid shape to a spherical conformation.

In addition to microtubules, platelets contain a dense actin cytoskeleton. An individual platelet consists of 2 million actin molecules expressed in constant dynamic equilibrium between monomeric (G-actin) and polymeric (F-actin) forms. In resting platelets, around 40 percent of actin present in platelet is found in the polymerized F-actin form creating around 2000-5000 linear actin filaments and the remaining 60 percent are free in the cytosol or stored as 1:1 complex with  $\beta$ 4-thymosin in the platelet cytoplasm, where they can be mobilised to create new actin filaments or elongations that drive cell spreading over the subendothelial matrix upon platelet activation (Hartwig & DeSisto, 1991; Safer & Nachmias, 1994; Nachmias, 2008).

### **1.2.7 Secretory granules**

Upon activation, platelets secrete a number of bioactive substances from three types of granule; dense granules,  $\alpha$ -granules and lysosomes. Deficiency of either the dense granules or  $\alpha$ -granules is known to lead to bleeding disorders in human patients – with patients lacking dense granules in Hermansky-Pudlak syndrome and  $\delta$ -storage pool disorder (Gunay-Aygun *et al.*, 2004), and  $\alpha$ -granules in the Gray platelet syndrome. These clinical findings suggest that secretions of these two granules are essential for platelets role in haemostasis. The  $\alpha$ - and dense granules can be distinguished in imaging studies though their distinct features -  $\alpha$ -granules are larger in diameter around 200 nm, more abundant 50-80/platelet compared to dense granules which are around 20 nm in diameter 3-8 inside the platelet (Mc Nicol & Israels, 1999; Harrison & Cramer 1993; Reed, 2007) The contents of each of these granules are distinct, leading to them providing different roles in normal haemostatic function. Dense granules are rich in autocrine signalling molecules such as ADP, ATP and serotonin that play a principal role in increasing the thrombus growth by activation and recruiting circulating platelets to the growing thrombus (Nesbitt *et al.*, 2003). In contrast, the  $\alpha$ -granules

store and release a variety of substances including adhesive proteins (vWF, fibrinogen, fibronectin), coagulation factors (Factor V), growth factors (PDGF, IGF-1, TGF $\beta$ ), serine protease inhibitors (alpha 2-macroglobulin, alpha 2-antiplasmin), chemokines (CXCL4), and angiogenesis regulatory proteins (endostatin and VEGF) (White, 1993; Italiano *et al.*, 2008).

In addition to the release of their luminal contents, insertion of membranes of these 2 granules into the OCS and surface membranes may alter platelet function, as these granules also contains transmembrane proteins including GLUT-3 for the  $\alpha$ -granule, MRP4 for the dense granule (Jedlitschky *et al.*, 2004), and P-selectin for both granules (Youssefian *et al.*, 1997). In addition the insertion of lipids may play a key role in mediating platelet spreading over the subendothelial lining. Unlike most other cells, upon activation platelets significantly increase their surface area as they spread. As *de novo* synthesis of lipids it is too slow to account for this expansion, it was hypothesised that insertion of lipids from platelet granules could account for this increase in the area of the surface membrane. In support of this previous studies have shown that exocytosis of  $\alpha$ -granules forms a reservoir of membrane in order to contribute towards expansion of plasma membrane and help facilitate platelet spreading on the damaged vessel wall (Peters *et al.*, 2012).

### **1.3 Thrombus formation requires an agonist-dependent rise in cytosolic Ca<sup>2+</sup> concentration in platelets**

When the blood vessel is injured, platelets are recruited to the damaged vessel wall where they undergo a series of activation events which results in the building of the thrombus (Figure 1.4). The first stage is adhesion to the damaged sub-endothelial wall. Platelets bind directly to collagen through glycoprotein VI (GPVI) and integrin

$\alpha_2\beta_1$ , as well as indirectly via glycoprotein Ib-IX-V- (GPIb-IX-V) and integrin  $\alpha_{IIb}\beta_3$ -binding to vWF. vWF acts as an initial point of adhesion for platelets, especially under high shear conditions, where the initial tethering of platelets to vWF appears to be essential to thrombus formation in these conditions (Savage *et al.*, 1998). The bonds formed between vWF and GPIb $\alpha$  are unstable because they both form and dissociate rapidly, hence the adhesion formed by interaction between GPIb $\alpha$  and vWF is not very firm - resulting in transient tethering and slow translocation of platelets across the damaged vessel wall (Nieswandt & Watson, 2003; Figure 1.5). Similarly, platelets also bind to collagen directly via glycoprotein VI, which also supports the initial tethering to the subendothelial matrix. These initial interactions trigger platelet signalling which can lead to the activation of integrin  $\alpha_{IIb}\beta_3$  and integrin  $\alpha_2\beta_1$  into high-affinity states, (Fig 1.5). These activated integrins can then trigger stable adhesion bound to collagen and vWF through these activated receptors (Mangin *et al.*, 2003; Nieswandt & Watson 2003; Kasirer-Friede *et al.* 2004; Marshall *et al.* 2004). Previous studies have demonstrated that this conversion from reversible to firm adhesion is dependent upon a maintained rise in the cytosolic  $Ca^{2+}$  concentration  $[Ca^{2+}]_{cyt}$  (Mazzucato *et al.*, 2002; Nesbitt *et al.*, 2002). These adherent platelets are then able to activate other circulating platelets through their ability to secrete autocooids from their dense granules and produce  $TxA_2$ . Both dense granule secretion and  $TxA_2$  are dependent on an agonist-evoked rises in  $[Ca^{2+}]_{cyt}$  (Rink *et al.*, 1982). This triggers simultaneous  $Ca^{2+}$  signals in both the circulating and adherent platelets. The circulating platelets forms a network with adherent platelets via GPIb/V/IX binding to surface expressed vWf. In response to this interaction  $Ca^{2+}$  signals elicited from adherent platelets serves as a nuclei to tether circulating platelets and secrete ADP whilst exposing its activated integrin  $\alpha_{IIb}\beta_3$  on the surface. The engagement between integrin  $\alpha_{IIb}\beta_3$  and the platelet

expressed vWF triggers further ADP release and elicits additional  $\text{Ca}^{2+}$  signals in nearby platelets thereby triggering integrin  $\alpha_{\text{IIb}}\beta_3$  activation in these cells, allowing the two activated cells to cohere to one another – thus promoting platelet aggregation. These simultaneous agonist-evoked rises in  $[\text{Ca}^{2+}]_{\text{cyt}}$  have been shown to be required for thrombus growth (Nesbitt *et al.*, 2003). This likely occurs due to the need to have activated integrin  $\alpha_{\text{IIb}}\beta_3$  on both cells, which can then bind fibrinogen to the surface of both platelets, cross (Weisel *et al.*, 1992) linking them and thus leading to platelet aggregation. The activation of this fibrinogen receptor on the platelets has been shown to be dependent upon  $\text{Ca}^{2+}$ -dependent activation of the  $\text{Ca}^{2+}$  and DAG regulated guanine nucleotide exchange factor I (Ca/DAG-GEFI) which can trigger integrin activation via an activation of the GTPase Rap1b (Stefanini *et al.*, 2009). Previous work has showed that prolonged rises in  $\text{Ca}^{2+}$  are also essential in facilitating thrombus growth. Both Mazzucato *et al.*, (2002) and Nesbitt *et al.*, (2003) demonstrated that the longer a  $\text{Ca}^{2+}$  signal lasted, the longer a platelet could bind to vWF under flow, and the more likely it was to adhere irreversibly. In addition to binding to the sub-endothelial matrix, prolonged  $\text{Ca}^{2+}$  signals also appear to be important in in facilitating platelet binding to a growing thrombus (Mazzucato *et al.*, 2002; Nesbitt *et al.* 2003).

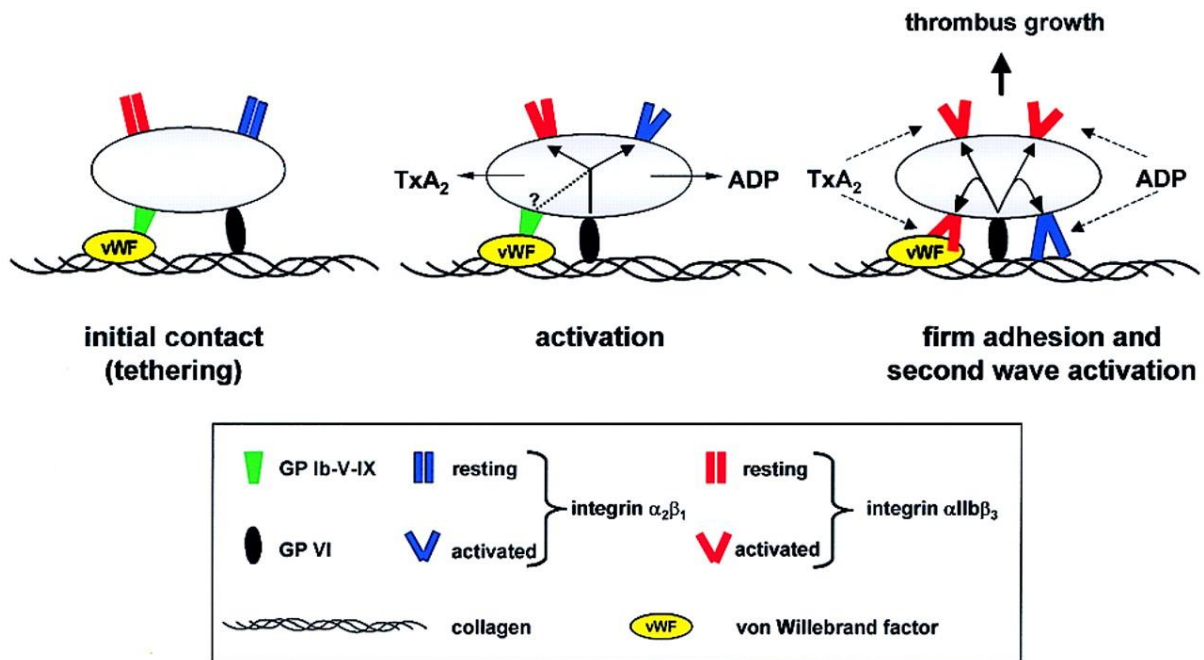


**Figure 1.5: Mechanisms of platelet adhesion to the subendothelial matrix.** Upon vascular damage the GPIIb $\alpha$  – VWF interactions at high shear rates  $> 500 \text{ s}^{-1}$  mediates the initial contact or tethering of platelets to the extracellular matrix. Next activation is triggered by GPVI collagen interactions that change the integrin to high affinity state resulting in release of agonist such as ADP and TxA<sub>2</sub>. This GPVI mediated activation may be caused by initial GPIIb $\alpha$  – VWF interactions but mandatory along with integrin up regulation for initial adhesion. Finally activated  $\alpha_2\beta_1$  and  $\alpha_{IIb}\beta_3$  mediates firm adhesion of platelets to the collagen in turn resulting in a continued GPVI signalling, enhanced release, phosphatidylserine exposure and procoagulant activity. Agonists ADP and TxA<sub>2</sub> mediates thrombus size and growth by activating integrins on adherent platelets and activating additional platelets. Reproduced from Nieswandt & Watson, (2003).

Van Gestel *et al.*, (2002) monitored thrombus formation *in vivo* in anaesthetised rabbits and showed that platelets that formed part of a thrombus underwent shape change and degranulation in combination with a prolonged rises in  $[Ca^{2+}]_{cyt}$  (van Gestel *et al.*, 2002). Whereas platelets that form emboli exhibited reduced, transient  $Ca^{2+}$  signals, and in turn demonstrated neither degranulation nor shape change. This is in line with more recent work which demonstrated that platelets need to have simultaneous rises in  $Ca^{2+}$  to aggregate together (Nesbitt *et al.* 2003).

Once the thrombus is formed it also needs to trigger the localised activation of the blood coagulation cascade to help create thrombin which in turn both helps activate more platelets (Furie & Furie, 2008) as well as create fibrin strands to help stabilise the thrombus (Furie & Furie, 2008). This is achieved through the exposure of anionic phospholipids such as phosphatidylserine on the surface of the platelet. Previous studies have shown that this only occurs on a subset of platelet within the thrombus (Munnix *et al.*, 2007). This subgroup of platelets are called pro-coagulant platelets, and are characterised by having high, sustained rises in  $[Ca^{2+}]_{cyt}$  (Kulkarni & Jackson, 2004). These data suggested that maintaining  $Ca^{2+}$  signals at higher levels is essential in determining both the extent of thrombus formation as well as the extent of activation of the blood coagulation cascade. Failure to trigger phosphatidylserine exposure is seen in patients with Scott's syndrome, who suffer from a bleeding diathesis (Suzuki *et al.*, 2010). Recent work has demonstrated that these patients have a loss of a  $Ca^{2+}$ -dependent lipid scramblase called TMEM16F (Yang *et al.*, 2012).

From the above outline description of thrombus formation, it is possible to see that platelets contain a number of  $Ca^{2+}$ -regulated processes which allow them to mediate their haemostatic functions. Therefore understanding both how resting platelets keep their  $[Ca^{2+}]_{cyt}$  low to prevent unwanted activation, and how  $[Ca^{2+}]_{cyt}$  are maintained at

high levels upon blood vessel damage will allow us to understand how thrombus formation is controlled.

### **1.3.1 Resting platelets keep cytosolic $\text{Ca}^{2+}$ concentration low**

In the undamaged circulation, platelets circulate in a quiescent, discoid state. From the initial stages of platelet adhesion to the final stages of clot retraction, all platelet-mediated events in blood clotting have a requirement for a rise in the  $[\text{Ca}^{2+}]_{\text{cyt}}$ . However in a resting platelet,  $[\text{Ca}^{2+}]_{\text{cyt}}$  is kept at very low at around 50-100 nM (Rink & Sage, 1990). The ability of platelet to tightly control the concentration of resting  $[\text{Ca}^{2+}]_{\text{cyt}}$  within their cytosol is essential in ensuring that platelets do not begin to aggregate inside undamaged blood vessels. At rest, platelets mediate tight control over their  $[\text{Ca}^{2+}]_{\text{cyt}}$  levels through their ability to exclude this divalent cation from this cell compartment through removing  $\text{Ca}^{2+}$  across their plasma membranes and sequestering it into their intracellular organelles.

### **1.3.2 $\text{Ca}^{2+}$ Removal**

Two subsets of proteins work cooperatively to remove  $\text{Ca}^{2+}$  across the plasma membrane they are: The plasma membrane  $\text{Ca}^{2+}$  ATPase (PMCA) and the  $\text{Na}^+/\text{Ca}^{2+}$  exchanger (NCX). PMCA is ubiquitously expressed with high expression found in a number of cells including erythrocytes, platelets, spermatozoa, heart, vascular smooth, muscle, kidney, skeletal muscle, stomach, intestine and brain (Okunade *et al* ., 2004; Stauffer *et al* ., 1995; Brandt *et al* ., 1992; Howard *et al* ., 1993; Jones *et al* ., 2010; Oceandy *et al* ., 2007; Pande *et al* ., 2006; Schuh *et al* ., 2004). PMCA4 isoform was reported to play an important structural role in tethering neuronal nitric oxide synthase (nNOS) to a highly segregated microdomain within the cardiac cell membrane. This structural role was later identified as the nNOS dependent

mechanism through which PMCA4 regulated  $\beta$ -adrenergic induced cardiac contractility (Mohamed *et al.*, 2011). Recent studies investigating the PMCA4 isoform in mouse models have confirmed its physiological function in regulating sperm motility and male fertility (Schuh *et al.*, 2004).

The platelet  $\text{Ca}^{2+}$  homeostasis is maintained by two ion transporters (PMCA, NCX) playing different roles, possessing different kinetic properties and  $\text{Ca}^{2+}$  affinities (Johansson & Haynes, 1988; Valant *et al.*, 1992). The PMCA is better suited for maintenance of basal  $[\text{Ca}^{2+}]_{\text{cyt}}$  because it possess a higher affinity for  $\text{Ca}^{2+}$  than the NCX, whereas in stimulated platelets the NCX plays a greater role in restoring  $[\text{Ca}^{2+}]_{\text{cyt}}$  to resting levels due to its higher capacity for  $\text{Ca}^{2+}$  transport (Johansson *et al.*, 1992). The main agent for  $\text{Ca}^{2+}$  efflux in platelets at rest is PMCA due to its high affinity, low capacity transport mechanisms. Platelets are known to express two isoforms of PMCA - PMCA1b and PMCA4b (Dean, 2010). However expression of PMCA1b is much lower than PMCA4b, suggesting that this is the predominant isoform in these cells (Dean, 2010) The PMCA has been shown to be predominantly localised to the OCS, with a particular association at the membrane complex (Cutler *et al.*, 1981). Although this transporter was traditionally thought to play a role in preventing platelet activation, previous work has shown that this transporter is more than a passive regulator of platelet function, with studies demonstrating that it can be localised to the filopodial region, through its interaction with the actin cytoskeleton – thus suggesting a potential to control platelet spreading on the sub-endothelium (Dean & Whiteheart, 2004). In addition to its control over its spatial localisation, further studies have demonstrated the PMCA activity can also be controlled through the action of Protein kinase A, Src family kinases, calpain, small GTPases and phosphoinositide's (Dean *et al.*, 1997; Rosado & Sage, 2000; Wan *et al.*, 2003). Alterations in this regulation have been

shown to potentially be responsible for the elevated agonist-evoked  $\text{Ca}^{2+}$  responses seen in patient groups who demonstrate platelet hyperactivity, such as those with hypertension and type II diabetes mellitus (Blankenship *et al.*, 2000; Rosado *et al.*, 2004). These results therefore suggest the potential for PMCA activity to be a key negative regulator of platelet activity in resting platelets

Platelets have been reported to possess at least two isoforms of  $\text{Na}^+/\text{Ca}^{2+}$  exchangers (NCX) NCX1 and NCX3 (Roberts *et al.*, 2012). Of these NCX3 is likely to be the dominant isoform as NCX1 expression has not been consistently discovered in western blot studies or proteomic screens of human platelets (Lewandrowski *et al.*, 2009; Harper *et al.*, 2010; Burkhart *et al.*, 2012; Roberts *et al.*, 2012). Previous work has demonstrated that the NCX accounts for rapid  $\text{Ca}^{2+}$  removal upon platelet activation (Valant *et al.*, 1992; Sage *et al.*, 2013) suggesting that like other cells, this exchanger plays a key role in mediating  $\text{Ca}^{2+}$  removal upon activation and not in resting cells (Blaustein & Lederer, 1999). Unlike the PMCA, little has been reported about the platelets regulation by post-translational modification or its ultrastructural localisation within the cell. In addition to the NCX isoforms described above, platelets have also been reported to contain a  $\text{K}^+$ -dependent NCX (NCKX), NCKX1 (Kimura *et al.*, 1993). The NCKX isoforms provide an exchanger whose mode of exchange is less influenced by changes in cytosolic  $\text{Na}^+$  concentration ( $[\text{Na}^+]_{\text{cyt}}$ ) – however little is known about the importance of this exchanger in human platelet physiology.

### 1.3.3 $\text{Ca}^{2+}$ Sequestration

In addition to  $\text{Ca}^{2+}$  removal across the plasma membrane, resting- and agonist-evoked rises in  $[\text{Ca}^{2+}]_{\text{cyt}}$  are also negatively regulated by sequestration of this divalent cation into intracellular  $\text{Ca}^{2+}$  stores. Previous measurements suggest that these stores

contain an average concentration of around 200  $\mu\text{M}$  inside them (Sage *et al.*, 2011) demonstrating that active transport mechanisms must be used to allow  $\text{Ca}^{2+}$  to be taken up against the concentration gradient present between these stores and the cytosol.

Previous studies in human platelets have suggested that there are at least two intracellular  $\text{Ca}^{2+}$  stores in platelets; a DTS-localised  $\text{Ca}^{2+}$  stores as well as an acidic  $\text{Ca}^{2+}$  stores (Rosado, 2011). These stores have distinct cellular mechanisms to control  $\text{Ca}^{2+}$  sequestration into them, as shown by their distinct pharmacological properties (Ruiz *et al.*, 2004, Sage *et al.*, 2011) which relates to the distinct molecular mechanisms available for them to take up  $\text{Ca}^{2+}$ . Both stores appear to possess a specific sarco / endoplasmic reticulum (SR) calcium transport ATPase (SERCA) isoform unique to that pool. The ability of platelet to sequester into these two distinct  $\text{Ca}^{2+}$  stores can be differentiated by their distinct sensitivity to thapsigargin and TBHQ (2, 5-di-(t-butyl)-1,4-hydroquinone; Rosado 2011). Sequestration of  $\text{Ca}^{2+}$  into the dense tubular system requires the SERCA2b isoform and is characterised by its sensitivity to low concentrations of the SERCA inhibitor thapsigargin, and its insensitivity to TBHQ. In contrast, the acidic  $\text{Ca}^{2+}$  stores are pharmacologically characterised by the presence of SERCA3 isoform which can be distinguished by its sensitivity to TBHQ, and its relative insensitivity to thapsigargin. Through both pharmacological and immunolocalisation studies, previous studies have confirmed that these two SERCA pumps are found within two distinct  $\text{Ca}^{2+}$  stores in human platelets (Papp *et al.*, 1991; Papp *et al.*, 1992; Lopez *et al.*, 2005). Currently the exact location(s) of the acidic  $\text{Ca}^{2+}$  stores in platelets is unknown but it is likely to include one or more of the platelet secretory granules (Ruiz *et al.*, 2004; Rosado, 2011).

Inside the platelet SERCA has been shown to act as a negative regulator of both resting and agonist-evoked rises in  $[Ca^{2+}]_{cyt}$  by sequestering  $Ca^{2+}$  into the intracellular stores (Sage *et al.*, 2011). The ability of SERCA to reduce  $[Ca^{2+}]_{cyt}$  can also be altered by post-translational modifications such as phosphorylation by PKA, PKC and nitrosylation that have been shown to accelerate SERCA-mediated  $Ca^{2+}$  reuptake into stores (Tao *et al.*, 1992; Trepakova *et al.*, 1999). However, SERCA is not the only mechanism for sequestering  $Ca^{2+}$  present in the intracellular  $Ca^{2+}$  stores – previous studies demonstrated that in the absence of SERCA activity, platelets are still able to sequester  $Ca^{2+}$  into their intracellular organelles (Sage *et al.*, 2011). This effect is not present when platelets are exposed to the protonophore, nigericin, which suggests there is a  $Ca^{2+}/H^+$  exchange mechanism present in the acidic stores of these cells. Further work will be required to identify the molecular identity of this exchanger which may be the activity of a single exchanger or a coupled-transport system requiring two or more  $Ca^{2+}$ - and  $H^+$ -dependent exchangers (Sage *et al.*, 2011)

#### **1.3.4 A rise in cytosolic $Ca^{2+}$ concentration is required to trigger platelet activation**

From the above description, it is possible to see that upon blood vessel damage platelets are exposed to a range of adhesive ligands (e.g. vWF, collagen, and fibrinogen) and soluble ligands (e.g. ATP, ADP, 5-HT, thrombin,  $TxA_2$ ) which trigger platelet activation. They do this through their ability to bind to an array of specific cell surface receptors, which in turn can trigger platelet activation through triggering an increase in  $[Ca^{2+}]_{cyt}$  (Rink & Sage, 1990). Like other cells this can be brought about in two ways, through release of  $Ca^{2+}$  from intracellular  $Ca^{2+}$  stores and via  $Ca^{2+}$  entry across the plasma membrane.

### 1.3.5 Ca<sup>2+</sup> release

As stated above human platelets consist of two distinct intracellular Ca<sup>2+</sup> stores which can be mobilised upon agonist stimulation - a DTS-localised Ca<sup>2+</sup> store and an acidic Ca<sup>2+</sup> store which is likely to be one or more of the platelet secretory granules (lysosome,  $\alpha$ - and dense granule; Rosado, 2011). In addition to their distinct sequestration mechanisms, these two stores are also mobilised in response to the creation of two different second messenger systems.

The principal agonist-sensitive Ca<sup>2+</sup> store is contained within the DTS, which is able to release Ca<sup>2+</sup> via the opening of IP<sub>3</sub> receptors (IP<sub>3</sub>Rs; Sage *et al.*, 2011). Nearly all platelet agonist release Ca<sup>2+</sup> from this store through the stimulated breakdown of phosphatidylinositol 4,5-bisphosphate (PIP<sub>2</sub>) to inositol 1,4,5-trisphosphate (IP<sub>3</sub>) and diacylglycerol (DAG) triggered by the activation of phospholipase C (PLC). However, how the pathway by which this is triggered is distinct for soluble agonists such as thrombin, ADP, TxA<sub>2</sub> and platelet-activating factor (PAF), and adhesive ligands such as collagen, fibrinogen and vWF (Rink & Sage, 1990). Soluble agonists trigger the activation of the Gq protein via G-protein coupled receptors, which then goes onto trigger an increase in activity of PLC $\beta$  (Heemskerk & Sage, 1994). In contrast, adhesive ligands trigger the activation of src family kinases which then go on to trigger the activation of phospholipase C $\gamma$  (Senis *et al.*, 2014).

Previous work has identified all three known isoforms of IP<sub>3</sub>Rs in human platelets (Rosado & Sage, 2000). Controversy prevails over the isoforms subcellular localisation in human platelets with some reports stating that type I, II and III IP<sub>3</sub>Rs being present in both intracellular- and plasma membrane-associated platelet fractions (Bourguignon *et al.*, 1993; Quinton & Dean, 1996; El-Daher *et al.*, 2000).

However, the consensus appears to be that type III isoform is localised in plasma membrane, type I isoform appears to be predominantly intracellular while the type II isoform might split between both these locations. Therefore, based on these suggestions that type I and type II IP<sub>3</sub>R may be involved in Ca<sup>2+</sup> release, whilst type III IP<sub>3</sub>R may be involved in mediating Ca<sup>2+</sup> entry (El-Daher *et al.*, 2000), although no evidence yet exists to show that this latter pathways occurs physiologically. In addition to the basic regulation of this Ca<sup>2+</sup>-permeable ion channel by IP<sub>3</sub>, IP<sub>3</sub>R-mediated Ca<sup>2+</sup> release has also been shown to be positively regulated by allosteric Ca<sup>2+</sup> binding to the IP<sub>3</sub>R leading to Ca<sup>2+</sup>-induced Ca<sup>2+</sup> release in these cells (van Gorp *et al.*, 1997; Sage *et al.*, 2011). In addition, nitric oxide may mediate its negative effects on platelet Ca<sup>2+</sup> signalling through inhibition of the type I IP<sub>3</sub>R via its ability to increase cGMP rises and activate Protein Kinase G, which in turn phosphorylates the associated protein, IRAG (van Gorp *et al.*, 1997).

In addition to the DTS platelets also contain, a secondary Ca<sup>2+</sup> acidic store which has been previously shown to release Ca<sup>2+</sup> in response to a rise in cytosolic NAADP (Nicotinic acid adenine dinucleotide phosphate; Lopez *et al.*, 2006). In contrast to IP<sub>3</sub>, NAADP appears to only be made to strong platelet agonists such as collagen and thrombin (Coxon *et al.*, 2012). However, the manner by which this second messenger is created in platelets upon receptor stimulation is currently unclear. Recent work has demonstrated a role for the TPCN2 channel in mediating NAADP-dependent Ca<sup>2+</sup> release from the dense granule of platelets – suggesting that this Ca<sup>2+</sup> release may play a key role in modulating dense granule secretion (Ambrosio *et al.*, 2015).

### 1.3.6 Ca<sup>2+</sup> entry

Platelets possess three main Ca<sup>2+</sup>-permeable ion channels through which Ca<sup>2+</sup> can enter the platelet upon agonist binding. These are the store-operated channel, a TRPC6-containing second messenger-operated channel, and the P<sub>2X1</sub> purinoreceptor. When cells are activated they release Ca<sup>2+</sup> from their intracellular stores, leading to a decrease in the Ca<sup>2+</sup> concentration inside their organelles. This drop in intracellular Ca<sup>2+</sup> stores is then able to elicit the activation of a plasma membrane-localised Ca<sup>2+</sup>-permeable ion channels – known as store-operated channels (SOC). In non-excitabile cells, such as human platelets, store-operated Ca<sup>2+</sup> entry (SOCE) is a key mechanism of Ca<sup>2+</sup> entry (Rink & Sage, 1990). Recent work has identified two important proteins in mediating the activation of this pathway – these are STIM1 (stromal interaction molecule 1) and Orai1.

STIM1 is a transmembrane protein resident in the endoplasmic reticulum of all cells, and has a Ca<sup>2+</sup>-binding EF hand domain which extends in the lumen of this organelle which allows it to sense changes in Ca<sup>2+</sup> concentration of the intracellular stores. When the stores are filled with Ca<sup>2+</sup>, STIM1 binds a Ca<sup>2+</sup> ion and is unable to activate the SOC. However when Ca<sup>2+</sup> stores empty upon opening of IP<sub>3</sub>Rs, Ca<sup>2+</sup> debinds from STIM1 eliciting a change in conformation which allows it to bind to and activate the SOC. Patients with mutations in the STIM1 molecule causing it to take a constitutively active form are found to have higher basal Ca<sup>2+</sup> signals, reduced SOCE and a mild bleeding tendency, showing that this channel plays a key role in underlying platelet activation (Misceo *et al.*, 2014; Markello *et al.*, 2015). This is in line with data from STIM1 knockout mice, who are found to have reduced agonist-evoked Ca<sup>2+</sup> signals as well as impaired thrombus formation (Varga-Szabo *et al.*, 2008). Orai1 has been discovered to be an essential component of the platelet SOC – with Orai1 knockout

mice found to have a similar phenotype to the STIM1 knockout mouse with defective SOCE, reduced agonist-evoked  $\text{Ca}^{2+}$  signalling and impaired thrombus formation (Braun *et al.*, 2009; Gilio *et al.*, 2010). Putative SOC blockers were found to also inhibit functional responses in human platelets (van Kruchten *et al.*, 2012). However intriguingly there are no features of haemostatic defects in patients with Orai1 and STIM1 mutations – suggesting that these channels are less essential to normal function in humans compared to mice (McCarl *et al.*, 2009, Picard *et al.*, 2009). Platelets have also been shown to elicit a rise in intracellular  $\text{Ca}^{2+}$  in response to the DAG created by receptor-dependent activation of PLC (Hassock *et al.*, 2002). This DAG dependent pathway is thought to be elicited through TRPC6, which is relatively highly-expressed in these cells (Tolhurst *et al.*, 2008). However recent work in TRPC6-knockout mice has elicited conflicting evidence regarding the likelihood that this channel plays any significant functional role within platelets (Paez Espinosa *et al.*, 2012; Ramanathan *et al.*, 2012; Harper *et al.*, 2013). In contrast, work in human platelets has suggested a role in modulating platelet dense granule secretion and aggregation (Lopez *et al.*, 2015; Vemana *et al.*, 2015). Recent work has suggested that TRPC6 is absent from the plasma membrane of resting human platelets, and may be inserted upon platelet activation, which may explain some of these discrepancies (Harper *et al.*, 2013).

Platelets also express the ionotropic  $\text{P}_{2\text{X}_1}$  receptor, which is a non-selective cation channel which allows  $\text{Ca}^{2+}$  entry in the presence of extracellular ATP (MacKenzie *et al.*, 1996). Upon vascular damage ATP is secreted by dense granules, injured endothelial cells and damaged red blood cells. Secreted ATP immediately interacts with  $\text{P}_{2\text{X}_1}$  receptors leading to  $\text{Ca}^{2+}$  influx, shape change, granule centralisation and finally platelet activation (Mahaut-Smith *et al.*, 2004, Mahaut-Smith *et al.*, 2011). Unlike

other  $\text{Ca}^{2+}$  mobilising systems in human platelets the  $\text{P}_{2\text{x}1}$  purinoreceptor is not inhibited by elevated cytosolic cyclic nucleotides elicited by the endothelial-derived platelet inhibitors (Mahaut-Smith *et al.*, 2011). *In vitro* measurements of the  $\text{Ca}^{2+}$  influx mediated by this channel only yielded small responses, however this could possibly be due to desensitisation of  $\text{P}_{2\text{x}1}$  purinoreceptor when platelets are extracted from the human body due to the reduced ability to remove ATP and ADP by ectonucleotidases present both in plasma as well as circulating leukocytes and endothelial cells (Robson, 2001; Rolf *et al.*, 2001; Heptinstall *et al.*, 2005). A previous report has also suggested that  $\text{P}_{2\text{x}1}$  receptors may function to amplify  $\text{Ca}^{2+}$  signals which may play a key role in facilitating effecting thrombus formation under the high shear stress conditions found in small arteries and arterioles (Jones *et al.*, 2014).

### **1.3.7 $\text{Ca}^{2+}$ Effectors**

A rise in  $[\text{Ca}^{2+}]_{\text{cyt}}$  in human platelets triggers a range of changes in the structural and functional properties of platelets. These effects are mediated via a number of distinct  $\text{Ca}^{2+}$  effector proteins which bind  $\text{Ca}^{2+}$  and trigger the activation of a range of responses which underlie these changes in platelet structure and function.

Shape change is known to be the first measurable response elicited by platelets upon exposure to physiological agonists. Upon activation, platelets undergo a marked change in their morphology from the discoid form found in resting cells, into a spherical form. This shape change has been shown to be mediated through both  $\text{Ca}^{2+}$ -dependent and independent pathways (Paul *et al.*, 1999). The  $\text{Ca}^{2+}$ -dependent pathway involves binding of this divalent cation to calmodulin, which can then bind to and trigger the activation of the myosin light chain kinase (MLCK). This turn

phosphorylates and activates myosin eliciting the shape change (Daniel *et al.*, 1984). However, previous studies have also demonstrated the possibility of a  $\text{Ca}^{2+}$  independent pathway in which RhoA kinase phosphorylates p160<sup>ROCK</sup>, which acts to inhibit the myosin phosphatase, leading to and myosin light chain phosphorylation thus triggering shape change independent of the  $\text{Ca}^{2+}$ /Calmodulin-dependent pathway. (Nakai *et al.*, 1997; Bauer *et al.*, 1999). This data is based on the demonstration that agonist-evoked shape change is resistant to loading of the platelets with the fast  $\text{Ca}^{2+}$  chelator, dimethyl-BAPTA.

In addition to this initial shape change, platelets can also further change their morphology through rearrangements of the actin cytoskeleton in a  $\text{Ca}^{2+}$ -dependent manner which help the platelet to spread over the sub-endothelial matrix. For instance gelsolin plays an important role in  $\text{Ca}^{2+}$ -regulated actin severing during platelet activation (Witke *et al.*, 1995; Goshima *et al.*, 1999). Rodriguez Del Castillo *et al.*, (1992) demonstrated that scinderin, another  $\text{Ca}^{2+}$ -dependent actin filament-severing protein might involve in regulation of platelet actin network mechanisms.

$\text{Ca}^{2+}$  also plays a role in the recruitment of platelets to the growing thrombus through controlling the release of autocrine stimulants. This includes facilitating the production of TxA<sub>2</sub> via the ability of  $\text{Ca}^{2+}$  to activate cytosolic PLA<sub>2</sub> (Borsch-Haubold *et al.*, 1995). In addition  $\text{Ca}^{2+}$  also plays a key role in triggering the secretion of platelet granules as  $\text{Ca}^{2+}$ -dependent proteins such as calpain, protein kinase C and Munc13-4 are thought to be critically involve in regulating platelet granule secretion (Croce *et al.*, 1999; Strehl *et al.*, 2007; Ren *et al.*, 2010, Boswell *et al.*, 2012; Golebiewska & Poole, 2013).

Platelet aggregation requires the activation of the fibrinogen receptor, integrin  $\alpha_{\text{IIb}}\beta_3$ , onto the platelet surface to facilitate platelet-platelet adhesion in the growing thrombus.

Ca<sup>2+</sup>-binding proteins such as CalDAG-GEFI and CIB1 are thought to be involved in mediating the activation of this integrin (Naik *et al.*, 2009; Stefanini *et al.*, 2009).

Lastly in all mammalian cells including blood platelets phospholipids are asymmetrically arranged between the outer and inner leaflets of plasma membrane. However localised activation of the coagulation cascade requires platelet expression of acidic phospholipids such as phosphatidylserine on the extracellular face of the platelets. When platelets undergo agonist induced activation the phospholipid symmetry is disrupted by a scrambling process and they expose phosphatidylserine on their surface to allow the localised recruitment and activation of clotting factors involved in triggering the activation of the coagulation cascade. Failure to trigger this scrambling is found in patients with Scott's syndrome, who suffer from a mild bleeding disorder. Recent studies have identified a role for TMEM16F as a protein that supports Ca<sup>2+</sup>-dependent phospholipid scrambling (Yang *et al.*, 2012; van Kruchten *et al.*, 2013; Fujii *et al.*, 2015)

### **1.3.8 Platelets can selectively respond to cytosolic Ca<sup>2+</sup> signals**

The previous discussion above has demonstrated that Ca<sup>2+</sup> functions as an important secondary messenger in the platelet activation cascade, as increased cytosolic Ca<sup>2+</sup> concentration is accountable for activation of all stages of platelet activation including adhesion, shape change, secretion, aggregation and transition to a procoagulant phenotype through its ability to activate a number of distinct Ca<sup>2+</sup>-dependent effectors (Grette, 1962; Born, 1972; Heptinstall, 1976). This central role of Ca<sup>2+</sup> has attracted researchers to try to identify the molecular mechanisms that generate and modulate these agonist-evoked rises in platelet cytosolic Ca<sup>2+</sup>, in the hope of discovering novel targets for anti-thrombotic drugs that can function by blocking specific Ca<sup>2+</sup> entry

pathways. But all of the main  $\text{Ca}^{2+}$ -permeable channels detailed above are not selectively expressed in platelets, and as such opens up the likelihood of non-specific interactions with other cells leading to unwanted side effects. Furthermore, using blockers that significantly inhibit all agonist-evoked  $\text{Ca}^{2+}$  rises could put the patient at risk of bleeding defects.

Previous studies have demonstrated that individual platelets respond heterogeneously within the thrombus *in vivo* suggesting that platelets are able to selectively activate each of the different  $\text{Ca}^{2+}$ -dependent effectors mentioned in the previous section. Munnix *et al.*, (2007) demonstrated that both *in vitro* and *in vivo* models of thrombus formation there were distinct sub-populations of platelet demonstrating either activation of integrin  $\alpha\text{IIb}\beta\text{3}$  or exposure of phosphatidylserine, thus suggesting that within the growing thrombus platelets segregate into discrete microdomains or patches with aggregatory or procoagulant functions (Munnix *et al.*, 2007). More recently Stalker *et al.*, (2013), demonstrated that platelets within the growing thrombus could be defined by the degree of platelet activation and packing density. For instance, the inner core is composed of densely-packed thrombin activated platelets with P-selectin surface expression (indicative of granule secretion), restricted plasma entry and heavily influenced by contact dependent signalling. Conversely the outer shell is composed of loosely arranged platelets with no P-selectin expression or fibrin mesh, and is highly permeable to plasma. Therefore, these data suggest that platelets within the platelet aggregate can be differentially activated to create these different sub-populations (Stalker *et al.*, 2013).

These data thus suggest that  $\text{Ca}^{2+}$ -dependent functions must be able to be selectively activated within the platelets. If we can understand how platelets are able to use  $\text{Ca}^{2+}$  signalling pathways to selectively activate specific  $\text{Ca}^{2+}$ -dependent functions, then this

might help us design treatments that can selectively block certain  $\text{Ca}^{2+}$ -dependent effects inside the platelets. For example, the differences in duration of  $\text{Ca}^{2+}$  signal in procoagulant and pro-aggregatory platelets suggest that being able to limit the duration of  $\text{Ca}^{2+}$  signals could reduce the proportion of procoagulant platelets in a thrombus, without affecting the recruitment of pro-aggregatory platelets. Therefore any anti-platelet drug that limits the duration of  $\text{Ca}^{2+}$  signalling could reduce the extent of activation of the blood coagulation system and thereby prevent thrombi from occluding blood vessels without significantly increasing the bleeding risk posed by anti-thrombotic medication currently.

### **1.3.9 Platelets can create localised $\text{Ca}^{2+}$ signals**

Studies in other cell types (such as neurons and striated muscle cells) have demonstrated that they are able to create selective responses to  $\text{Ca}^{2+}$  signals by co-localising  $\text{Ca}^{2+}$  channels and  $\text{Ca}^{2+}$  effectors in spatially-distinct microdomains of the cell (Gabella, 1971; Devine et al., 1972; Verboomen *et al.*, 1992). However, the small size of the platelet would appear to preclude this possibility, as elementary calcium signals observed in these other cell types are significantly bigger than the size of the platelet. For example,  $\text{Ca}^{2+}$  puffs generated from the opening of a single cluster of  $\text{IP}_3$ Rs averages about 5  $\mu\text{m}$ , whilst the platelet is only 2  $\mu\text{m}$  in diameter (Niggli & Shirokova, 2007). As platelets are reported to contain around 5000 copies of the various  $\text{IP}_3$  receptor isoforms alone, it would appear that platelets should not be able to compartmentalise  $\text{Ca}^{2+}$  signalling, as  $\text{Ca}^{2+}$  signals would be expected to spread throughout the entire platelet cytosol.

Despite these apparent structural difficulties previous single cell imaging studies have presented evidence for a link between localized  $\text{Ca}^{2+}$  signals with redistribution of

signalling receptors and effector proteins in activated human platelets (Ariyoshi Salzman, 1996). In addition, previous work by Tsunoda *et al.*, (1988) also reported  $\text{Ca}^{2+}$  gradients in resting platelets. These data support the existence of a specialised mechanism able to controlling the spread of  $\text{Ca}^{2+}$  signals in platelets, which allows them to use the localised signals to selectively control its  $\text{Ca}^{2+}$ -dependent functions.

### **1.3.10 Nanojunctions permit the creation of isolated cytosolic $\text{Ca}^{2+}$ nanodomains**

When the membranes of two organelles are tethered in close apposition (10-30nm wide), these structures are termed as nanojunctions. In striated and smooth muscle cells, nanojunctions made up of close appositions (within  $\approx 20$  nm) of specialised portions of the plasma membrane and the sarcoplasmic reticulum are responsible for controlling the spatial spread of  $\text{Ca}^{2+}$  signals. Both the ultrastructure and electrostatic properties of nanojunction generates an environment of restricted  $\text{Ca}^{2+}$  diffusion that facilitates the creation of a cytosolic nanodomain (van Breemen *et al.*, 2013). By creating a local environment that is able to slow  $\text{Ca}^{2+}$  diffusion, they can create cytosolic nanodomains in which control of  $\text{Ca}^{2+}$  concentration can be locally controlled by the channels and transporters localised here, and  $\text{Ca}^{2+}$  effector proteins localised here can be selectively activated. Human platelets possess an analogous nanojunction to those seen in muscles cells, called the membrane complex. This structure is made up of the close apposition of the main platelet intracellular  $\text{Ca}^{2+}$  store, the DTS, and the invaginated plasma membrane of the OCS. As such the MC may create the cellular architecture needed to facilitate selective platelet activation.

In recent studies from our lab, we have provided initial evidence for a key role for the membrane complex in triggering agonist-evoked  $\text{Ca}^{2+}$  signalling in human platelets.

This work proposed that  $\text{Ca}^{2+}$  release from intracellular  $\text{Ca}^{2+}$  stores occurs initially into a cytosolic nanodomain enclosed within the membrane complex from which diffusion is restricted into the bulk cytosol. From this cytosolic nanodomain, the  $\text{Ca}^{2+}$  is spread via removal by the  $\text{Na}^+/\text{Ca}^{2+}$  exchanger (NCX) into the OCS, where it can accumulate. Due to the tiny volume of the lumen of the OCS,  $\text{Ca}^{2+}$  is spread pericellularly through the lumen of this system and then recycled back into the cytosol through  $\text{Ca}^{2+}$ -permeable ion channels (as shown in Fig 1.6). The  $\text{Na}^+/\text{Ca}^{2+}$  exchanger (NCX) is hypothesised to be resident in the OCS within membrane complex. One of the predictions of this model of agonist-evoked  $\text{Ca}^{2+}$  signalling is that the platelet possesses two functional cytosolic subcompartments for  $\text{Ca}^{2+}$  signalling the bulk cytosol and that encompassed within the membrane complex. Through selective partitioning of  $\text{Ca}^{2+}$ -dependent effectors between these sub compartments, this could therefore explain selective activation of  $\text{Ca}^{2+}$ -dependent processes in platelets. In this project we aimed to provide evidence of the presence of a cytosolic nanodomain which controls  $\text{Ca}^{2+}$  signalling in human platelets.

#### **1.4 Megakaryocytes as a model system for studying the platelet membrane complex**

Platelets are relatively small in size ranging from 2-4  $\mu\text{m}$  in diameter therefore it is extremely challenging to view subcellular events with the platelet under confocal microscopy. Additionally platelets lack a nucleus precluding genetic modification and are difficult to patch clamp due to their ability to undergo contact-induced activation when exposed to the glass patch pipette and the high sheer pressure required to seal the patch (Hussain & Mahaut-Smith, 1999; Tolhurst *et al.*, 2005).

Since megakaryocytes are the larger precursor cells of platelets (around 20 - 100  $\mu\text{m}$  in diameter) they might be an appropriate model system in which to study platelet signalling events. Previous work has shown that CD34<sup>+</sup>-cultured megakaryocytes start to develop a number of Ca<sup>2+</sup>-transporting proteins found in platelet such as TRPC and Orai1 channels (Ramanathan & Mannhalter, 2015).

A recent study has also demonstrated that NCX function can be found in cultured megakaryocytes, and that the expression of this exchanger can be modulated by culturing in the presence of 1,25-dihydrocholecalciferol (calcitriol; Schmid *et al.*, 2015). Therefore, megakaryocytes contain much of the same Ca<sup>2+</sup>-transporting as platelets. Megakaryocytes also contain analogous cellular structures to platelets. During the earliest stages of megakaryopoiesis, the developing cells start to make an invaginated membrane system analogous to the platelet OCS, called the demarcation membrane system (DMS). The DMS was initially called this as it was initially thought to delineate small territories, from which platelets would be produced, however recent studies have suggested this is not the case (Behnke, 1968; Nakao & Angrist, 1968). Like the OCS, the DMS has been found to be continuous with the extracellular environment and creates an intricate membrane system which spreads throughout the interior of the megakaryocyte. Furthermore recent work has demonstrated a close association of the DMS with the smooth endoplasmic reticulum – creating a nanojunction in megakaryocytes analogous to the platelet membrane complex (Eckly *et al.*, 2014; White 1972). These data suggest the possibility that those megakaryocytes may also use this structure to control their Ca<sup>2+</sup> signalling. Based on these findings we can conclude that megakaryocytes might present a model system in which we can investigate development, structure and function of the platelet membrane complex. However there is very limited data about the structure of the ER-DMS nanonjunction

in these cells and how they might relate to the MC. Similarly there is no information regarding the spatial localisation of  $\text{Ca}^{2+}$  channels and transporters in these cells. Therefore, in this project we will examine the role of the NCX in the  $\text{Ca}^{2+}$  signalling

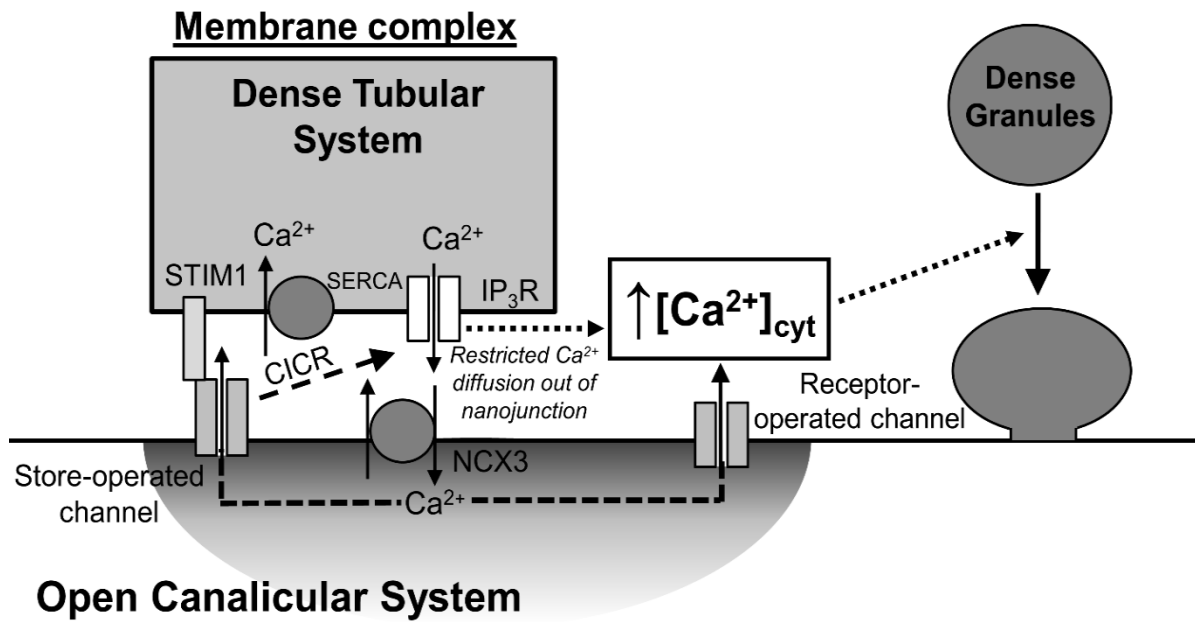


**Figure 1.6 The pericellular  $\text{Ca}^{2+}$  recycling hypothesis.** Reproduced from Sage et al., (2013). Upon thrombin stimulation the IP<sub>3</sub> receptors are activated and cause  $\text{Ca}^{2+}$  release from dense tubular system. Nanojunctions have restricted  $\text{Ca}^{2+}$  diffusion due to its geometrical structure in nanometer scale. Additionally, the cytosol is equipped with a high  $\text{Ca}^{2+}$  buffering capacity that reduces the  $\text{Ca}^{2+}$  diffusion therefore  $\text{Ca}^{2+}$  released from the dense tubular system is unable to diffuse effectively from the membrane complex to the bulk cytosol. Instead the  $\text{Ca}^{2+}$  is removed from this nanodomain by the NCX working in forward mode activity, thereby transporting it into the pericellular region within the open canalicular system. The elevated pericellular  $\text{Ca}^{2+}$  concentration cause the  $\text{Ca}^{2+}$  to recycle back into the bulk cytosol down its concentration gradient through  $\text{Ca}^{2+}$ -permeable ion channels. cause a dense granule secretion that in turn would create a rise in the bulk  $[\text{Ca}^{2+}]_{\text{cyt}}$ .

of megakaryocytic cells cultured from human CD34<sup>+</sup> cells, and examine whether this can be modulated by culture in the presence of calcitriol. These will provide an initial assessment of whether NCX may participate in a similar pericellular Ca<sup>2+</sup> recycling system in human megakaryocytes.

### **1.5 Aims of the current project**

Previous work in our lab has hypothesised that platelets release Ca<sup>2+</sup> from their intracellular stores into a specialised cytosolic nanodomain which is closely apposed to the NCX in the OCS membrane (Sage *et al.*, 2013; Walford *et al.*, 2015). In this study we aimed to begin to test this hypothesis and thereby provide the first experimental evidence for the presence of an NCX-associated cytosolic nanodomain in human platelets. In addition we also aimed to assess the role this cytosolic nanodomain plays in regulating Ca<sup>2+</sup>-dependent changes in platelet function.

Due to the difficulty in imaging and genetically-interfering with the membrane complex in human platelets, there is also currently a need to find a model system in which to try to study this cellular architecture. Due to the close similarity of the proteins and structures found in human platelets and megakaryocytes, we hypothesised that CD34<sup>+</sup> may use the NCX to control agonist-evoked Ca<sup>2+</sup> signalling in a similar manner to human platelets. The aim of this would be to provide initial evidence for a pericellular Ca<sup>2+</sup> recycling system similar to that found in the platelet in these cells, such that it would be possible to use CD34<sup>+</sup>-cultured human megakaryocytes as a model system in which to study the platelet MC in the future.

## **2. Materials and Methods**

### **2.1 Materials**

Calcitriol, Hoechst 33342, Fura-2/AM and SBFI/AM were obtained from Cambridge Biosciences (Cambridge, UK). Thrombin was from Merck Chemicals (Nottingham, UK). Fluo-4 K<sup>+</sup> salt was from Invitrogen (Paisley, UK). KB-R7943, SN-6, Cytochalasin D, Nicergoline and Y-27632 were from Tocris Bioscience (Bristol, UK). Apyrase, Methyl- $\beta$ -cyclodextrin, DNase I, 5-5'-Dimethyl-BAPTA/AM, 2-APB, ML-7 and Poly-L-Lysine solution were from Sigma Aldrich (Gillingham, UK). Human CD34<sup>+</sup> cells from bone marrow were obtained from Lonza (Blackley, UK), Serum-Free Expansion Medium II (SFEM II) was from StemCell Technologies (Cambridge, UK). Fetal calf Serum was from Labtech International Ltd. (Lichfield, UK) Interleukin-6 (IL-6), Interleukin-9 (IL-9), Stem cell factor (SCF) and Thrombopoietin (TPO) were from Peprotech Inc. (Hamburg Germany). Primary - Goat NCX3 (C-15) antibody was from Insight Biotechnology (Wembley, UK), Secondary - Preabsorbed Alexa Fluor555-conjugated Donkey anti-goat antibody from Abcam (Cambridge, UK), Sheep anti-mouse IgG HRP conjugated antibody GE Healthcare (Little Chalfont, UK). Nunc 8-well chambered cover slides were obtained from R+D systems (Rochester, NY). All other reagents were of analytical grade.

### **2.2 Methods for human platelet studies**

#### **2.2.1 Human Platelet Preparation**

This study was approved by Keele University Research Ethics Committee. Healthy, drug free volunteers donated blood after giving written informed consent. Blood was collected via venepuncture and mixed with one-sixth volume of acid citrate dextrose

anticoagulant (ACD; 85 mmol L<sup>-1</sup> sodium citrate, 78 mmol L<sup>-1</sup> citric acid, and 111 mmol L<sup>-1</sup> glucose). This blood was then subjected to centrifugation for 8 min at 700g. Platelet rich plasma (PRP) was then collected from above the buffy coat and immediately treated with 100 µmol.L<sup>-1</sup> aspirin and 0.1 U.mL<sup>-1</sup> apyrase.

### **2.2.2 Monitoring Cytosolic Ca<sup>2+</sup> concentration ([Ca<sup>2+</sup>]<sub>cyt</sub>) in washed platelet suspensions**

Fura-2/AM was added to PRP to a final concentration of 2.5 µmol.L<sup>-1</sup> and then incubated for 45 min at 37°C. Washed platelets were extracted by centrifugation of platelet rich plasma PRP at 350g for 20 min, and the platelet pellet was subsequently resuspended in HEPES-buffered saline (HBS; 145 mmol.L<sup>-1</sup> NaCl, 5 mmol.L<sup>-1</sup> KCl, 1-mmol.L<sup>-1</sup> MgSO<sub>4</sub>, 10 mmol.L<sup>-1</sup> HEPES (N-2-hydroxyethylpiperazine-N'-2ethanesulfonic acid), 5 mmol L<sup>-1</sup> KCl, 1 mmol L<sup>-1</sup> MgSO<sub>4</sub>, pH 7.45) which was supplemented on the day with 10 mmol.L<sup>-1</sup> D-glucose, 0.1% [w/v] bovine serum albumin (BSA), 200 µmol.L<sup>-1</sup> CaCl<sub>2</sub> and 0.1 U.mL<sup>-1</sup> apyrase (supplemented HBS). Fluorescence was recorded from these 1.2 mL magnetically-stirred aliquots of platelet suspension at 37°C using a Cairn Research spectrophotometer (Cairn Research, Faversham, U.K.) with excitation wavelengths set at 340 and 380 nm, and emission wavelengths recorded between 470-550 nm. All [Ca<sup>2+</sup>]<sub>cyt</sub> changes were monitored using the 340/380 nm fluorescence ratio, and calibrated according to the method of Grynkiewicz *et al.*, (1985). Thrombin-evoked changes in [Ca<sup>2+</sup>]<sub>cyt</sub> were quantified by the integration of the change in fluorescence records from basal with respect to time for 3.5 minutes after thrombin addition.

### 2.2.3 Monitoring cytosolic Na<sup>+</sup> concentration ([Na<sup>+</sup>]<sub>cyt</sub>) in washed platelet suspensions

PRP was subjected to centrifugation at 350 g for 20 min, and platelet pellets were resuspended in HBS supplemented with 10 mmol.L<sup>-1</sup> D-glucose, 200 µmol.L<sup>-1</sup> CaCl<sub>2</sub> and 0.1 U.mL<sup>-1</sup> apyrase (BSA-free supplemented HBS). The SBFI/AM stock was prepared by mixing 10% pluronic F-127 dissolved in dimethylsulfoxide (DMSO) resulting in a 5 mmol.L<sup>-1</sup> stock solution. This was then added to washed platelets to give a final concentration of 10 µmol.L<sup>-1</sup>, and incubated for 45 min at 37°C. After this incubation, 10% [v/v] ACD was added to the washed platelets prior to centrifugation at 6000 g for 1 min. The platelet pellet was then resuspended in supplemented HBS to a final density of 2x10<sup>8</sup> cells.mL<sup>-1</sup> and SBFI fluorescence was measured using a Cairn Research spectrophotometer as stated for Fura-2 above. Agonist-evoked changes in [Na<sup>+</sup>]<sub>cyt</sub> were monitored using the SBFI 340/380 nm fluorescence ratio. Since previous studies have already described a small quenching effect of KB-R7943 on SBFI (Harper & Sage, 2007), the fluorescence ratios were normalised to a percentage of the maximum fluorescence. This was done by comparison of the recorded value to the basal fluorescence (F<sub>0</sub>) recorded prior to thrombin addition and a maximum fluorescence value obtained after treatment with each sample with 50-µmol.L<sup>-1</sup> gramicidin at the end of each run (F<sub>max</sub>), using the following equation:

$$\% \text{ Maximum fluorescence} = 100 \times \left( \frac{F - F_0}{F_{max} - F_0} \right)$$

Thrombin-evoked changes in [Na<sup>+</sup>]<sub>cyt</sub> were quantified by the integration of the change of the records of percentage maximum fluorescence from basal with respect to time for 3.5 minutes after thrombin addition.

#### **2.2.4 Monitoring extracellular $\text{Ca}^{2+}$ concentration in washed platelet suspensions ( $[\text{Ca}^{2+}]_{\text{ext}}$ )**

Immediately prior to the start of the experiment, Fluo-4  $\text{K}^+$  salt was added to 1.2 mL aliquots of washed human platelets to a final concentration of  $2.5 \mu\text{mol.L}^{-1}$   $[\text{Ca}^{2+}]_{\text{ext}}$  was monitored under constant magnetic stirring at  $37^\circ\text{C}$  using a Cairn Research Spectrophotometer with the excitation wavelength set at 480 nm, and emission wavelengths collected between 500-550 nm. Thrombin-evoked changes in  $[\text{Ca}^{2+}]_{\text{ext}}$  were quantified by the integration of the change in fluorescence records from basal with respect to time for 3.5 minutes after thrombin addition.

#### **2.2.5 Imaging of agonist-evoked changes in $[\text{Ca}^{2+}]_{\text{ext}}$ in single human platelets**

$\text{Ca}^{2+}$  removal into the pericellular region of individual platelets was monitored in washed platelet suspensions to which Fluo-4  $\text{K}^+$  salt had been added. Washed platelets were collected by centrifugation of PRP at 350 g for 20 min and resuspended in supplemented HBS at a density of  $2 \times 10^8$  cells.  $\text{mL}^{-1}$ . Washed platelets were then treated with a variety of compounds, before being allowed to settle for 5 min at room temperature on poly-L-lysine-coated Nunc chambered cover slides. Excess cell suspension was removed and replaced with supplemented HBS to which  $1 \text{ mmol.L}^{-1}$  EGTA and  $5 \mu\text{mol.L}^{-1}$  Fluo-4  $\text{K}^+$  salt was added. Transmitted light and fluorescent images were recorded using a Fluoview FV 1200 laser scanning confocal microscope (Olympus, UK) with a 60x oil immersion objective using a  $100\text{-}\mu\text{m}$  confocal aperture. Fluorescence images were recorded at a frequency of 0.5 Hz for 5 min using an excitation wavelength of 473 nm and collecting emitted light between 520-560 nm.

### **2.2.6 Immunofluorescent imaging of NCX3 in single platelets**

Unstimulated, washed human platelet suspensions were treated with either 100- $\mu\text{mol.L}^{-1}$  nicergoline or an equal volume of its vehicle, DMSO, for 10 min at 37°C under continuous magnetic stirring. Treated platelets were then fixed by addition of 3% [w/v] formaldehyde and stored at 4°C until use. Fixed platelets were washed by centrifugation in minifuge at 6000 g for 1 min and resuspended in HBS containing a 1:1000 dilution of Horseradish Peroxidase-conjugated Sheep anti-mouse secondary antibody and 5 mg.mL<sup>-1</sup> BSA and incubated for 30 min at room temperature to block non-specific antibody binding sites. Cells were recollected by centrifugation platelets resuspended in HBS containing a 1:25 dilution of goat NCX3 antibody and 5mg.mL<sup>-1</sup> BSA. Antibodies were incubated at room temperature for 30 min. Cells were recollected by centrifugation and resuspended in HBS containing a 1:1000 dilution of pre-absorbed Alexa Fluor 555-conjugated Donkey anti-goat antibody and 5mg.mL<sup>-1</sup> BSA. The platelet were incubated with this fluorophore-conjugated secondary antibody at room temperature for 30 min. Cells were recollected one last time by centrifugation and resuspended in HBS containing 5 mg.mL<sup>-1</sup> BSA. Labelled cells were loaded onto poly-L-lysine-coated Nunc Chambered cover slides and allowed to adhere to the surface for 10 min at room temperature. Platelet suspension was then removed and slides were washed with HBS containing 5 mg.mL<sup>-1</sup> BSA. Fluorescent images were captured using a Fluoview FV1200 laser scanning confocal microscope (Olympus, UK) with a PLAPON 100x oil immersion objective. Images were recorded at a frequency of 0.5 Hz for 5 min with excitation at 473 nm and emission light at 520-560 nm were collected.

### **2.2.7 Monitoring platelet shape change using light transmission aggregometry**

Washed platelets were collected by centrifugation of PRP at 350 *g* for 20 min and resuspended in supplemented HBS. Cells were pre incubated with their assigned treatments under magnetic stirring at 37°C. Treated cells had external Ca<sup>2+</sup> chelated by addition of 1 mmol.L<sup>-1</sup> EGTA, and 450 µL was then transferred into aggregometer cuvettes (Kartell, Italy). Readings were taken under continuous magnetic stirring at 37°C using a 2 channel Chronolog light transmission aggregometer (Labmedics, Oxfordshire, UK). Readings were made against a baseline level of an aggregometer cuvette containing supplemented HBS.

## **2.3 Methods used for human megakaryocyte studies**

### **2.3.1 Culturing human megakaryocytes from human CD34<sup>+</sup> cells**

Human CD34<sup>+</sup> cells were resuscitated from liquid nitrogen following the manufacturer's instruction. Liquid cultures were set-up by plating CD34<sup>+</sup> cells in 24-well plates at a density of 2x10<sup>4</sup> cells.mL<sup>-1</sup> in SFEMII medium (Stem cell Technologies) containing 30-50ng.mL<sup>-1</sup> TPO, 1 ng.mL<sup>-1</sup> SCF, 7.5-20 ng.mL<sup>-1</sup> IL-6 and 13.5ng.mL<sup>-1</sup> IL-9. Cells were cultured in a humidified environment containing 5% CO<sub>2</sub> and O<sub>2</sub>. On day 2 and day 5 cultures were gently mixed and supplemented with fresh SFEMII containing the same cytokine cocktail as described above. Cells were used in experiments between day 7 and day 9 of the culture in line with previous studies demonstrating CD34<sup>+</sup> cell maturation into human megakaryocytic cell lineages (Dr A. Al-Ghannam and Dr A.G.S. Harper, personal communication).

### **2.3.2 Single cell imaging of morphological changes in CD34<sup>+</sup>-cultured human megakaryocytes:**

On day 7 megakaryocytes cultures were supplemented with 0.1 U.mL<sup>-1</sup> apyrase and incubated with 1 μmol.L<sup>-1</sup> Fluo-5N/AM, for 2 hours and 5 μg.ml L<sup>-1</sup> Hoechst 33342 for 1 hour at 37°C. Cells were then recollected by centrifugation at 6000 g for 1 min and finally resuspended in supplemented HBS to a cell density of 5x10<sup>4</sup> cells.mL<sup>-1</sup>. Cells were then allowed to adhere to poly-L-lysine-coated Nunc chambered cover slides for 30 min prior to imaging in the presence of 5 μmol.L<sup>-1</sup> Rhod-5N K<sup>+</sup> salt. Fluorescent images were captured using a Fluoview FV1200 laser scanning confocal microscope (Olympus, UK) with a PLAPON 100x oil immersion objective. Images were recorded at a frequency of 0.5 Hz for 5 min with excitation at 473 nm and emission light at 520-590 nm were collected. The mean Fluo-5N and Rhod-5N fluorescence levels of all the cells scanned in the field were compared between control and treated conditions for both dyes. The emission wavelength of (BA 490-525 nm) and excitation wavelength of (473 nm) were collected for Fluo-5N and emission wavelength of (BA 560-620 nm) and excitation wavelength of (543 nm) were collected for Rhod -5N accordingly.

### **2.3.3 Monitoring [Ca<sup>2+</sup>]<sub>cyt</sub> from CD34<sup>+</sup>-cultured human megakaryocytes**

Experiments were performed from cells taken after 7-9 days of culture. Cells were loaded with 2.5 μmol.L<sup>-1</sup> Fura 2/AM in the presence of 0.1 U.mL<sup>-1</sup> apyrase for 1 h at 37°C. By centrifugation 8400 g for 1 min and resuspended in supplemented HBS to a final cell density of 5x10<sup>4</sup> cells.mL<sup>-1</sup>. Cells were treated with 50μmol.L<sup>-1</sup> KB-R7943, SN-6 or an equivalent volume of DMSO under continuous magnetic stirring for 10 min at 37°C. 100 μL aliquots of each sample were transferred into 96-well plates and the extracellular Ca<sup>2+</sup> was either increased to a final concentration of 1 mM, or removed

by chelation by addition of 1 mM EGTA. Fluorescence was then recorded using a BioTek Synergy 2 microplate reader using a 360 nm excitation wavelength filter and collected using a 440 nm emission filter. The recorded value to basal fluorescence, recorded before thrombin addition were compared and a maximal fluorescence value was obtained after treatment of each sample with 10% triton at the end of each run. Changes in  $[Ca^{2+}]_{cyt}$  was quantified by the incorporation of the change in fluorescence records from basal with respect to time for 5 minutes after thrombin addition.

#### **2.3.4 Monitoring $[Na^+]_{cyt}$ from CD34<sup>+</sup>-cultured human megakaryocytes**

Experiments were performed from cells taken after 7-9 days of culture. SBF1/AM was prepared by mixing 10% [w/v] pluronic F-127 dissolved in DMSO resulting in a 5-mmol.L<sup>-1</sup> stock solution. On day 9 of the culture, cells were treated with 0.1 U.mL<sup>-1</sup> apyrase and washed by centrifugation at 8400 g for 1 min. Washed cell pellets were resuspended in BSA-free supplemented HBS and SBF1 stock solution was added to give a final concentration of 10  $\mu$ mol.L<sup>-1</sup> SBF1/AM. Cells were incubated for 40 min at 37°C. Labelled CD34<sup>+</sup> cells were then washed by centrifugation at 8400 g for 1 min and resuspended in supplemented HBS to a final concentration of 5x10<sup>4</sup> cells.mL<sup>-1</sup>. Cells were treated with 50  $\mu$ mol.L<sup>-1</sup> KB-R7943, SN-6 or an equivalent volume of DMSO under continuous magnetic stirring for 10 min at 37°C. 100  $\mu$ L aliquots of each sample were transferred into 96-well plates and the extracellular Ca<sup>2+</sup> was then either increased to a final concentration of 1 mmol.L<sup>-1</sup>, or removed by chelation by addition of 1 mmol.L<sup>-1</sup> EGTA. Fluorescence was then recorded using a BioTek Synergy 2 microplate reader using a 360 nm excitation wavelength filter and collected using a 440 nm emission filter. The fluorescence ratios were normalised to a percentage of

the maximum fluorescence by comparison of the basal fluorescence ( $F_0$ ) values recorded prior to thrombin addition. Following this a maximum fluorescence value was obtained after treatment with each sample with  $50 \mu\text{mol.L}^{-1}$  gramicidin at the end of each run ( $F_{\text{max}}$ ), using the following equation:

$$\% \text{ Maximum fluorescence} = 100 \times \left( \frac{F - F_0}{F_{\text{max}} - F_0} \right)$$

Changes in  $[\text{Na}^+]_{\text{cyt}}$  was quantified by the integration of the change of the records of percentage maximum fluorescence from basal with respect to time for 5 minutes after thrombin addition.

### **2.3.5 Fixed Cell Imaging of NCX3 antibody in single Megakaryocyte demarcation membrane system.**

Megakaryocytes samples from day 7 of the culture were fixed by addition of 3% [w/v] formaldehyde and stored at  $4^\circ\text{C}$  until use. Megakaryocytes were washed by centrifugation at  $8400 g$  for 1 min and resuspended in a blocking solution made up of HBS containing 1:1000 dilution of mouse IgG secondary antibody and  $5 \text{ mg.mL}^{-1}$  BSA and incubated for 30 min at room temperature. Cells were washed again by centrifugation at  $8400 g$  for 1 min and resuspended in HBS containing a 1:25 dilution of goat NCX3 antibody stock and  $5 \text{ mg.mL}^{-1}$  BSA and incubated at room temperature for 30 min. Cells were recollected by centrifugation at  $8400 g$  for 1 min and resuspended in HBS containing a 1:1000 dilution of Alexa Fluor 555-conjugated Donkey anti-goat antibody and  $5 \text{ mg.mL}^{-1}$  BSA and incubated at room temperature for 30 min. Cells were recollected again by centrifugation at  $8400 g$  for 1 min and finally resuspended in HBS containing  $5 \text{ mg.mL}^{-1}$  BSA to a density of  $1 \times 10^5 \text{ cells.mL}^{-1}$ . Labelled megakaryocytes were transferred to the chambered cover slides and allowed

to adhere to substrate for 10 min. Megakaryocyte suspension was then removed and slides were washed with HBS containing 5 mg.mL<sup>-1</sup>. Fluorescent images were captured using a Fluoview FV 1200 laser scanning confocal microscope (Olympus, UK) with a 100x oil immersion objective. Images were recorded at a frequency of 0.5 Hz for 5 min with excitation at 473 nm and emission light at 520-590 nm was collected.

## **2.4 Statistical Comparison**

Results are reported as the mean  $\pm$  SEM of the number of independent observations (n) made. Statistical significance was assessed using either Student's paired t-test or a one way ANOVA test followed by a post hoc Tukey test was performed to calculate the statistical significance.  $P < 0.05$  was considered statistically significant.

### 3. Results

#### 3.1 Identification and characterisation of a cytosolic nanodomain in DM-BAPTA-loaded human platelets

##### 3.1.1 Thrombin-evoked rises in extracellular $\text{Ca}^{2+}$ concentration ( $[\text{Ca}^{2+}]_{\text{ext}}$ ) can be observed in the absence of any detectable rise in cytosolic $\text{Ca}^{2+}$ concentration ( $[\text{Ca}^{2+}]_{\text{cyt}}$ ) in human platelets.

Previously our lab has presented a pericellular recycling hypothesis which suggested that  $\text{Ca}^{2+}$  is released from the DTS into a cytosolic nanodomain enclosed within the confines of the MC (Sage *et al.*, 2013). This model further suggested that  $\text{Ca}^{2+}$  in the MC can then be removed into the OCS by the action of the NCX (Sage *et al.*, 2013). This work therefore predicts that platelets possess two functional cytosolic sub-compartments for  $\text{Ca}^{2+}$  signalling; the bulk cytosol and the nanodomain encompassed within the MC. To examine whether it was possible to identify such an NCX-associated cytosolic nanodomain in human platelets, we have examined the  $\text{Ca}^{2+}$  responses of platelets loaded with Dimethyl BAPTA (DM-BAPTA). DM-BAPTA is, a fast  $\text{Ca}^{2+}$  chelator whose high  $\text{Ca}^{2+}$  affinity and rapid on-rate of binding can efficiently completely buffer  $\text{Ca}^{2+}$  rises in the bulk cytosol. However due to its inability to instantaneously bind  $\text{Ca}^{2+}$ , this divalent cation is still able to diffuse around 20 nm before it is efficiently buffered by this chelator. Therefore, DM-BAPTA is unable to buffer  $\text{Ca}^{2+}$  within around 20 nm of the  $\text{Ca}^{2+}$  channel pore (Parekh, 2008; Neher & Almers, 1986; FIG 3.1). This is around the same distance found between the membranes in other cell types (van Breemen *et al.*, 2013), including the MC of platelets (van Nispen tot Pannerden *et al.*, 2010). DM-BAPTA-loading will thus buffer  $\text{Ca}^{2+}$  rises in the bulk cytosol, but not within the cytosolic nanodomains contained within any present nanojunction. Therefore, if  $\text{Ca}^{2+}$  is released from the DTS into a restricted cytosolic nanodomain within the MC,

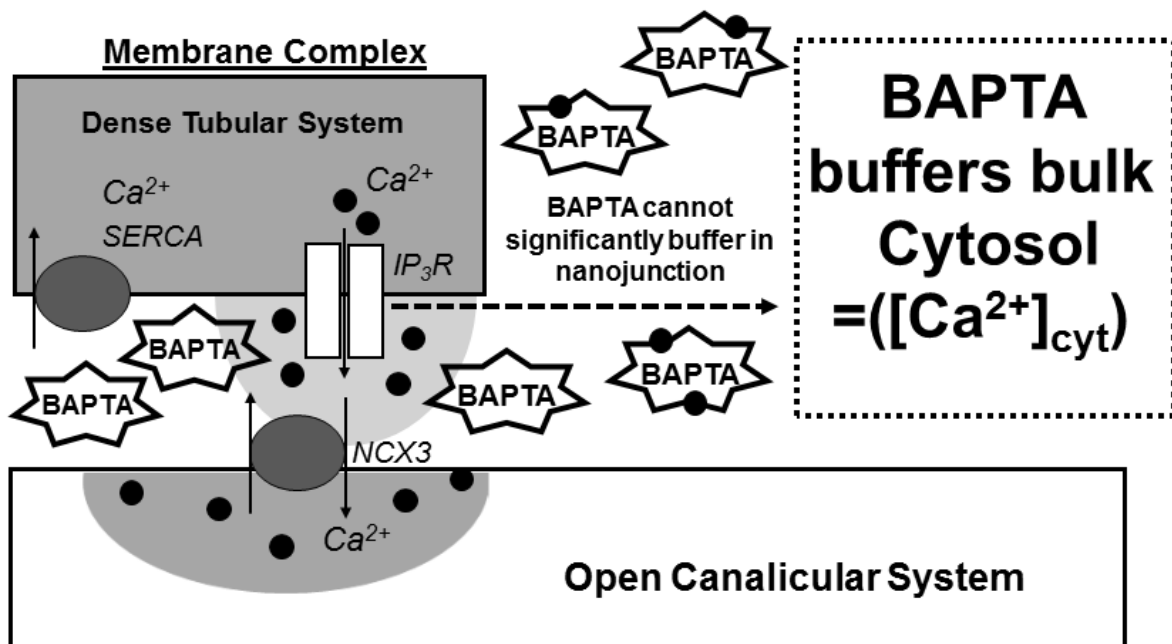


**Fig 3.1 A model of how DM-BAPTA- regulates spatial spread of  $\text{Ca}^{2+}$  from microdomain**  
*In DM-BAPTA-loaded cells, the thrombin-evoked rise in bulk  $[\text{Ca}^{2+}]_{\text{cyt}}$  is prevented. But  $\text{Ca}^{2+}$  entry or release into nanojunction could occur reasonably unaffected. The presence of NCX in the open canalicular system functions in forward mode direction extruding  $\text{Ca}^{2+}$  release from DTS into the pericellular region creating pericellular  $\text{Ca}^{2+}$  hotspot. DM-BAPTA is a fast  $\text{Ca}^{2+}$  chelator whose high  $\text{Ca}^{2+}$  affinity and rapid on-rate binding efficiently buffers  $\text{Ca}^{2+}$  rise in bulk cytosol. Very close to the microdomain it is unable to immediately bind  $\text{Ca}^{2+}$  within around 20 nm of its point of entry but could restrict the spatial spread of  $\text{Ca}^{2+}$  signals determined by its on-rate. (Parekh, 2008).*

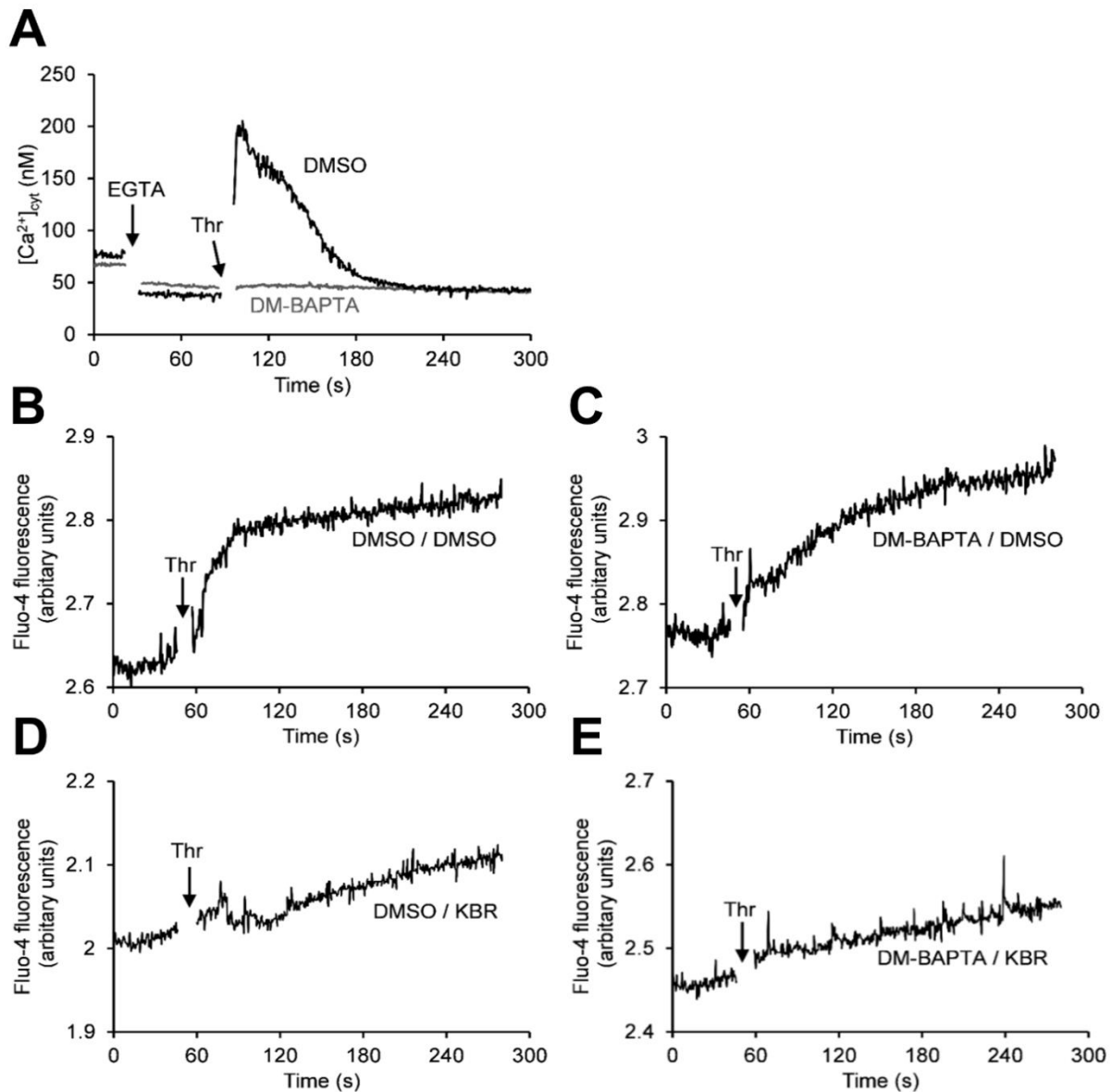


**Figure 3.2** Thrombin-evoked rises in  $[Ca^{2+}]_{ext}$  can be observed in the absence of any detectable rise in  $[Ca^{2+}]_{cyt}$  in human platelets. (A) Fura-2-loaded human platelets suspended in supplemented HBS were pre incubated with either  $30 \mu\text{mol.L}^{-1}$  dimethyl-BAPTA/AM, or an equivalent volume of its vehicle, DMSO, for 10 min at  $37^\circ\text{C}$ . Extracellular  $Ca^{2+}$  was then chelated with  $1 \text{mmol.L}^{-1}$  EGTA and then 1 min later stimulated with  $0.5 \text{U.mL}^{-1}$  thrombin. (B-D) Washed human platelets suspended in supplemented HBS were pre-treated with  $30 \mu\text{mol.L}^{-1}$  dimethyl-BAPTA/AM (C,E), or an equivalent volume of its vehicle, DMSO (B,D), for 10 min at  $37^\circ\text{C}$ . Cells were also treated with either  $50 \mu\text{mol.L}^{-1}$  KB-R7943 (D,E), or an equivalent volume of its vehicle, DMSO (B,C), for the last 5 min of this incubation. A final concentration of  $2.5 \mu\text{mol.L}^{-1}$  Fluo-4 salt was then added immediately before the experiment. Extracellular  $Ca^{2+}$  was then chelated with  $1 \text{mmol.L}^{-1}$  EGTA (not shown) and then 1 min later stimulated with  $0.5 \text{U.mL}^{-1}$  thrombin.

where it is removed by the NCX, the presence of DM-BAPTA-loading should not significantly prevent thrombin-evoked  $\text{Ca}^{2+}$  removal from the cell. Experiments were performed to examine the effect of DM-BAPTA loading on  $\text{Ca}^{2+}$  removal in thrombin-stimulated platelets. All experiments were performed in the absence of extracellular  $\text{Ca}^{2+}$  to isolate  $\text{Ca}^{2+}$  signals elicited by intracellular  $\text{Ca}^{2+}$  release from the intracellular stores, from those elicited by  $\text{Ca}^{2+}$  entry across the plasma membrane.

Previous experiment in our lab have showed that pre incubation of cells with  $30 \mu\text{mol.L}^{-1}$  DM-BAPTA/AM for 10 min at  $37^\circ\text{C}$  could prevent thrombin-evoked cytosolic  $\text{Ca}^{2+}$  rises detected in the bulk cytosol by Fura-2 (Sage *et al.*, 2013). These results were confirmed in positive control experiments on each donor, with DM-BAPTA-loading abolishing any notable rise in  $[\text{Ca}^{2+}]_{\text{cyt}}$  when platelets were stimulated with thrombin in the absence of extracellular  $\text{Ca}^{2+}$  ( $1.0 \pm 0.6$  % of control;  $n = 4$ ;  $P < 0.05$ ; Fig 3.2A). But even in the absence of any observable thrombin-evoked rise in  $[\text{Ca}^{2+}]_{\text{cyt}}$ , it was still possible to see a rise in  $[\text{Ca}^{2+}]_{\text{ext}}$ , although it occurs slower than in control cells ( $69.7\% \pm 10.5\%$  of untreated controls;  $n = 7$ ;  $P < 0.05$ ; Fig 3.2B,C). This is consistent with our previous finding that DM-BAPTA-loading slows thrombin-evoked  $\text{Ca}^{2+}$  release, suggesting that this prevents calcium-induced calcium release (Sage *et al.*, 2013). These results therefore suggest that  $\text{Ca}^{2+}$  release from intracellular stores principally occurs into a nanodomain of cytosol which is unaffected by DM-BAPTA-loading and too small to be detected by Fura-2.

The pericellular recycling hypothesis also suggested that  $\text{Ca}^{2+}$  removal from this nanodomain would be dependent on activity of the NCX. Therefore, experiments were also simultaneously performed to examine the effect of pre incubating platelets with the NCX inhibitor, KB-R7943. Previous work in our labs have demonstrated that this

compound is able to significantly inhibit forward-mode exchange in human platelets in a manner which does not directly blocking  $\text{Ca}^{2+}$  permeable ion channels in the plasma membrane or intracellular stores (Sage *et al.*, 2013). Pre-treatment with KB-R7943, reduced the thrombin-evoked rises in  $[\text{Ca}^{2+}]_{\text{ext}}$  in cells not treated with DM-BAPTA to  $37.5\% \pm 3.3\%$  of control ( $n = 7$ ,  $P < 0.05$ , Fig 3.2B,D), in line with our previous findings (Sage *et al.*, 2013). Similarly pre-treatment with KB-R7943 elicited a significant reduction in thrombin evoked rise in  $[\text{Ca}^{2+}]_{\text{ext}}$  in DM-BAPTA-loaded cells ( $35.4\% \pm 7.7\%$  of control;  $n = 7$ ;  $P < 0.05$ ; Fig 3.2C,E). These data demonstrate that  $\text{Ca}^{2+}$  removal from the cytosolic nanodomain is largely blocked by treatment with NCX inhibitor.

To further these findings, additional experiments were performed to examine the effect of KB-R7943 on thrombin-evoked rises in  $[\text{Na}^+]_{\text{cyt}}$ . If NCX-mediated  $\text{Ca}^{2+}$  removal is blocked, then KB-R7943 should reduce thrombin-evoked rises in  $\text{Na}^+$  due to the influx of  $\text{Na}^+$  brought in on this exchanger. In line with this model, KB-R7943-pretreatment was able to significantly inhibit thrombin-evoked rises in  $[\text{Na}^+]_{\text{cyt}}$  in DM-BAPTA-loaded platelets ( $28.6 \pm 10.1\%$  of control;  $n = 6$ ;  $P < 0.05$ ; Fig 3.3). Thus suggesting that  $\text{Ca}^{2+}$  removal is elicited from the cytosolic nanodomain by forward mode activity of the NCX, as previous suggested by our earlier studies (Harper *et al.*, 2009; Sage *et al.*, 2013).

These results support our hypothesis that  $\text{Ca}^{2+}$  release initially accumulates within an NCX-associated cytosolic nanodomain that is functionally restricted from the bulk platelet cytosol.

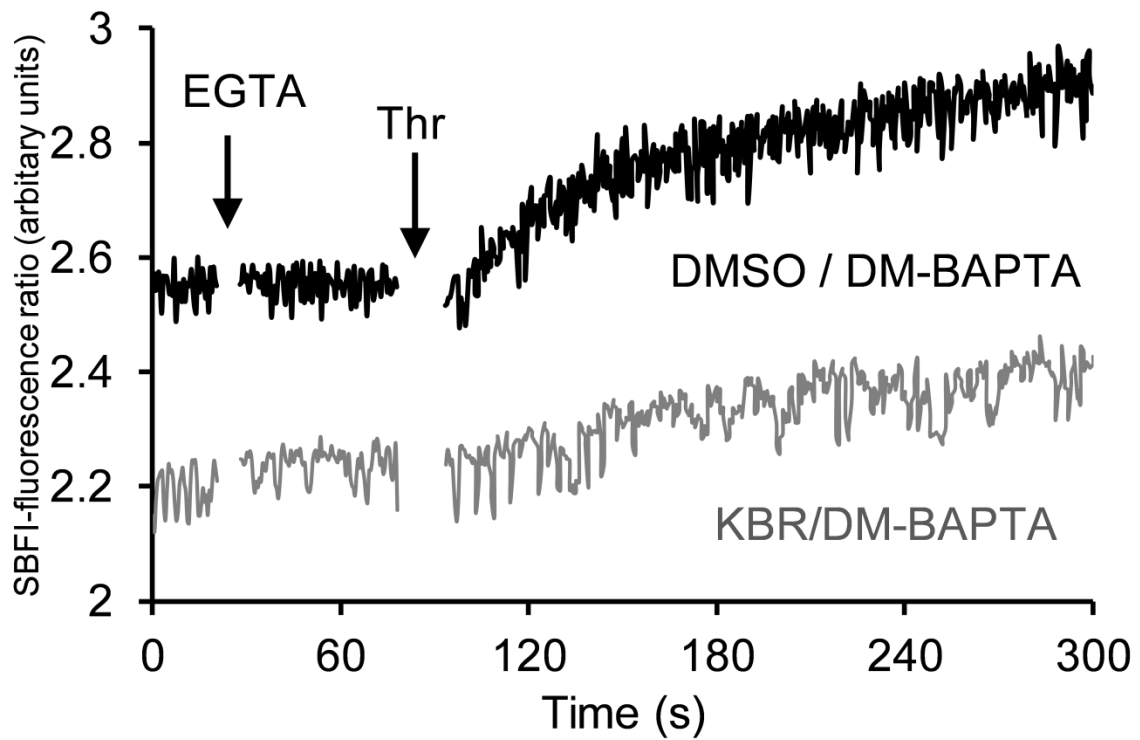


**Figure 3.3** Thrombin-evoked rises in  $[Na^+]_{cyt}$  are inhibited by pretreatment with KB-R7943 in DM-BAPTA-loaded human platelets. SBF1-loaded human platelets suspended in supplemented HBS were preincubated with  $30 \mu\text{mol.L}^{-1}$  dimethyl-BAPTA/AM for 10 min at  $37^\circ\text{C}$ . Cells were also treated with either  $50 \mu\text{mol.L}^{-1}$  KB-R7943, or an equivalent volume of its vehicle, DMSO for the last 5 min of this incubation. Extracellular  $Ca^{2+}$  was then chelated with  $1 \text{mmol.L}^{-1}$  EGTA and then 1 min later stimulated with  $0.5 \text{U.mL}^{-1}$  thrombin.

### **3.2 Nicergoline-induced disruption of the subcellular localisation of the DTS inhibits thrombin-evoked rises in $[Ca^{2+}]_{ext}$ and $[Na^+]_{cyt}$ in DM-BAPTA-loaded platelets.**

Recently we have demonstrated that pre-treatment of nicergoline disrupts pericellular  $Ca^{2+}$  accumulation through triggering a microtubule-dependent reorganisation of the DTS (Walford *et al.*, 2015). If the cytosolic nanodomain in which  $Ca^{2+}$  release from the DTS is tightly coupled to NCX-mediated removal is contained within the MC, then nicergoline-induced disorganisation of the DTS should be expected to inhibit the thrombin-evoked rise in  $[Ca^{2+}]_{ext}$  in DM-BAPTA-loaded cells, as the stores are further away from the NCX such that  $Ca^{2+}$  can be buffered by DM-BAPTA before reaching the plasma membrane. Experiments were therefore performed to examine whether nicergoline-induced disruption of the DTS is able to affect thrombin-evoked rises in  $[Ca^{2+}]_{ext}$ . Dimethyl-BAPTA loading prevented thrombin-evoked rise elicited in the absence of extracellular  $Ca^{2+}$  signals to  $(3.8 \pm 1.6 \%$  of control;  $n = 4$ ;  $P < 0.05$ ; Fig 3.4A). Pre-treatment with nicergoline significantly inhibited thrombin-evoked rises in  $[Ca^{2+}]_{ext}$  in cells from the same donors to  $51.0 \pm 19.6 \%$  of control ( $n = 9$ ;  $P < 0.05$ ; Fig 3.4B,C).

If nicergoline-induced DTS reorganisation removes the resident  $IP_3R$  away from the vicinity of the NCX in the plasma membrane, then nicergoline should also block the NCX-mediated thrombin-evoked rises in  $[Na^+]_{cyt}$  elicited by forward mode exchange in DM-BAPTA-loaded platelets. Experiments demonstrated that nicergoline pre-treatment blocked thrombin-evoked rises in  $[Na^+]_{cyt}$  in DM-BAPTA-loaded platelets stimulated in the absence of extracellular  $Ca^{2+}$  to  $43.1 \pm 14.1 \%$  of control ( $n = 6$ ;  $P < 0.05$ ; Fig 3.5), in line with our proposed mechanism of action of nicergoline whereby it spatially decouples these  $Ca^{2+}$  transporting proteins in the cytosolic nanodomain.

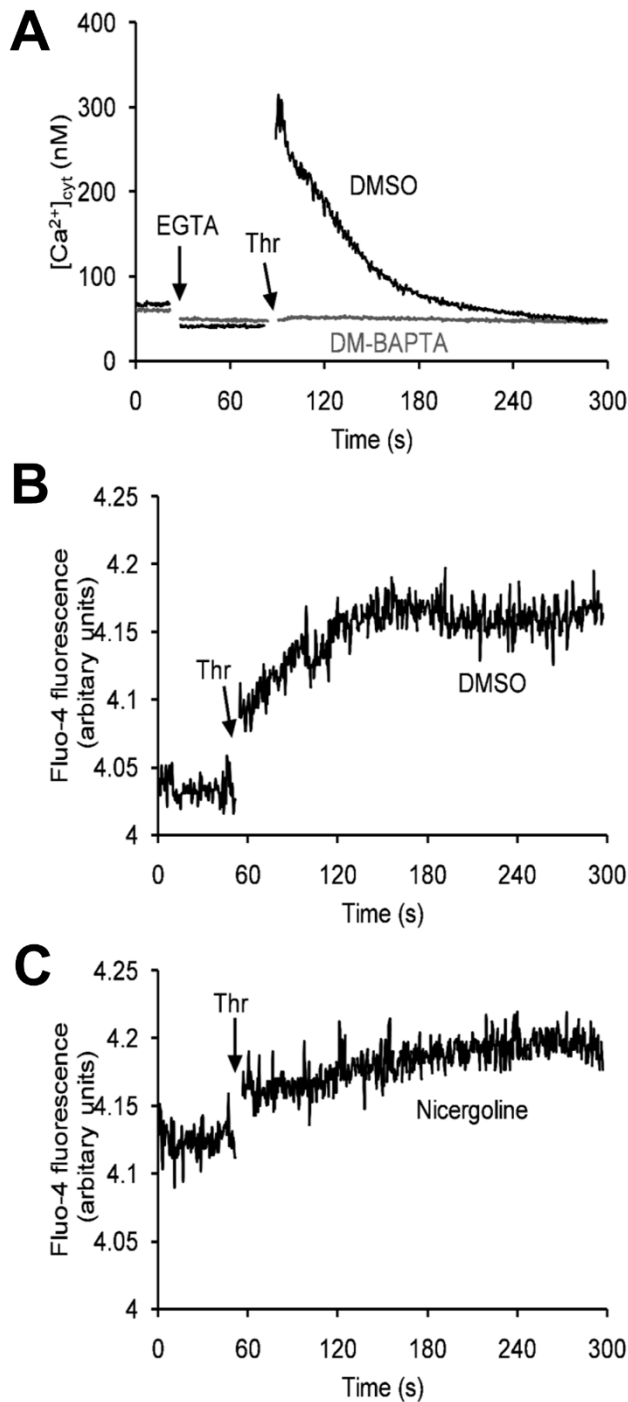


**Figure 3.4 Nicergoline-induced disruption of the subcellular localisation of the DTS inhibits thrombin-evoked rises in  $[Ca^{2+}]_{ext}$  in DM-BAPTA-loaded platelets.** (A) Fura-2-loaded human platelets suspended in supplemented HBS were preincubated with either  $30 \mu\text{mol.L}^{-1}$  dimethyl-BAPTA/AM, or an equivalent volume of its vehicle, DMSO, for 10 min at  $37^\circ\text{C}$ . Extracellular  $Ca^{2+}$  was then chelated with  $1 \text{mmol.L}^{-1}$  EGTA and then 1 min later stimulated with  $0.5 \text{U.mL}^{-1}$  thrombin. (B,C) Washed human platelets were suspended in supplemented HBS were pre-treated with  $30 \mu\text{mol.L}^{-1}$  dimethyl-BAPTA/AM as well as either  $100 \mu\text{mol.L}^{-1}$  nicergoline (B), or an equivalent volume of its vehicle, DMSO (C) for 10 min at  $37^\circ\text{C}$ . A final concentration of  $2.5 \mu\text{mol.L}^{-1}$  Fluo-4 salt was then added immediately before the experiment. Extracellular  $Ca^{2+}$  was then chelated with  $1 \text{mmol.L}^{-1}$  EGTA (not shown) and then 1 min later stimulated with  $0.5 \text{U.mL}^{-1}$  thrombin.

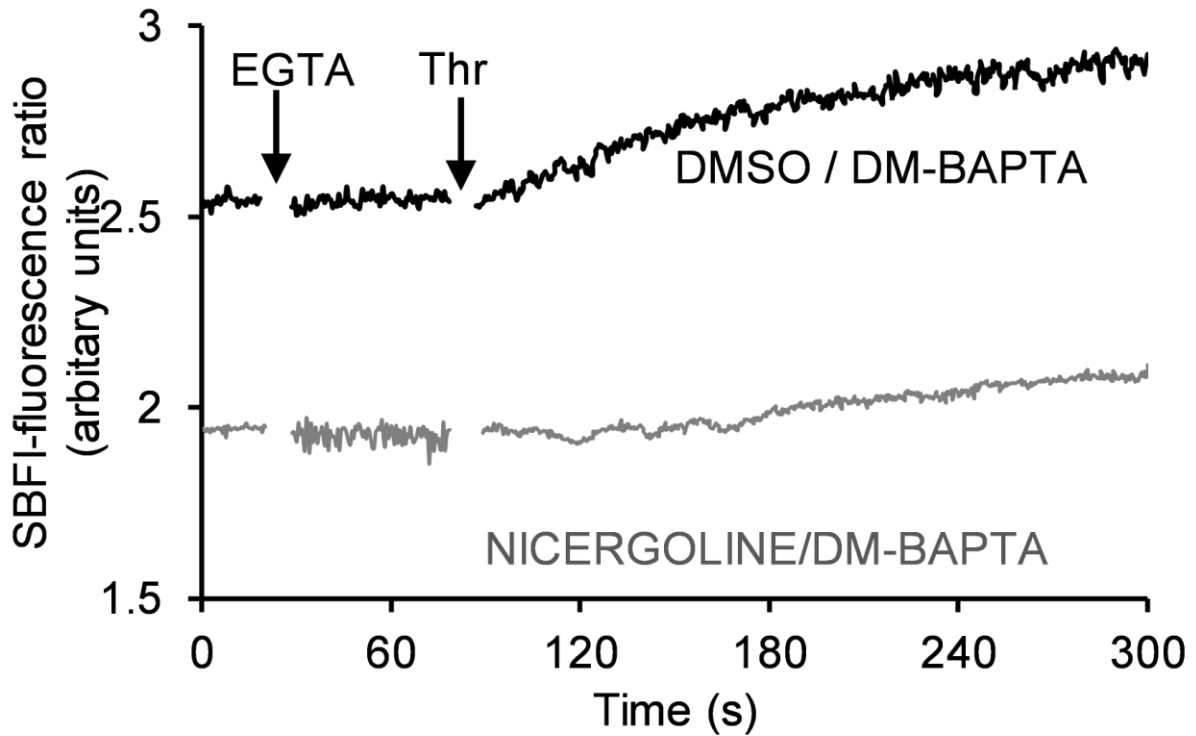


**Figure 3.5** Thrombin-evoked rises in  $[Na^+]_{cyt}$  are inhibited by pre-treatment with nicergoline in DM-BAPTA-loaded human platelets.. SBF1-loaded human platelets suspended in supplemented HBS were preincubated with  $30 \mu\text{mol.L}^{-1}$  dimethyl-BAPTA/AM and either,  $100 \mu\text{mol.L}^{-1}$  Nicergoline, or an equivalent volume of its vehicle, DMSO for 10 min at  $37^\circ\text{C}$ . Extracellular  $Ca^{2+}$  was then chelated with  $1 \text{mmol.L}^{-1}$  EGTA and then 1 min later stimulated with  $0.5 \text{U.mL}^{-1}$  thrombin.

These results show that NCX-mediated  $\text{Ca}^{2+}$  removal from the DM-BAPTA-insensitive cytosolic nanodomain is reliant on the normal positioning of the DTS. These results therefore support the hypothesis that the cytosolic nanodomain is present within the MC (Sage *et al.*, 2013; Walford *et al.*, 2016)

### **3.3 Disruption of the actin cytoskeleton does not prevent $\text{Ca}^{2+}$ removal from the cytosolic nanodomain, but instead significantly potentiates it.**

Previous studies have demonstrated a role for the platelet actin cytoskeleton in regulating platelet  $\text{Ca}^{2+}$  signalling (Bourguignon *et al.*, 1993; Ariyoshi & Salzman, 1996; Rosado *et al.*, 2000; Harper & Sage, 2006; Harper & Sage, 2007). It was thus considered whether the actin cytoskeleton may play a role in scaffolding the membrane complex and thus facilitate the  $\text{Ca}^{2+}$  removal from the platelet cytosolic nanodomain. Therefore, experiments were conducted to examine whether disruption of the actin cytoskeleton could interfere with  $\text{Ca}^{2+}$  removal from DM-BAPTA-loaded platelets. These experiments were performed using a prolonged incubation with the actin polymerisation inhibitor, cytochalasin D, which has been shown to reduce the F-actin content of platelets as well as cause the breakdown of the cortical actin ring into localised foci of F-actin (Rosado, Graves *et al.* 2000; Rosado and Sage 2000). Consistent with our previous experiments, the positive control experiments again demonstrated that pre-incubating platelets with DM-BAPTA prevented any significant thrombin-evoked rises in  $[\text{Ca}^{2+}]_{\text{cyt}}$  ( $3.8 \pm 1.7$  % of control;  $n = 4$ ;  $P < 0.05$ ; Fig 3.6A). Pre-treatment of DM-BAPTA-loaded platelets from the same donor with Cytochalasin D elicited a significant potentiation of the thrombin-evoked rise in  $[\text{Ca}^{2+}]_{\text{ext}}$  to  $156.0 \pm 19.6$  % of untreated, DM-BAPTA-loaded control cells ( $n = 12$ ;  $P < 0.05$ ; Fig 3.6B). These data suggest that the actin cytoskeleton has an inhibitory effect on thrombin-

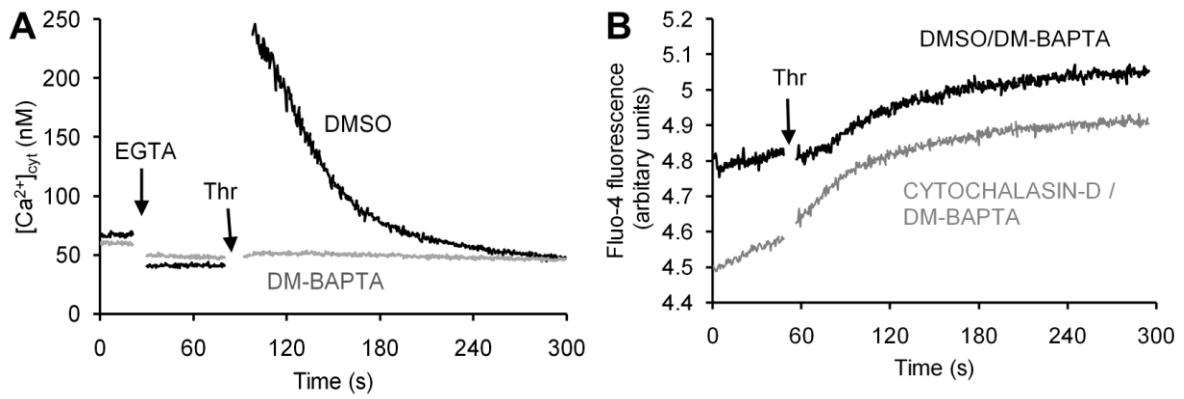


**Figure 3.6 Cytochalasin D significantly potentiates thrombin-evoked rises in  $[Ca^{2+}]_{ext}$  in DM-BAPTA-loaded human platelets.** (A) *Fura-2*-loaded human platelets suspended in supplemented HBS were preincubated with either  $30 \mu\text{mol.L}^{-1}$  dimethyl-BAPTA/AM, or an equivalent volume of its vehicle, DMSO, for 10 min at  $37^{\circ}\text{C}$ . Extracellular  $Ca^{2+}$  was then chelated with  $1 \text{mmol.L}^{-1}$  EGTA and then 1 min later stimulated with  $0.5 \text{U.mL}^{-1}$  thrombin. (B) Washed human platelets were suspended in supplemented HBS were pre-treated with either  $10 \mu\text{mol.L}^{-1}$  cytochalasin D or an equivalent volume of DMSO, for 40 min at  $37^{\circ}\text{C}$ . All cells were also pre-treated with  $30 \mu\text{mol.L}^{-1}$  dimethyl-BAPTA/AM for the final 10 min of the preincubation with cytochalasin D or DMSO. A final concentration of  $2.5 \mu\text{mol.L}^{-1}$  Fluo-4 salt was then added immediately before the experiment. Extracellular  $Ca^{2+}$  was then chelated with  $1 \text{mmol.L}^{-1}$  EGTA (not shown) and then 1 min later stimulated with  $0.5 \text{U.mL}^{-1}$  thrombin.

evoked  $\text{Ca}^{2+}$  signalling exerted within the nanodomain. These findings would be consistent with the findings of Harper & Sage (2006), who demonstrated that PAR4 was found at higher levels in the platelets treated with cytochalasin D, suggesting that they may elicit greater production of  $\text{IP}_3$  to the same dose of thrombin. These data also suggest that dynamically unstable sections of the cortical cytoskeleton are unlikely to play a role in scaffolding the membrane complex.

### **3.4 Disrupting lipid rafts inhibits thrombin-evoked rises in $[\text{Ca}^{2+}]_{\text{ext}}$ in DM-BAPTA-loaded platelets**

Cholesterol-rich lipid rafts are present in platelet membranes at physiological temperatures and combine to form microdomains that play a role in scaffolding together signalling cascades required for normal platelet activation (Gousset *et al.*, 2002). Earlier studies have from our lab demonstrated that lipid rafts play a key role in mediating thrombin-evoked rises in  $[\text{Ca}^{2+}]_{\text{cyt}}$  both in the presence and absence of extracellular  $\text{Ca}^{2+}$  (Brownlow *et al.*, 2004). This was thought to be related to its effect on the ability to facilitate coupling of  $\text{IP}_3\text{R}$  in the DTS and TRPC1 in the plasma membrane (Brownlow *et al.*, 2004), although more recent work has disproved this hypothesis (Harper & Sage, 2007). However Gousset *et al.*, (2002) and Grgurevich *et al.*, (2003) confirmed that disruption of the lipid rafts by treatment with the cholesterol sequestering compound, methyl- $\beta$ -cyclodextrin (MBCD) resulted in eversion and diminishment of the OCS (Gousset *et al.*, 2002; Grgurevich *et al.*, 2003). These data therefore suggested the possibility that lipid rafts are essential for holding together the OCS and the proteins contained here, and as such could be essential for scaffolding together the membrane complex by providing a platform for the creation of a multimolecular protein complex which holds the DTS and OCS together. Experiments

were therefore performed to examine whether lipid raft disruption prevented thrombin-evoked rises in  $[Ca^{2+}]_{cyt}$  in DM-BAPTA-loaded cells. Positive control experiments demonstrated that dimethyl-BAPTA-loaded platelets from the same donor showed no notable rise in  $[Ca^{2+}]_{cyt}$  when stimulated with thrombin ( $2.2 \pm 1.1\%$  of control;  $n = 4$ ;  $P < 0.05$ ; Fig 3.7A). When platelets were pre-treated with the lipid raft disrupting drug, MBCD, thrombin evoked rises  $[Ca^{2+}]_{ext}$  were reduced in DM-BAPTA-loaded cells to  $61.0 \pm 12.3\%$  of control ( $n = 9$ ;  $P < 0.05$ ; Fig 3.7B). These data suggested that disruption to the OCS caused by depletion of the lipid rafts disrupt  $Ca^{2+}$  removal from the cytosolic nanodomain.

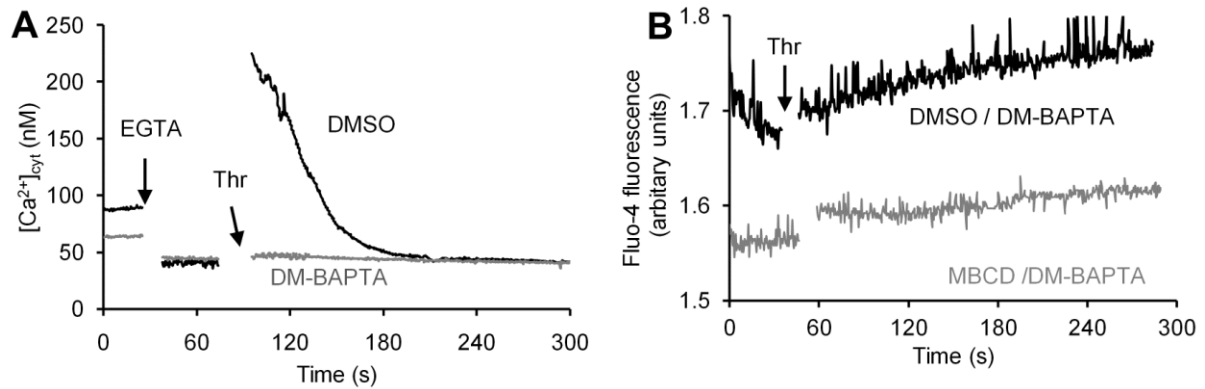


**Figure 3.7** MBCD significantly inhibits thrombin-evoked rises in  $[Ca^{2+}]_{\text{ext}}$  in DM-BAPTA-loaded human platelets. (A) *Fura-2*-loaded human platelets suspended in supplemented HBS were pre incubated with either  $30 \mu\text{mol.L}^{-1}$  dimethyl-BAPTA/AM, or an equivalent volume of its vehicle, DMSO, for 10 min at  $37^\circ\text{C}$ . Extracellular  $Ca^{2+}$  was then chelated with  $1 \text{mmol.L}^{-1}$  EGTA and then 1 min later stimulated with  $0.5 \text{U.mL}^{-1}$  thrombin. (B) Washed human platelets were suspended in supplemented HBS were pre-treated with either  $10 \text{mmol.L}^{-1}$  MBCD or an equivalent volume of DMSO, for 30 min at  $37^\circ\text{C}$ . All cells were also pre-treated with  $30 \mu\text{mol.L}^{-1}$  dimethyl-BAPTA/AM for the final 10 min of the pre incubation with MBCD or DMSO. A final concentration of  $2.5 \mu\text{mol.L}^{-1}$  Fluo-4 salt was then added immediately before the experiment. Extracellular  $Ca^{2+}$  was then chelated with  $1 \text{mmol.L}^{-1}$  EGTA (not shown) and then 1 min later stimulated with  $0.5 \text{U.mL}^{-1}$  thrombin.

### **3.5 Disruption of lipid rafts with MBCD appears to interfere with platelet Ca<sup>2+</sup> signalling by dissipating the Na<sup>+</sup> gradient across the plasma membrane.**

To further examine whether lipid raft disruption might reduce thrombin-evoked Ca<sup>2+</sup> removal in DM-BAPTA-loaded cells by interfering with the normal recruitment of the NCX to this subcellular domain in the DTS, experiments were performed to examine whether MBCD pre-treatment could interfere with forward mode NCX activity in DM-BAPTA loaded cells by examining thrombin-evoked rises in [Na<sup>+</sup>]<sub>cyt</sub> in chelated cells. After MBCD pre-treatment there was a significant increase in the basal SBFI fluorescence when compared to the DMSO-treated control (193.3 ± 5.8% of control; n = 5; *P* < 0.05; Fig 3.8A). Furthermore, treatment with either thrombin or the Na<sup>+</sup> ionophore gramicidin, at the end of the run was unable to further increase the fluorescence ratio, with the maximum fluorescence observed being 150.6 ± 12.2% of control in MBCD-treated cells (n = 5; *P* < 0.05; Fig 3.8A). As gramicidin should saturate the SBFI with Na<sup>+</sup> eliciting the same response in both treatment conditions, a greater maximum fluorescence suggests the possibility that MBCD interferes with the normal functioning of the SBFI dye

To examine if this difference was due to an auto fluorescence of the MBCD, further experiments examined the direct effect of MBCD addition on SBFI fluorescence were directly observed. As can be seen in (Fig 3.8B), addition of 10 mmol.L<sup>-1</sup> MBCD to SBFI-loaded platelets triggered a small initial rise in the fluorescence ratio, followed by a slower rise to the maximum fluorescence ratio over the course of the 30 min incubation period. Both the fast and slow responses are associated with reciprocal changes in the emissions of the dye at 340 nm and 380 nm in line with this being a

rapid increase in  $[Na^+]_{cyt}$ , rather than an artefact elicited by an auto fluorescence of the MBCD.

This was further supported by additional checks which showed that adding MBCD to a sample of HBS at a final concentration of  $10 \text{ mmol.L}^{-1}$  elicited only a marginal increase in the 340 nm and 380 nm fluorescence (data not shown). The lack of effect of MBCD on resting  $[Ca^{2+}]_{cyt}$  (Brownlow *et al.*, 2004) suggests that the effect of MBCD is selective for  $Na^+$  ions. These data therefore suggest that MBCD inhibits thrombin-evoked  $Ca^{2+}$  signalling by dissipating the  $Na^+$  gradient across the plasma membrane, and thus exerting effect on thrombin-evoked  $Ca^{2+}$  signalling through an indirect inhibition of the  $Na^+/Ca^{2+}$  exchanger. The ability of MBCD to raise basal  $Na^+$  over a long time scale as well as increase the maximal fluorescence seen after gramicidin treatment seen would suggest an effect of this drug is not on facilitating  $Na^+$  entry but preventing  $Na^+$  removal. It may be that MBCD decouples the  $Na^+/K^+$ -ATPase from  $Na^+$ -permeable channels leading to the changes in  $[Na^+]_{cyt}$  observed. However further experiments will be required to clarify this effect.

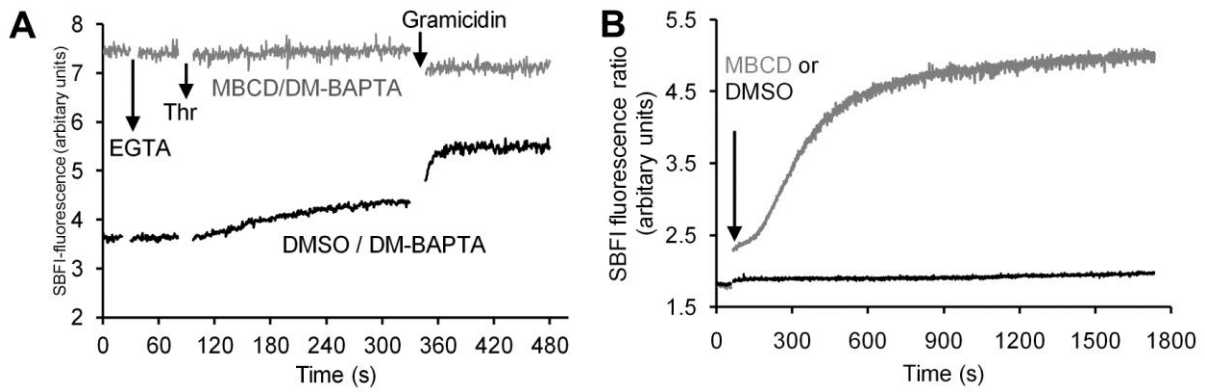


**Figure 3.8 Pre-treatment with MBCD dissipates the  $\text{Na}^+$  gradient across the plasma membrane in DM-BAPTA-loaded human platelets.** (A) SBFI-loaded human platelets suspended in supplemented HBS  $10 \text{ mmol.L}^{-1}$  MBCD or an equivalent volume of DMSO, for 30 min at  $37^\circ\text{C}$ . All cells were also pre-treated with  $30 \mu\text{mol.L}^{-1}$  dimethyl-BAPTA/AM for the final 10 min of the preincubation with MBCD or DMSO. Extracellular  $\text{Ca}^{2+}$  was then chelated with  $1 \text{ mmol.L}^{-1}$  EGTA and then 1 min later stimulated with  $0.5 \text{ U.mL}^{-1}$  thrombin. (B) SBFI-loaded human platelets suspended in supplemented HBS and pre-warmed for 10 min at  $37^\circ\text{C}$ . Cells were then exposed to either  $10 \text{ mmol.L}^{-1}$  MBCD or an equivalent volume of DMSO.

### **3.6 DM-BAPTA-loading does not prevent the production of pericellular Ca<sup>2+</sup> hotspots in thrombin-stimulated human platelets**

Previous studies have demonstrated that it is possible to observe pericellular Ca<sup>2+</sup> signals in single platelets stimulated with thrombin (Sage *et al.*, 2013; Walford *et al.*, 2016). These thrombin-evoked pericellular Ca<sup>2+</sup> rises were found to occur within the boundaries of the cell and appeared to spread away from the source in a directionally-restricted manner, consistent with their creation in the OCS. In addition, they were found to originate within a specific sub-region of the cell – which was hypothesised to be linked to the membrane complex (Sage *et al.*, 2013). If the pericellular hotspots are being created by NCX-mediated Ca<sup>2+</sup> removal from a cytosolic nanodomain enclosed within the membrane complex, then they should be resistant to DM-BAPTA-loading. Therefore, experiments were performed to examine whether pericellular Ca<sup>2+</sup> hotspots could be observed in DM-BAPTA-loaded cells, and whether any signal could be blocked by pre incubation with the NCX inhibitor, KB-R7943.

Examination of control cells showed that pericellular Ca<sup>2+</sup> hotspots could be observed in the majority of DM-BAPTA-loaded cells during the recording period after thrombin stimulation ( $66.1 \pm 5.8\%$  of cells per field;  $n = 7$ ;  $P < 0.05$ ; Fig 3.9 A, C). This is slightly lower than previous observations of untreated platelets where over 90% of platelets were shown to exhibit a signal (Sage *et al.*, 2013; Kang *et al.*, 2014; Walford *et al.*, 2016). In addition, the signals appeared to be of lower amplitude and more spatially restricted than in previous studies. In our studies very few platelets it was rare to see any spread of Ca<sup>2+</sup> away from the pericellular Ca<sup>2+</sup> hotspot across the other side ( $5.4 \pm 2.5\%$  of cells per field;  $n = 7$ ), in contrast to our previous observation of that half of the cells in a field on untreated platelets showed this behaviour (Walford *et al.*, 2015)

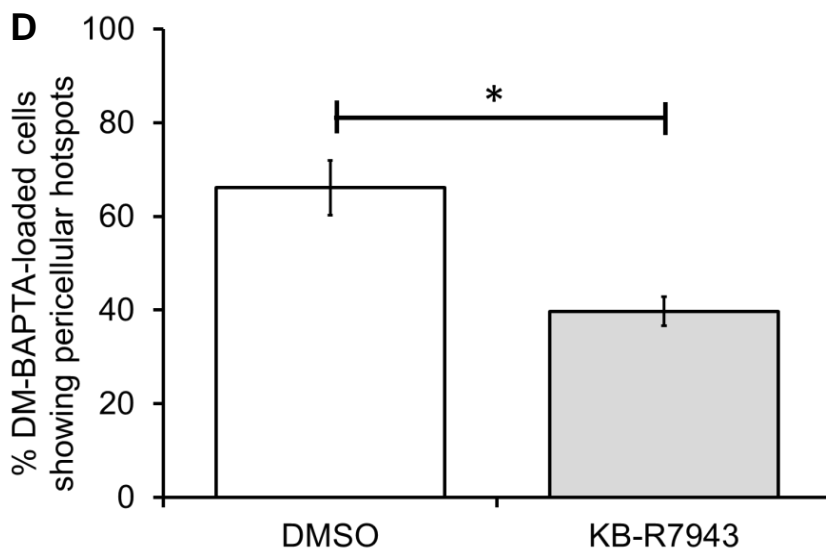
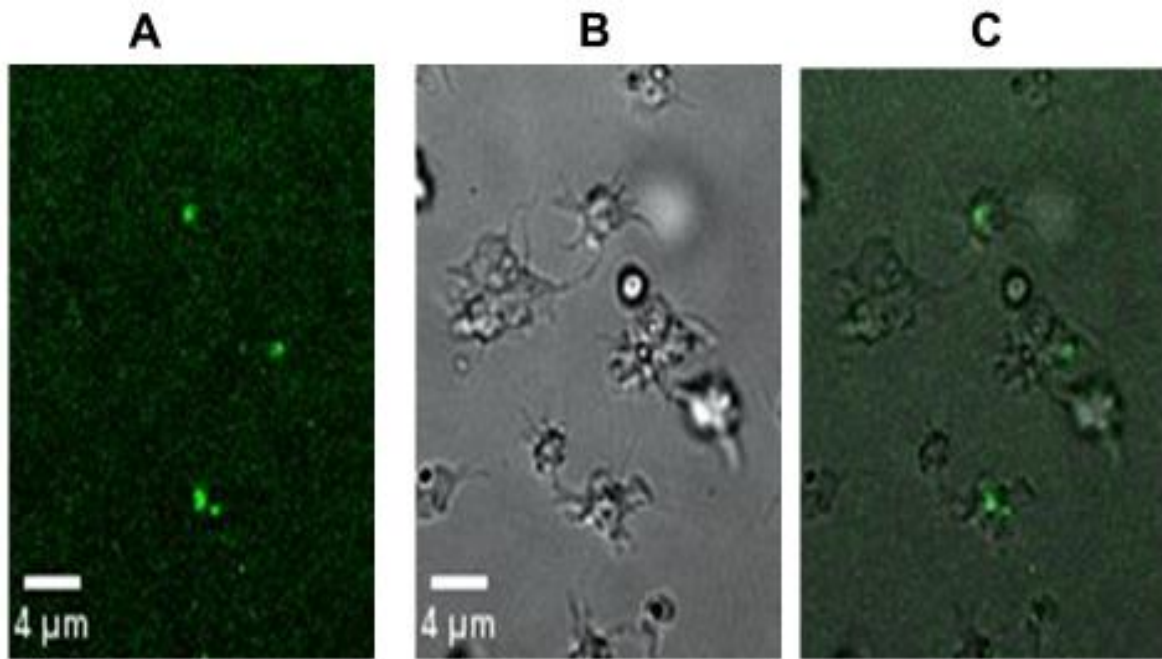


**Figure 3.9** Thrombin-evoked pericellular signals are resistant to DM-BAPTA loading in untreated human platelets (A-C) but are significantly inhibited when pretreated with KB-R7943 (D). Washed human platelets were suspended in supplemented HBS were pre-treated with  $30 \mu\text{mol.L}^{-1}$  dimethyl-BAPTA/AM. Cells were also treated with either  $50 \mu\text{mol.L}^{-1}$  KB-R7943 (D) or an equivalent volume of its vehicle, DMSO (B,C), for the last 5 min of this incubation. Platelets were added to poly-lysine-coated chambered cover slides and allowed to adhere for 5 minutes. Extracellular  $\text{Ca}^{2+}$  was then chelated by addition of  $1 \text{ mmol.L}^{-1}$  EGTA and Fluo-4 salt was added a final concentration of  $2.5 \mu\text{mol.L}^{-1}$ . Cells were then stimulated with  $0.5 \text{ U.mL}^{-1}$  thrombin and observed for 5 minutes. (D) Bar charts illustrates that in DM-BAPTA loaded platelets 66.1% of cells showed pericellular  $\text{Ca}^{2+}$  hotspots while the percentage of cells showing pericellular  $\text{Ca}^{2+}$  hotspot was significantly reduced to 39.7% in KB-R7943 treated cells.

These differences in the frequency and characteristics of the pericellular  $\text{Ca}^{2+}$  signal in DM-BAPTA-loaded cells can be reconciled by the previous demonstration that DM-BAPTA-loading significantly slows thrombin-evoked  $\text{Ca}^{2+}$  release from intracellular stores, by interfering with a process of  $\text{Ca}^{2+}$ -induced  $\text{Ca}^{2+}$  release (Sage *et al.*, 2013). When cells were pre incubated with the NCX inhibitor, KB-R7943, the proportion of cells showing a pericellular  $\text{Ca}^{2+}$  hotspot was significantly reduced to  $39.7 \pm 3.1\%$  of cells per field ( $n = 10$ ;  $P < 0.05$ ). In addition,  $\text{Ca}^{2+}$  spread from the source was also reduced ( $1.6 \pm 1.3\%$  of cells per field;  $n = 7$ ;  $P > 0.05$ ; Fig 3.9D), although this was not significantly different. Thus, these data suggest that the creation of the pericellular hotspot is relatively insensitive to DM-BAPTA-loading, but its amplification and spread across the cell is. This is consistent with a model that the  $\text{Ca}^{2+}$  enters the pericellular space at the membrane complex, but through its recycling back into the cell can trigger further  $\text{Ca}^{2+}$  release which can then be removed from the cell and amplify the  $\text{Ca}^{2+}$  signal allowing for  $\text{Ca}^{2+}$  spread from the pericellular hotspot.

### **3.7 Subcellular localisation of NCX3 isoform in fixed human platelets.**

Recent hypothesis from our lab suggest that NCX 3 isoform coupled with  $\text{IP}_3$  receptor could be specifically located in the cytosolic nanodomain enclosed within the membrane complex (Sage *et al.*, 2013). Proteomic studies and western blot analysis have both indicated NCX3 expression within the platelet plasma membrane (Lewandrowski *et al.*, 2009; Harper *et al.*, 2010; Roberts *et al.*, 2012). But no data exist for subcellular localization of NCX3 isoform within the platelet. Therefore, experiments were performed in fixed cells to examine whether NCX3 was found in the

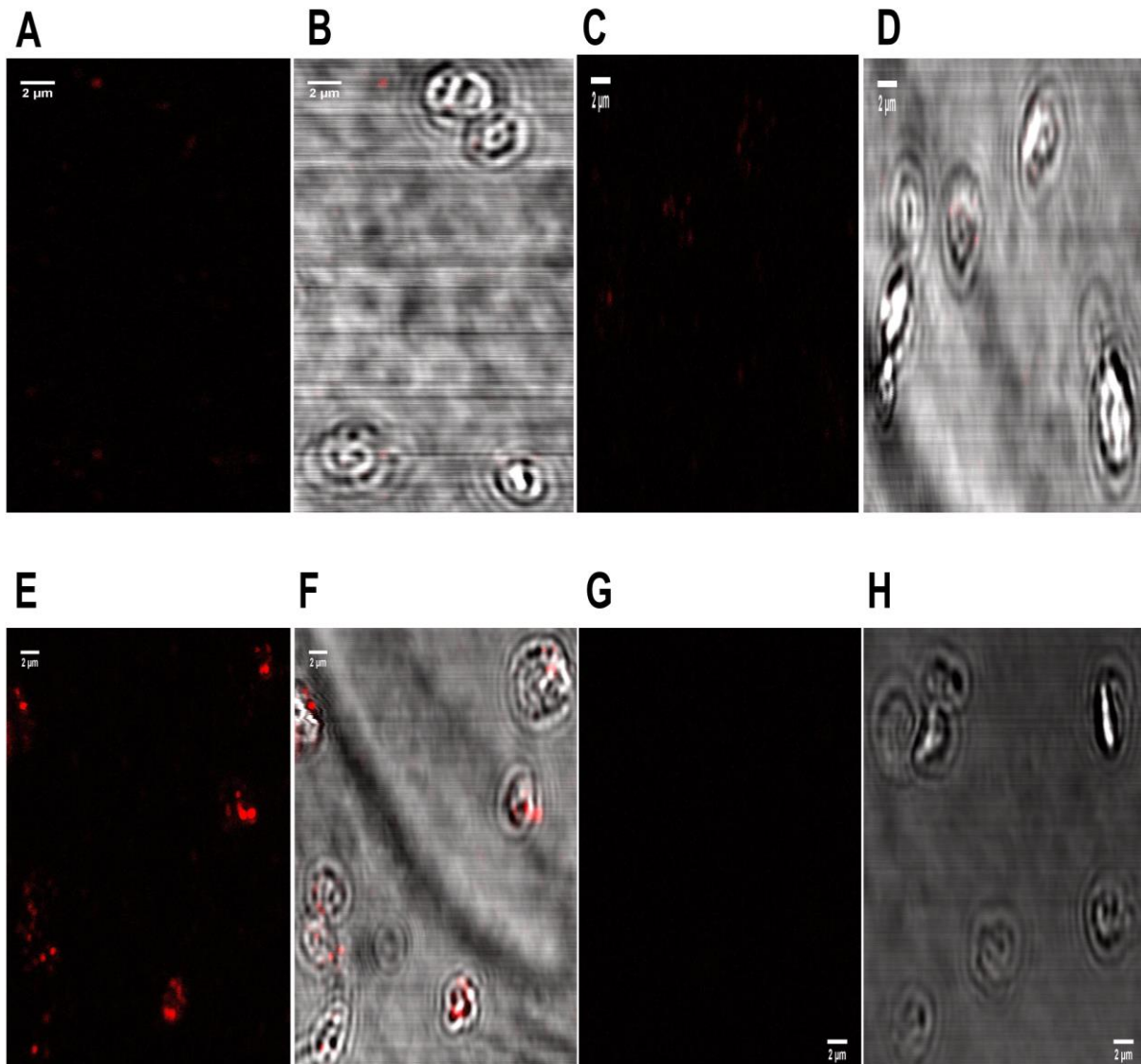


**Figure 3.10 NCX3 appears to be localised in a manner consistent with its presence within the open canalicular system.** Fixed platelets were pre incubated with a blocking buffer of HBS containing  $1 \text{ mg.mL}^{-1}$  BSA and a 1:100 dilution of a mouse secondary antibody for 30 min at room temperature. Cells were washed and then resuspended into HBS containing  $1 \text{ mg.mL}^{-1}$  BSA and either a 1:25 (E,F), 1:50 (C,D), 1:100 (A,B) dilution of an Goat NCX3 primary antibody or no antibody (G,H) for 30 min at room temperature. Cells were then washed again and incubated in HBS containing  $1 \text{ mg.mL}^{-1}$  BSA and a 1:1000 dilution of a fluorophore-conjugated secondary antibody for 30 min at room temperature. Cells were washed and resuspended into HBS containing  $1 \text{ mg.mL}^{-1}$  BSA. The labelled cells were allowed to settle for 10 min on poly-L-lysine-coated chambered slide. Fluorescent images were captured using a Fluoview FV 1200 laser scanning confocal microscope (Olympus, UK). Images for fluorescence alone (left) or overlaid over the transmitted light image (right) are shown. The results presented are representative of 3 experiments respectively.

surface membrane or in a location within the platelet boundary indicative of its localisation within the OCS.

A pilot study utilising a range of dilutions of the fluorescently-labelled secondary antibody (1:100, 1:1000, antibody free control) was performed on cells from two different donors to identify the appropriate secondary antibody concentration to utilise for NCX3 localization experiments. These experiments identified that whilst 1:1000 showed no significant non-specific antibody binding compared to the antibody free control, cells treated with a 1:100 dilutions could be observed to have a significant fluorescence after treatment (data not shown). Therefore, the 1:1000 dilution was utilised in optimisation studies for the primary antibody.

Previous studies have demonstrated the presence of NCX3 using a primary antibody raised to an extracellular epitope of this exchanger (Harper *et al.*, 2010). Therefore, experiments initially tested incubating platelets for 30 min at room temperature with three different dilutions of a primary antibody (1:100, 1:50, 1:25) and a primary antibody free control to determine the optimal antibody concentration to use for further immunofluorescent studies. 1:25 dilution was found to consistently show immunofluorescent labelling on the surface of the platelet, whereas at 1:50 the effect was more inconsistent. Therefore 1:25 dilution was used for all subsequent studies.

Fluorescent imaging of the labelled cells found that cells possessed a varied bright punctate distribution of NCX3 protein predominantly within the platelet margin indicating its origin of the open canalicular system (Fig 3.10 E,F). These results are consistent with our previous work that predicted a functional role for NCX 3 protein preferentially located in cytosolic nanodomain within membrane complex and orchestrating pericellular Ca<sup>2+</sup> accumulations (Sage *et al.*, 2013; Walford *et al.*, 2016).

### **3.8 Nicergoline-induced reorganization of the DTS affects the subcellular localization and distribution of NCX3 in human platelets**

The close proximity of the two membrane systems at the membrane complex would suggest the need for a protein scaffold to hold these structures in alignment. This protein scaffold may therefore play a role in holding NCX3 in its normal location. Therefore, experiments were performed to examine whether the microtubule-dependent reorganisation of the DTS could alter the localisation of NCX3 within the platelets. Consistent with our previous experiment, control cells showed a punctate distribution away from the surface membrane, and in an eccentric location consistent with the exchanger primarily being found at the MC (Fig 3.11A-B). Pre-treatment with nicergoline elicited a more spread distribution of fluorescence throughout the interior platelet boundaries indicating that NCX3 localisation is affected by the nicergoline-induced disruption to the cortical microtubules and DTS (Fig 3.11E-F). The primary-free control cells did not show any fluorescent binding (Fig 3.11C-D). Quantitative analysis of this alteration in NCX3 fluorescence revealed that the mean skew of the pixel fluorescence distribution of all the DMSO-treated cells was significantly greater than found in nicergoline-treated cells ( $2.5 \pm 0.2$  and  $1.6 \pm 0.4$  in DMSO- and nicergoline-treated cells respectively;  $n = 4$ ;  $P < 0.05$ ) indicating that nicergoline induces a more homogenous distribution of NCX3 through these cells.

These results therefore suggest that NCX3 localisation requires an intact cortical microtubule bundle and/or DTS localisation to hold it in place. These results suggest the possibility that a common scaffolding system could hold both the intracellular  $\text{Ca}^{2+}$  stores and NCX3 together at the MC. Nicergoline-induced rearrangement of the NCX3 distribution could therefore prevent accumulation of  $\text{Ca}^{2+}$  in the pericellular space and therefore inhibit thrombin-evoked rises in  $[\text{Ca}^{2+}]_{\text{cyt}}$  (Walford *et al.*, 2016).

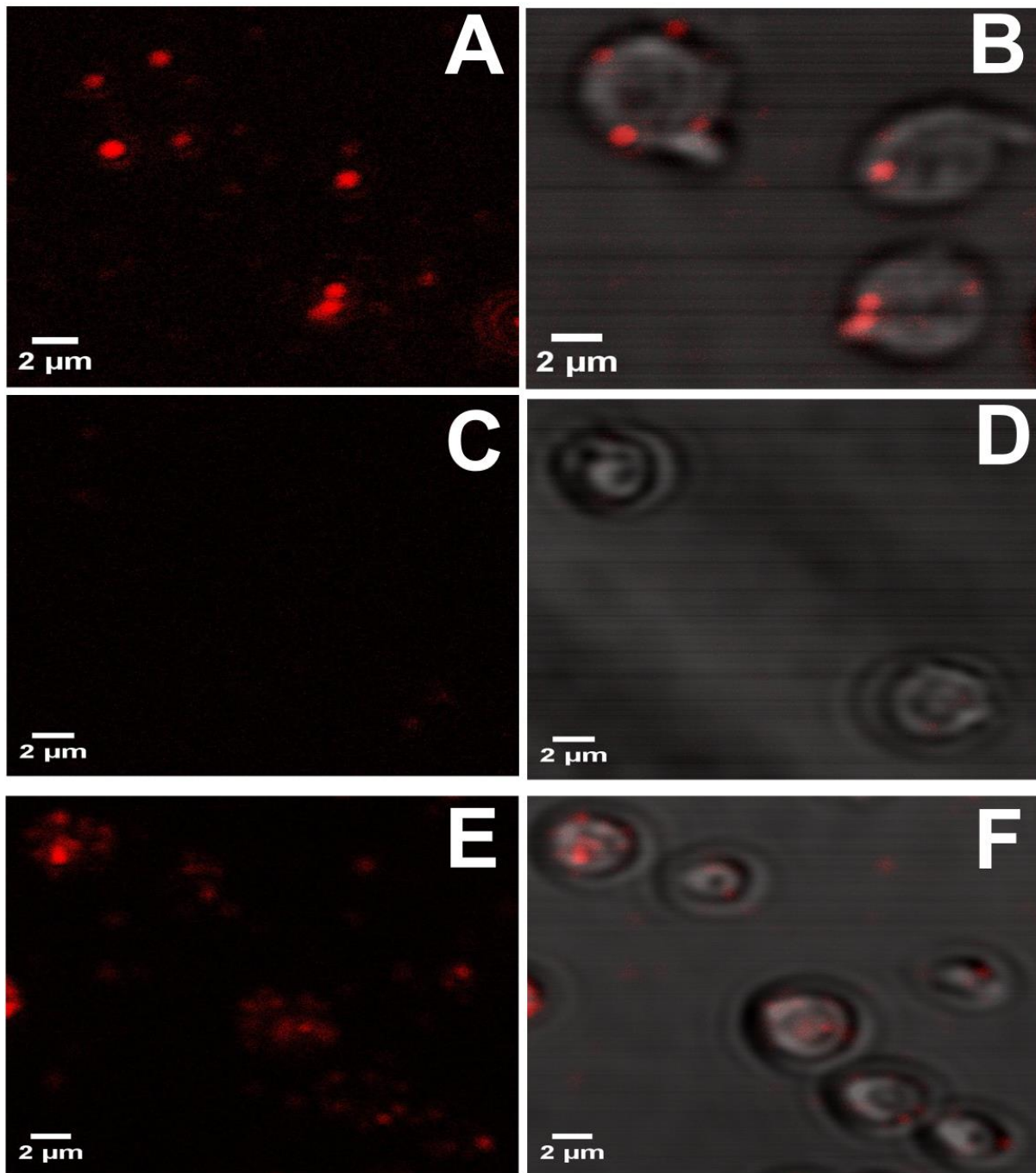


**Figure 3.11 Nicergoline disrupts the normal localisation of NCX3 within resting platelets.** Washed human platelets were pre-treated with either  $100 \mu\text{mol.L}^{-1}$  nicergoline (E,F), or an equivalent volume of its vehicle, DMSO (A,B) for 10 min at  $37^\circ\text{C}$ . Cells were then fixed with 3% [w/v] formaldehyde and stored at  $4^\circ\text{C}$  until use. Fixed platelets were preincubated with a blocking buffer of PBS containing  $1 \text{ mg.mL}^{-1}$  BSA and a 1:100 dilution of a mouse secondary antibody for 30 min at room temperature. Cells were washed and then resuspended into PBS containing  $1 \text{ mg.mL}^{-1}$  BSA and either a 1:25 dilution of an NCX3 primary antibody (E-F) or no antibody (C,D) for 30 min at room temperature. Cells were then washed again and incubated in PBS containing  $1 \text{ mg.mL}^{-1}$  BSA and a 1:1000 dilution of a fluorophore-conjugated secondary antibody for 30 min at room temperature. Cells were washed and resuspended into PBS containing  $1 \text{ mg.mL}^{-1}$  BSA. The labelled cells were allowed to settle for 10 min on poly-L-lysine-coated chambered slide. Fluorescent images were captured using a Fluoview FV 1200 laser scanning confocal microscope (Olympus, UK).

#### **4. Investigating the functional effects of a cytosolic nanodomain in platelets**

The presence of a cytosolic nanodomain which is specialised to regulate  $\text{Ca}^{2+}$  signalling functionally isolated from the bulk cytosol, provides a potential mechanism for altering the  $\text{Ca}^{2+}$  responsiveness of the various  $\text{Ca}^{2+}$ -dependent processes involved in controlling platelet activation. The pericellular  $\text{Ca}^{2+}$  recycling model hypothesises that  $\text{Ca}^{2+}$  is released first in the tiny volume of the cytosolic nanodomain, from where it spreads to the bulk cytosol via pericellular recycling from the OCS. If  $\text{Ca}^{2+}$  effectors are preferentially localised in either the cytosolic nanodomain and the bulk cytosol, this could alter both their sensitivity to agonist-evoked  $\text{Ca}^{2+}$  signals. For instance,  $\text{Ca}^{2+}$  effector proteins preferentially localised in the cytosolic nanodomain would be expected to be activated by any stimuli that triggered  $\text{Ca}^{2+}$  release due to the accumulation of large amounts of  $\text{Ca}^{2+}$  in this tiny volume, whereas those effectors found predominantly in the bulk cytosol may need a stronger signal to be triggered due to the need for the  $\text{Ca}^{2+}$  to escape the nanodomain and spread into the large volume of this cellular sub compartment. In addition,  $\text{Ca}^{2+}$  effectors present in the nanodomain would be expected to be activated with a shorter latency than those in the bulk cytosol due to the shorter diffusion distance of  $\text{Ca}^{2+}$  from the stores into this compartment.

To test this hypothesis, we have examined the properties of the platelet shape change in DM-BAPTA-loaded platelets in which  $\text{Ca}^{2+}$  signalling can only occur within the cytosolic nanodomain. Previous studies have demonstrated that unlike thrombin-evoked granule secretion and aggregation, shape change initiated by this ligand is resistant to DM-BAPTA-loading (Davies *et al.*, 1989; Paul *et al.*, 1999) suggesting that  $\text{Ca}^{2+}$  effectors for this process could be localised within the nanodomain. In addition, platelet shape change is triggered with a short latency by all platelet agonists. These

data therefore suggest that  $\text{Ca}^{2+}$  effectors involved in triggering the platelet shape change such as calmodulin (Hathaway *et al.*, 1981, Dandona *et al.*, 1996) might be localised within the cytosolic nanodomain. To examine this possibility experiments have been performed to examine whether interfering with  $\text{Ca}^{2+}$ -signalling system can alter the shape change response of DM-BAPTA-loaded platelets.

#### **4.1 Blockade of NCX activity induces shape change in unstimulated DM-BAPTA-loaded human platelets, and maintains the thrombin-evoked response.**

As described above, blockade of the NCX with KB-R7943 prevents  $\text{Ca}^{2+}$  removal from DM-BAPTA-loaded platelets suggesting that this exchanger is responsible for controlling the  $\text{Ca}^{2+}$  concentration found in this sub-region. These results suggest that blocking this exchanger should enhance and prolong agonist-evoked  $\text{Ca}^{2+}$  signals in this cellular sub compartment, and thus potentiate any  $\text{Ca}^{2+}$ -dependent responses observed. Thus we examined the effect of pre-treating platelets with KB-R7943 on the shape change observed in DM-BAPTA-loaded platelets. As KB-R7943 is poorly soluble when added directly to solutions, KB-R7943 (or an equivalent volume of its vehicle, DMSO) was solubilised at high concentrations into HBS by magnetic stirring at 37°C. This pre-solubilised KB-R7943 was then added to the washed platelet suspension to give final concentrations of 25  $\mu\text{mol.L}^{-1}$  and 50  $\mu\text{mol.L}^{-1}$ . The addition of these drug-containing solutions caused an initial increase in light transmittance (shown as a drop in the trace) due to its effect of diluting the platelet suspension. No further effect was seen in platelets treated with DMSO-containing HBS (decrease in light transmittance =  $-0.0\% \pm 0.2\%$  of basal;  $n = 9$ ; Fig 4.1A, B). However, when platelets were exposed to KB-R7943, there was a rapid, dose-dependent decrease in light transmittance, consistent with this drug initiating a shape change (decrease in light

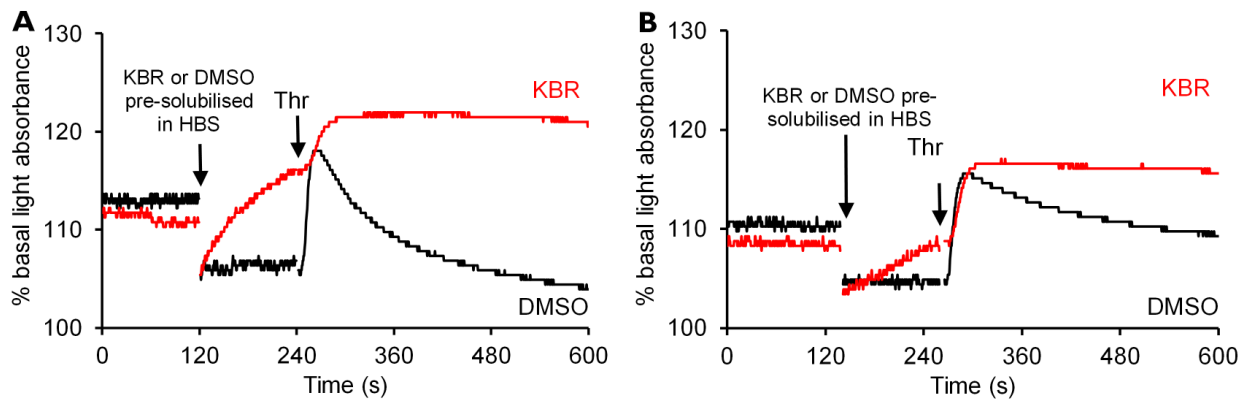


**Fig 4.1 Blockade of NCX activity induces shape change in unstimulated DM-BAPTA-loaded human platelets, and maintains the thrombin-evoked response.** Washed human platelets suspended in supplemented HBS were pre incubated with  $30 \mu\text{mol.L}^{-1}$  dimethyl-BAPTA/AM for 10 min at  $37^\circ\text{C}$ . Extracellular  $\text{Ca}^{2+}$  was then chelated with  $1 \text{mmol.L}^{-1}$  EGTA. Cells were then treated with HBS containing either KB-R7943 or an equivalent volume of DMSO, to give a final concentration of either  $50 \mu\text{mol.L}^{-1}$  (A) or  $25 \mu\text{mol.L}^{-1}$  (B) KB-R7943. 2 min later cells were stimulated with  $0.5 \text{U.mL}^{-1}$  thrombin.

transmittance =  $5.6\% \pm 0.3\%$  and  $8.5\% \pm 0.3\%$  of basal for  $25 \mu\text{mole.L}^{-1}$  and  $50 \mu\text{mole.L}^{-1}$  KB-R7943 respectively; both  $n = 9$ ; both  $P < 0.05$  compared to DMSO control; Fig 4.1). This KB-R7943-induced shape change has previously also been observed in the absence of prior DM-BAPTA-loading (Harper, 2007). These data suggest that blocking NCX-mediated removal in unstimulated platelets can elicit an increase in the  $\text{Ca}^{2+}$  concentration within the cytosolic nanodomain which can trigger the onset of shape change.

After the pre-incubation period with KB-R7943 or DMSO, platelets were stimulated with thrombin. As shown in Fig 4.1, thrombin-induces a rapid decrease in light transmittance consistent with the onset of the platelet shape change in DMSO-treated platelets, which then slowly returns towards baseline over the course of the observation period. In cells treated with KB-R7943 there is a further decrease in light transmittance, which then declines only slightly towards basal during the observation period. This decrease in light transmittance compared to the baseline level at the end of the recording period was significantly reduced in DMSO-treated cells (decrease in light transmittance =  $5.2\% \pm 0.4\%$  of basal;  $n = 9$ ; Fig 4.1) compared to KB-R7943-treated cells than in the control cells (decrease in light transmittance =  $14.5\% \pm 0.7\%$ , and  $12.6\% \pm 0.8\%$  of basal for  $25 \mu\text{mole.L}^{-1}$  and  $50 \mu\text{mole.L}^{-1}$  KB-R7943-treated cells respectively; both  $n = 9$ ; both  $P < 0.05$  compared to DMSO control; Fig 4.1). These data suggest that the shape change is reversible in DM-BAPTA-loaded cells stimulated with thrombin in the absence of extracellular  $\text{Ca}^{2+}$  due to  $\text{Ca}^{2+}$  being removed from the cytosolic nanodomain by NCX. When this transporter is blocked,  $\text{Ca}^{2+}$  remains elevated in this cellular sub compartment and allow the  $\text{Ca}^{2+}$ -dependent shape change to be prolonged.

#### **4.2 Pretreatment of DM-BAPTA-loaded platelets with the myosin light chain kinase inhibitor, ML-7, prevents KB-R7943- and thrombin-evoked shape change.**

Platelet shape change is mediated at least partially through a  $\text{Ca}^{2+}$ -dependent signalling pathway. This pathway involves  $\text{Ca}^{2+}$ -binding to calmodulin, which in turn can bind to and activate myosin light chain kinase (MLCK; Adelstein *et al.*, 1973; Hathaway & Adelstein, 1979; Adelstein, 1982). This  $\text{Ca}^{2+}$ /Calmodulin dependant signalling pathway is the principal mechanism by which the platelet shape change is elicited when stimulated by physiological agonists such as thrombin (Daniel *et al.*, 1981; Hathaway *et al.*, 1981; Daniel *et al.*, 1984). A number of studies have shown that ML-7, a synthetic inhibitor of myosin light chain kinase, is able to inhibit this calcium-dependent myosin light chain phosphorylation of the myosin light chain, and thus shape change, in thrombin-activated platelets (Itoh *et al.*, 1992). If the KB-R7943- and thrombin-induced shape changes are mediated by a rise in  $\text{Ca}^{2+}$  concentration ML-7 should prevent these platelet responses. Experiments were therefore performed to investigate whether pre-treatment with ML-7 was able to prevent the effects of, KB-R7943-pretreatment and thrombin-stimulation in DM-BAPTA-loaded cells. As can be seen in Fig 4.2, ML-7 almost completely abolished the thrombin-evoked shape change in DM-BAPTA-loaded cells pretreated with DMSO (decrease in light transmittance =  $10.9\% \pm 0.9\%$  and  $1.1\% \pm 0.4\%$  of basal in DMSO- and ML-7 treated cells respectively;  $n = 6$ ;  $P < 0.05$  Fig 4.2A). Similarly, in KB-R7943-treated cells, ML-7 also almost completely blocks both the KB-R7943- and thrombin- shape change (decrease in light transmittance =  $13.0\% \pm 1.5\%$  and  $1.0\% \pm 0.3\%$  of basal in DMSO- and ML-7 treated cells in presence of KB-R7943 respectively;  $n = 6$ ;  $P < 0.05$ ; Fig 4.2B). These results suggest that KB-R7943 mediates platelet shape change triggering activation

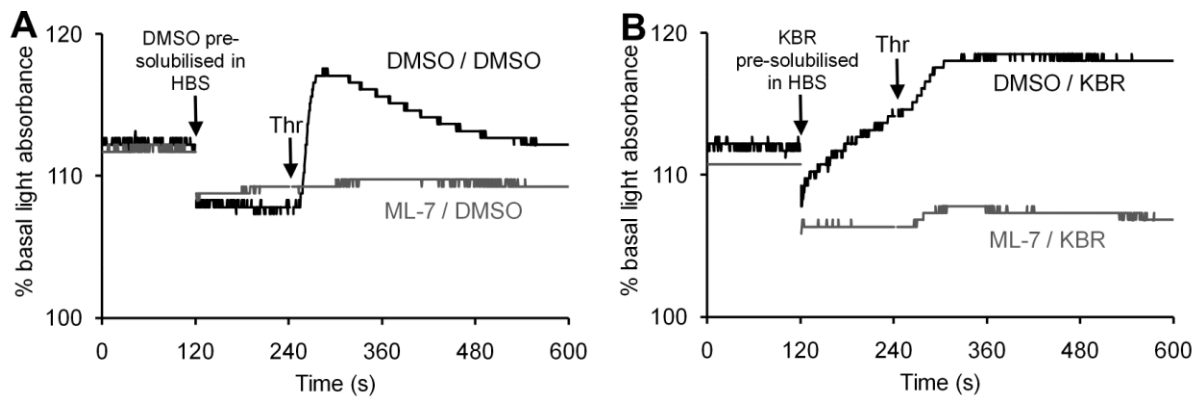


**Fig 4.2 Pretreatment with ML-7 inhibits KB-R7943- and thrombin-induced shape change in DM-BAPTA-loaded platelets.** Washed human platelets suspended in supplemented HBS were preincubated with  $30 \mu\text{mol.L}^{-1}$  dimethyl-BAPTA/AM and either  $25 \mu\text{mol.L}^{-1}$  ML-7 or an equivalent volume of its vehicle, DMSO, for 10 min at  $37^\circ\text{C}$  (A). Extracellular  $\text{Ca}^{2+}$  was then chelated with  $1 \text{mmol.L}^{-1}$  EGTA. Cells were then treated with HBS containing either KB-R7943 (B) or an equivalent volume of DMSO (B), to give a final concentration of  $50 \mu\text{mol.L}^{-1}$  KB-R7943. 2 min later cells were stimulated with  $0.5 \text{U.mL}^{-1}$  thrombin.

of the Ca<sup>2+</sup>-dependent MLCK by raising the Ca<sup>2+</sup> concentration within the cytosolic nanodomain of DM-BAPTA-loaded cells.

#### **4.3 Pre-treatment with the Rho-kinase inhibitor, Y-27632, has no significant effect on KB-R7943-evoked shape change in DM-BAPTA-loaded platelets.**

In addition to the Ca<sup>2+</sup>-dependent activation of MLCK, previous studies have demonstrated the presence of a Ca<sup>2+</sup>-independent signalling pathway for the activation of platelet shape change (Paul *et al.*, 1999). This pathway involves the activation of Rho Kinase, which indirectly increases the myosin light chain phosphorylation by decreasing the myosin phosphatase activity (Nakai *et al.*, 1997; Bauer *et al.*, 1999). Experiments were therefore performed to examine whether this signalling pathway may play a role in eliciting shape change in response to KB-R7943 or thrombin-stimulation in DM-BAPTA-loaded platelets. These experiments showed that pre-treatment with Y-27632 had no effect on thrombin-stimulation in DMSO-treated cells (decrease in light transmittance = 10.6% ± 2.0% and 11.4% ± 1.3% of basal in DMSO- and Y-27632-treated cells respectively; n = 6; P > 0.05; Fig 4.3A), or any effect on KB-R7943- (8.1% ± 1.5% and 11.1% ± 0.7% in DMSO- and Y-27632-treated-cells respectively; n = 6; P > 0.05; Fig 4.3B) or thrombin-induced shape change in KB-R7943-treated platelets. (13.6% ± 2.0% and 14.1% ± 0.7% in DMSO- and Y-27632-treated-cells respectively; n = 6; P > 0.05; Fig 4.3B) These data confirm that the shape changes elicited in these cells are elicited by the Ca<sup>2+</sup>-dependent MLCK pathway.

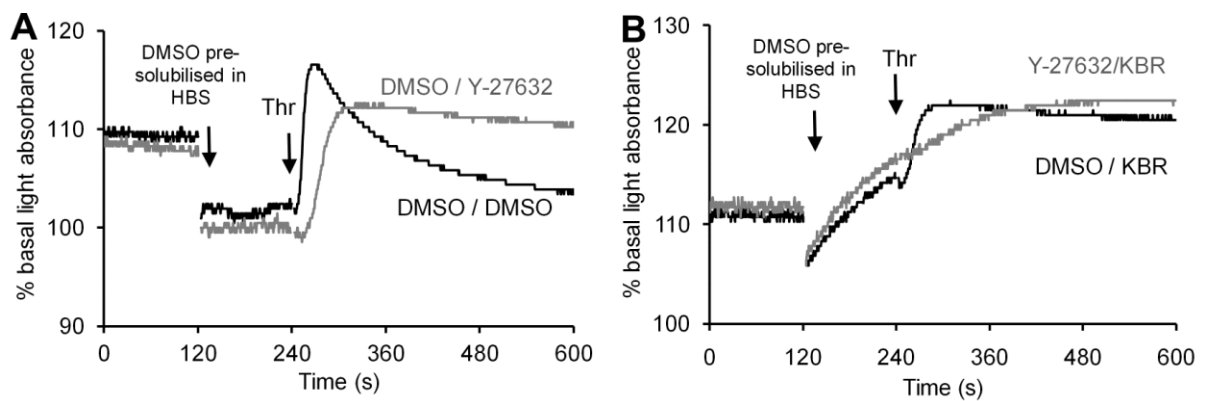


**Fig 4.3 Pretreatment with Y-27632 has no significant effect on KB-R7943- and thrombin-induced shape change in DM-BAPTA-loaded platelets.** Washed human platelets suspended in supplemented HBS were pre incubated with  $20 \mu\text{mol.L}^{-1}$  Y-267632 or an equivalent volume of its vehicle, DMSO, for 10 min at  $37^\circ\text{C}$  (A). All cells were also incubated with  $30 \mu\text{mol.L}^{-1}$  dimethyl-BAPTA/AM for the last 10 min of this incubation. Extracellular  $\text{Ca}^{2+}$  was then chelated with  $1 \text{mmol.L}^{-1}$  EGTA. Cells were the treated with HBS containing either KB-R7943 (B) or an equivalent volume of DMSO (B), to give a final concentration of  $50 \mu\text{mol.L}^{-1}$  KB-R7943. 2 min later cells were stimulated with  $0.5 \text{U.mL}^{-1}$  thrombin

#### **4.4 The IP<sub>3</sub>R inhibitor, 2-APB, inhibits KB-R7943- and thrombin-induced shape change in DM-BAPTA loaded cells.**

The previous experiments demonstrated that the NCX inhibitor KB-R7943 may trigger platelet shape change by preventing Ca<sup>2+</sup> removal from the cytosolic nanodomain. However, for there to be an accumulation in response to a blockage of this Ca<sup>2+</sup> removal pathway there must also be a constant entry of Ca<sup>2+</sup> into this domain which is counteracted by the action of the NCX. As all the experiments reported here occur in the absence of extracellular Ca<sup>2+</sup>, this suggests that the DTS is the most likely source of this Ca<sup>2+</sup>. This might either be through Ca<sup>2+</sup> blips from individual IP<sub>3</sub>Rs or the known Ca<sup>2+</sup> leak pathway from the DTS, which has been suggested to be mediated through proteins, such as the presenillins and Sec61 complexes. To attempt to initially identify the possible source of Ca<sup>2+</sup> for the KB-R7943-mediated shape change, experiments were performed to examine the effect of the IP<sub>3</sub>R inhibitor, 2-APB. This compound has previously been used to block IP<sub>3</sub>R in human platelets (Driver et al., 2001) . As shown in Fig 4.4B, pre-treatment with 2-APB at concentrations previously shown to significantly inhibit thrombin-evoked Ca<sup>2+</sup> release, significantly inhibited KB-R7943-induced evoked shape change in DM-BAPTA-loaded platelets (8.1% ± 1.2% and 1.0% ± 2.4% in DMSO- and 2-APB-treated-cells respectively; n = 6; P < 0.05). 2-APB was also found to significantly reduce the peak shape change response observed after thrombin (12.5% ± 1.5% and 1.5% ± 2.3% in DMSO- and 2-APB-treated-cells respectively; n = 6; P < 0.05), as well as the maintained level of shape change seen at the end of the experiment in KB-R7943 treated cells (11.7% ± 1.4% and 2.8% ± 2.4% in DMSO- and 2-APB-treated-cells respectively; n = 6; P < 0.05; Fig 4.4B). These data indicate that the IP<sub>3</sub>R is important for mediating Ca<sup>2+</sup> release into the cytosolic Ca<sup>2+</sup> nanodomain in which the NCX resides.

Surprisingly 2-APB was found to have no significant effect on the magnitude of thrombin-induced shape change in DMSO-treated control cells ( $9.6\% \pm 0.7\%$  and  $6.5\% \pm 1.5\%$  in DMSO- and 2-APB-treated-cells respectively;  $n = 6$ ;  $P > 0.05$ ; Fig 4.4A). However, the latency to peak height after thrombin stimulation was significantly prolonged in 2-APB-treated cells ( $43.1 \pm 4.8\text{s}$  and  $84.7 \pm 12.6\text{s}$  in DMSO- and 2-APB-treated-cells respectively;  $n = 6$ ;  $P < 0.05$ ; Fig 4.4A). These results were surprising as thrombin-evoked  $\text{Ca}^{2+}$  signalling is largely mediated via  $\text{IP}_3$  production (Sage *et al.* 2011). However previous studies have demonstrated that 2-APB is a selective inhibitor of  $\text{IP}_3\text{R1}$  (Saleem *et al.*, 2014) and so does not affect the  $\text{IP}_3\text{R2}$  and  $\text{IP}_3\text{R3}$  isoforms also known to be present in platelets (Quinton & Dean, 1996; El-Daher *et al.*, 2000). As  $\text{IP}_3\text{R3}$  is only found in the plasma membrane it cannot play a role in mediating  $\text{Ca}^{2+}$  release. Together these results suggest that the 2-APB-sensitive  $\text{IP}_3\text{R1}$  may be the main mechanism for  $\text{Ca}^{2+}$  release at the membrane complex. However, the  $\text{IP}_3\text{R2}$  isoforms and/or the NAADP receptor may also contribute to this  $\text{Ca}^{2+}$  release, thus accounting for why a shape change can still be observed in 2-APB-treated cells, even though it is significantly delayed. These results suggest that the type I  $\text{IP}_3\text{R}$  is the principal means of eliciting  $\text{Ca}^{2+}$  release in the cytosolic nanodomain – further studies will be needed to consider this effect more closely.

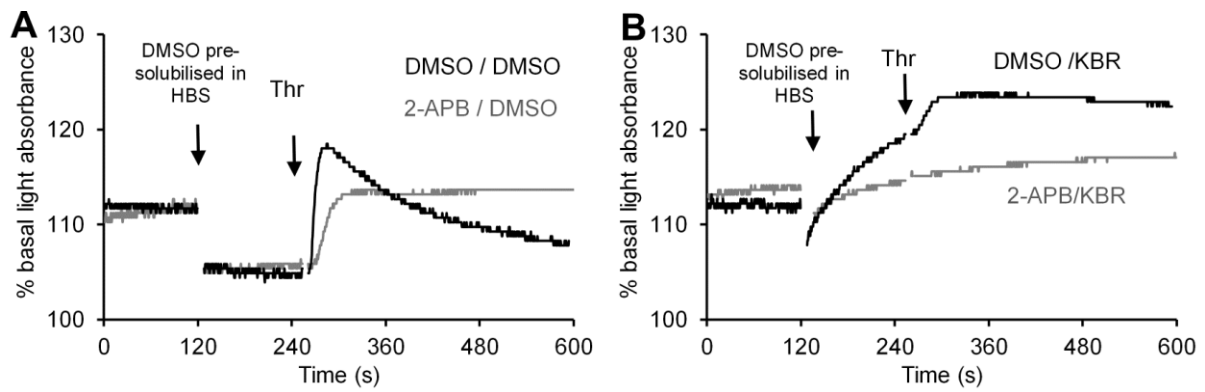


**Fig 4.4 Pre-treatment with 2-APB has no significant effect on KB-R7943- and thrombin-induced shape change in DM-BAPTA-loaded platelets.** Washed human platelets suspended in supplemented HBS were preincubated with  $30 \mu\text{mol.L}^{-1}$  dimethyl-BAPTA/AM for the 10 min at  $37^\circ\text{C}$ . For the last 5 min of this incubation cells were also treated with either  $100 \mu\text{mol.L}^{-1}$  2-APB or an equivalent volume of its vehicle, DMSO(A). Extracellular  $\text{Ca}^{2+}$  was then chelated with  $1 \text{mmol.L}^{-1}$  EGTA. Cells were the treated with HBS containing either KB-R7943 or an equivalent volume of DMSO, to give a final concentration of  $50 \mu\text{mol.L}^{-1}$  KB-R7943 (B). 2 min later cells were stimulated with  $0.5 \text{U.mL}^{-1}$  thrombin.

#### **4.5 Nicergoline pre-treatment prevents thrombin-induced shape change in DM-BAPTA-loaded cells.**

The previous experiments have suggested that in DM-BAPTA-loaded platelets that the thrombin-evoked shape change is mediated through the accumulation of  $\text{Ca}^{2+}$  within the cytosolic nanodomain, which triggers the activation of MLCK. If the cytosolic nanodomain is required for eliciting the activation of MLCK then pre-treatment with nicergoline should prevent the thrombin-evoked shape change. As shown in Fig 4.5, nicergoline pre-treatment nearly abolished thrombin-evoked shape change in human platelets (decrease in light transmittance =  $7.3\% \pm 1.7\%$  of basal and  $0.5\% \pm 0.4\%$  of basal in DMSO- and nicergoline-treated respectively;  $n = 6$ ;  $P < 0.05$  Fig 4.5). These data provide initial evidence that the membrane complex may play a key role in allowing selective activation of calmodulin over other  $\text{Ca}^{2+}$  effectors in human platelets.

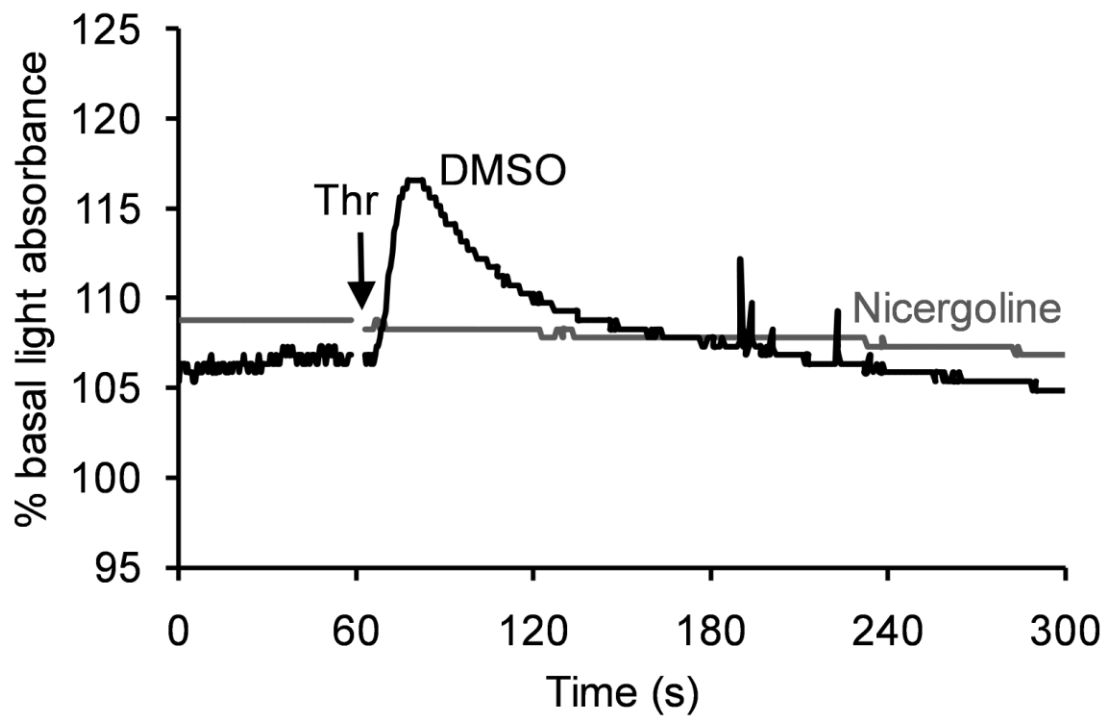


**Fig 4.5 Pretreatment with nicergoline inhibits thrombin-induced shape change in DM-BAPTA-loaded platelets.** Washed human platelets suspended in supplemented HBS were preincubated with  $30 \mu\text{mol.L}^{-1}$  dimethyl-BAPTA/AM and either  $100 \mu\text{mol.L}^{-1}$  nicergoline or an equivalent volume of its vehicle, DMSO for 10 min at  $37^\circ\text{C}$ . Extracellular  $\text{Ca}^{2+}$  was then chelated with  $1 \text{mmol.L}^{-1}$  EGTA. Cells were then treated with HBS containing either KB-R7943 or an equivalent volume of DMSO, to give a final concentration of  $50 \mu\text{mol.L}^{-1}$  KB-R7943. 2 min later cells were stimulated with  $0.5 \text{U.mL}^{-1}$  thrombin.

#### 4.6 ML-7 and Y-27632 inhibit thrombin-evoked rises in $[Ca^{2+}]_{ext}$ in DM-BAPTA-loaded platelets

The previous experiments demonstrated that  $Ca^{2+}$  release into the cytosolic nanodomain can trigger the activation of shape change via activation of MLCK. Here we considered whether MLCK is a passive mediator of  $Ca^{2+}$  signalling, or can work to shape the elicited  $Ca^{2+}$  signalling by providing feedback to the cell. Positive control experiments demonstrated pre incubating platelets with DM-BAPTA prevented thrombin-evoked  $[Ca^{2+}]_{cyt}$  signals ( $1.5 \pm 0.8$  % of control;  $n = 7$ ;  $P < 0.05$ ; Fig 4.6A) Pre incubating DM-BAPTA-loaded platelets from the same donor with both  $25 \mu\text{mol L}^{-1}$  ML-7 significantly inhibited thrombin-evoked rises in  $[Ca^{2+}]_{ext}$  to  $39.0 \pm 16.6$  % of control ( $n = 7$ ;  $P < 0.05$ ; Fig 4.6B). These results suggest that MLCK may also be a regulator of platelet  $Ca^{2+}$  signalling, and this may partly underlie the inhibitory effect of ML-7 on the thrombin-induced shape change. However additional work will need to be performed due to previous results which suggest that this compound may also be an inhibitor of TRPC6 (Shi *et al.*, 2007; Lei *et al.*, 2014)

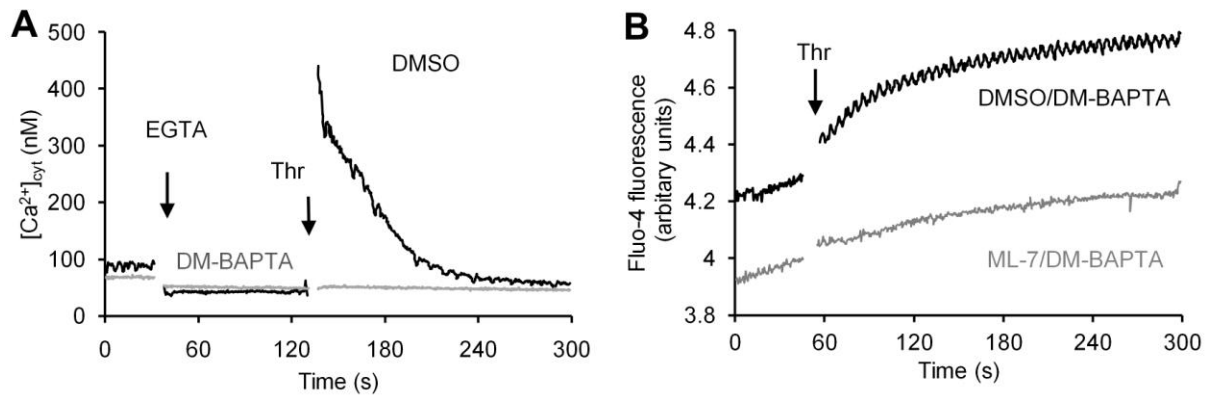


**Figure 4.6 ML-7 pretreatment inhibits thrombin-evoked rises in  $[Ca^{2+}]_{ext}$  in DM-BAPTA-loaded platelets.** (A) Fura-2-loaded human platelets suspended in supplemented HBS were preincubated with either  $30 \mu\text{mol.L}^{-1}$  dimethyl-BAPTA/AM, or an equivalent volume of its vehicle, DMSO, for 10 min at  $37^\circ\text{C}$ . Extracellular  $Ca^{2+}$  was then chelated with  $1 \text{mmol.L}^{-1}$  EGTA and then 1 min later stimulated with  $0.5 \text{U.mL}^{-1}$  thrombin. Washed human platelets were suspended in supplemented HBS were pre-treated with  $30 \mu\text{mol.L}^{-1}$  dimethyl-BAPTA/AM as well as either  $25 \mu\text{mol.L}^{-1}$  ML-7 (B), or an equivalent volume of its vehicle, DMSO (B) for 10 min at  $37^\circ\text{C}$ . A final concentration of  $2.5 \mu\text{mol.L}^{-1}$  Fluo-4 salt was then added immediately before the experiment. Extracellular  $Ca^{2+}$  was then chelated with  $1 \text{mmol.L}^{-1}$  EGTA (not shown) and then 1 min later stimulated with  $0.5 \text{U.mL}^{-1}$  thrombin.

Similar experiments were also performed examining the effect of the Rho Kinase inhibitor, Y-27632. Positive control experiments demonstrated pre incubating platelets with DM-BAPTA significantly prevented the thrombin-evoked  $[Ca^{2+}]_{cyt}$  signals to  $(1.9 \pm 1.1 \%$  of control;  $n = 4$ ;  $P < 0.05$ ; Fig 4.7A). Surprisingly, pre incubating DM-BAPTA-loaded platelets from the same donor with  $30 \mu\text{mol.L}^{-1}$  Y-27632 resulted in a significant reduction in thrombin-evoked rise in  $[Ca^{2+}]_{ext}$  to  $53.2 \pm 13.9 \%$  of control ( $n = 7$ ;  $P < 0.05$ ; Fig 4.7B). These results therefore support the ML-7 results and suggest the possibility that activation of myosin via phosphorylation of the myosin light chain may play a role in facilitating  $Ca^{2+}$  signalling in the cytosolic nanodomain

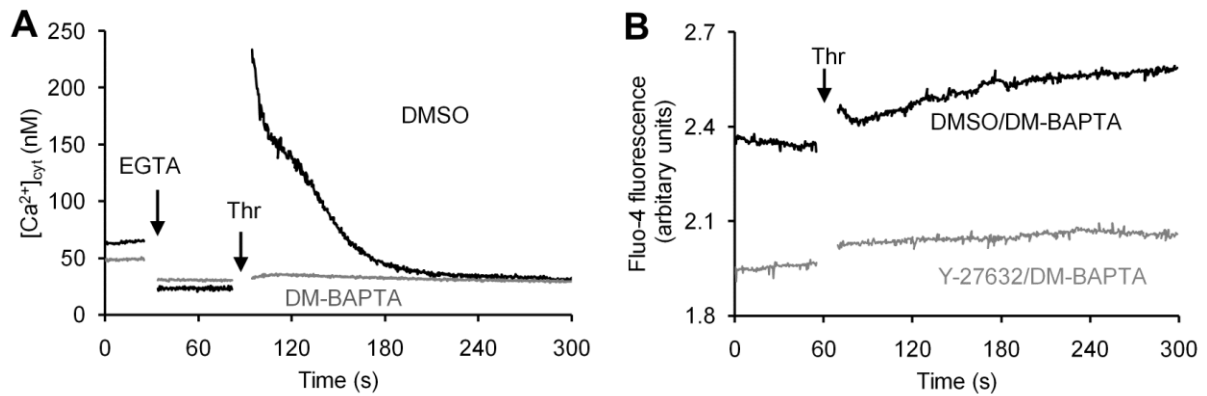


**Figure 4.7 Y-27632 pretreatment inhibits thrombin-evoked rises in  $[Ca^{2+}]_{ext}$  in DM-BAPTA-loaded platelets.** (A) Fura-2-loaded human platelets suspended in supplemented HBS were preincubated with either  $30 \mu\text{mol.L}^{-1}$  dimethyl-BAPTA/AM, or an equivalent volume of its vehicle, DMSO, for 10 min at  $37^\circ\text{C}$ . Extracellular  $Ca^{2+}$  was then chelated with  $1 \text{ mmol.L}^{-1}$  EGTA and then 1 min later stimulated with  $0.5 \text{ U.mL}^{-1}$  thrombin. (A) Washed human platelets were suspended in supplemented HBS were pre-treated with either  $20 \mu\text{mol.L}^{-1}$  Y-27632 (B), or an equivalent volume of its vehicle, DMSO (B), for 10 min at  $37^\circ\text{C}$ .  $30 \mu\text{mol.L}^{-1}$  dimethyl-BAPTA/AM for the final 10 min of the incubation at  $37^\circ\text{C}$ . A final concentration of  $2.5 \mu\text{mol.L}^{-1}$  Fluo-4 salt was then added immediately before the experiment. Extracellular  $Ca^{2+}$  was then chelated with  $1 \text{ mmol.L}^{-1}$  EGTA (not shown) and then 1 min later stimulated with  $0.5 \text{ U.mL}^{-1}$  thrombin

## **5. Investigating the role of the Na<sup>+</sup>/Ca<sup>2+</sup> exchanger in regulating agonist-evoked Ca<sup>2+</sup> signalling in CD34<sup>+</sup>-derived human megakaryocytes.**

The study of the platelet membrane complex is limited by its nanometer dimensions which preclude any direct live cell imaging, as well as our inability to try to selectively dismantle it by genetic disruption of potential scaffolding molecules. These limitations have led to us conducting pilot studies into the potential usefulness of culture-derived megakaryocytes as a model for platelet Ca<sup>2+</sup> signalling. This seems plausible given that number of similar Ca<sup>2+</sup>-signalling proteins such as Orai1, STIM1, TRPC6, P<sub>2X1</sub> and PAR receptors have been found to be expressed in these cells (Di Buduo *et al.*, 2014). Similarly more recent evidence has shown that megakaryocytes also possess a nanojunction akin to the platelet membrane complex, with the smooth endoplasmic reticulum and demarcation membrane system being shown to be closely apposed (Eckly *et al.*, 2014). If similar roles for the NCX in regulating agonist-evoked Ca<sup>2+</sup> signalling can be demonstrated in these human megakaryocytic cell lineages, then it might be possible to use the larger and genetically-accessible human megakaryocyte as a model system in which to test ideas on the proteins that mediate Ca<sup>2+</sup> signalling or provide a mechanical scaffold to hold this structure together.

### **5.1 Cultured CD34<sup>+</sup> cells exhibit development of features of mature megakaryocytes as well as an extensive network of intracellular Ca<sup>2+</sup> stores. These morphological features are not affected by culturing with calcitriol.**

Previous studies have demonstrated the effectiveness of culturing human megakaryocytic lineages from bone marrow- and cord-derived CD34<sup>+</sup> cells in liquid

culture (Pineault *et al.*, 2013) We have utilised the method of Pineault *et al.*, (2013) to culture human megakaryocytic lineages from these cells. Recent work in our laboratory have defined that the use of a liquid culturing incorporating a cytokine cocktail of TPO, IL-6, IL-9 and SCF is able to induced cells with a number of features of mature megakaryocytic cells within 7-9 days of initiation of the liquid culture. These features include a significant expansion in diameter to above 20  $\mu\text{m}$ , development of a multi-lobular nucleus and demarcation membrane system, and increased expression of cell surface markers of this lineage such as CD41a and CD42b (A. Al-Ghannam and A.G.S. Harper, personal communication).

Previous studies have provided evidence for an increase in  $\text{Na}^+/\text{Ca}^{2+}$  exchange activity in cells additionally exposed to calcitriol (1,25-dihydroxycholecalciferol) in the latter stages of the culture system. Initial studies were conducted to examine whether the inclusion of calcitriol into the culture system can alter the normal development of the  $\text{CD}34^+$  cells. Cells were cultured for 4 days in the conditions previously described with Pineault *et al.*, (2013). On this day the cultures were further supplement with either calcitriol or an equivalent volume of its vehicle DMSO, and these cells were then cultured for a further 3 days. On Day 7 the cells were loaded with the nuclear dye, Hoechst 33342, and an indicator of intracellular  $\text{Ca}^{2+}$  stores, Fluo-5N (Sage *et al.*, 2011). These cells were then imaged in the presence of Rhod-5N as an indicator of the extracellular fluid to help visualise the demarcation membrane system using an analogous method to (Mahaut Smith *et al.*, 2003) Fluo-5N fluorescence in both DMSO- and Calcitriol-treated megakaryocytes had a punctate distribution demonstrating a widespread distribution of the stores throughout the cells. The mean Fluo-5N fluorescence level was same in both culture conditions, with no significant difference in both DMSO- and calcitriol-treated cells ( $264.0 \pm 65.8$  and  $355.0 \pm 75.0$  arbitrary

units for DMSO- and calcitriol-treated cells respectively;  $n = 4$ ;  $P = 0.45$ ; Fig 5.1) Similarly Rhod -5N fluorescence was found widely distributed within the inner boundary of the megakaryocytes consistent with the presence of a DMS in both cell significantly difference in both DMSO- and calcitriol-treated cells ( $612.4 \pm 218.0$  and  $620.0 \pm 167.2$  arbitrary units for DMSO- and calcitriol-treated cells respectively;  $n = 4$ ;  $P = 0.97$ ; Fig 5.1). Hoechst 33342 fluorescence indicated the presence of bi- or multi-lobular nuclei characteristic of more mature megakaryocytic lineages in both the DMSO- and Calcitriol-treated cell populations. These results demonstrate that calcitriol pre-treatment has no detectable effect on the development of the intracellular structures within the CD34<sup>+</sup>-cultured megakaryocytes.

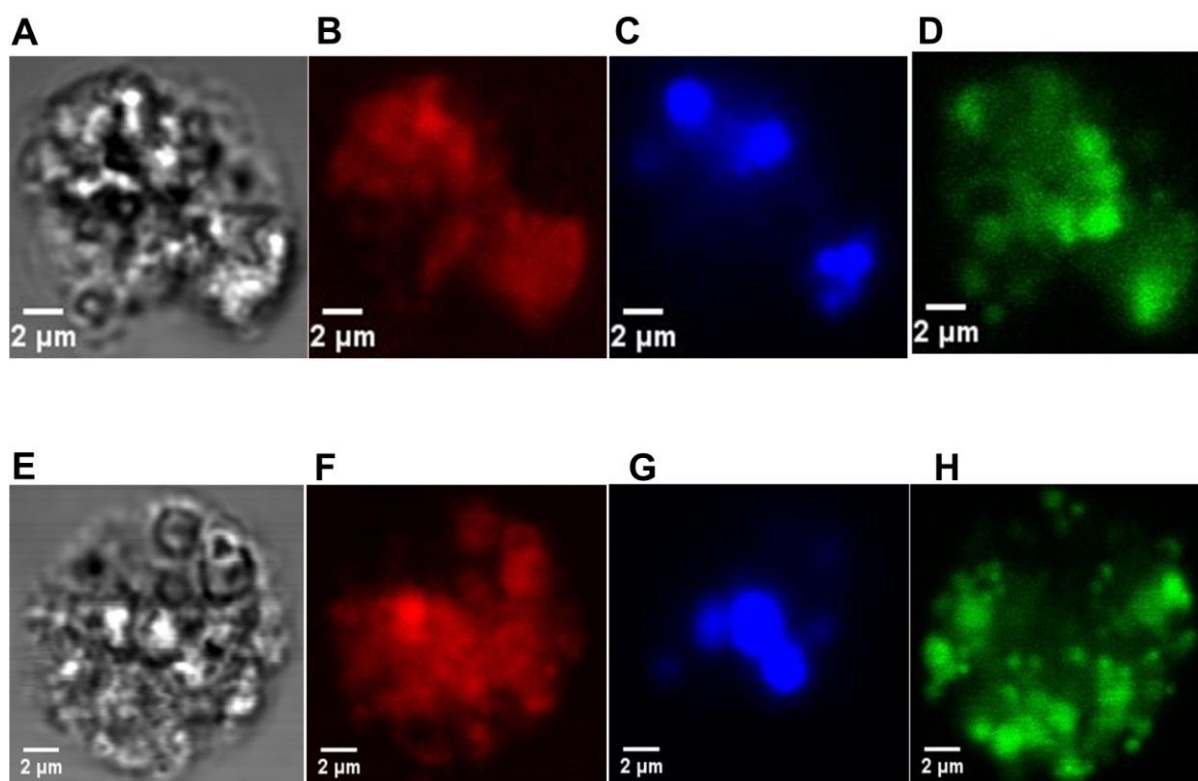


**Fig 5.1 Treatment with calcitriol has no significant effect on the morphology of CD34<sup>+</sup>-cultured human megakaryocytes.** Megakaryocytic CD34<sup>+</sup> cell cultures were supplemented on day 4 with either 100 nM calcitriol (E-H), or an equivalent volume of sterile DMSO(A-D). On Day 7 cells were loaded with Fluo-5N and Hoechst 33342. Cells were washed and resuspended into supplemented HBS containing 1 mmol.L<sup>-1</sup> CaCl<sub>2</sub> and 5 μmol.L<sup>-1</sup> Rhod-5N salt. Cells were allowed to adhere and spread on poly-L-lysine-coated coverslips. Fluorescence was then monitored with a Fluoview FV 1200 laser scanning confocal microscope. Fluo-5N fluorescence (D, H; green image), Rhod 5N fluorescence (B,F ; red image), Hoechst fluorescence (C, G; blue image) and transmitted light (A,E) images of cells are shown.

## 5.2 Pre-treatment with NCX inhibitor, KB-R7943, alters thrombin-evoked Ca<sup>2+</sup> signalling in CD34<sup>+</sup>-derived megakaryocytic cells.

Ca<sup>2+</sup> signalling plays a key role in regulating human megakaryocytic function (Di Buduo *et al.*, 2014). Previous studies have demonstrated that maturing megakaryocytes from CD34<sup>+</sup> cells develop thrombin-evoked Ca<sup>2+</sup> signalling (den Dekker *et al.*, 2001). To see if these cells may elicit Ca<sup>2+</sup> signalling in an analogous manner to human platelets, experiments were performed to examine whether pre-treatment of CD34<sup>+</sup>-cultured megakaryocytic cells with KB-R7943 elicits similar effects to those previously seen in the presence and absence of extracellular Ca<sup>2+</sup> (Sage *et al.*, 2013).

When stimulated in the absence of extracellular Ca<sup>2+</sup>, KB-R7943 pre-treatment yielded a significant reduction in thrombin-evoked rise in [Ca<sup>2+</sup>]<sub>cyt</sub> to 63.2 ± 10.4 % of control (n = 7; P < 0.05; Fig 5.2A), in line with our previous findings in human platelets (Sage *et al.*, 2013). Whereas KB-R7943 pre-treatment had no significant effect on thrombin-evoked rises in [Ca<sup>2+</sup>]<sub>cyt</sub> elicited in the presence of extracellular Ca<sup>2+</sup> (96.6 ± 13.1 % of control; n = 12; P > 0.05; Fig 5.2B). This lack of consistent effect on thrombin-evoked signalling was unexpected as the data would have expected some effect.

We therefore considered whether the results were due to a maturation-dependent effect on NCX expression and/or function, as similar experiments have suggested that megakaryocyte maturation can alter the Ca<sup>2+</sup> signalling proteins they express (den Dekker *et al.*, 2001). This suggests the possibility that the variability in the level of maturation of the megakaryocyte between cultures may account for the lack of

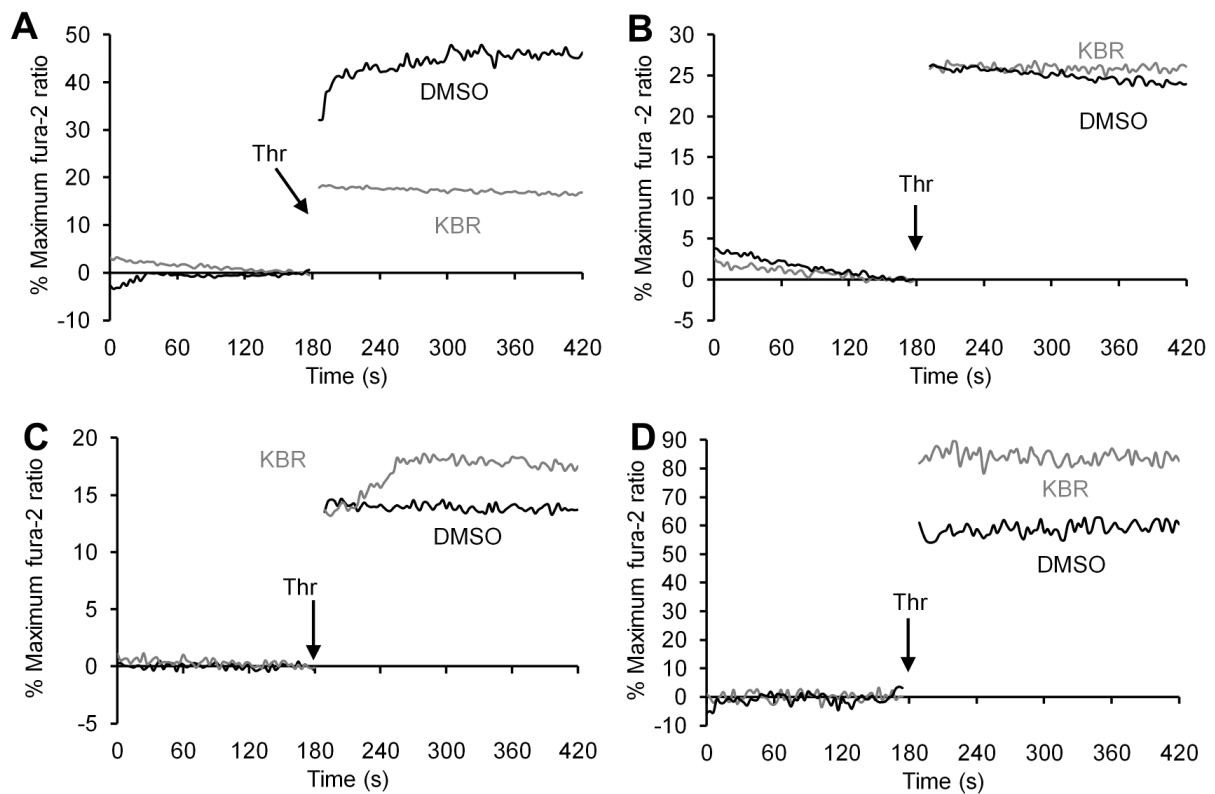


**Figure 5.2** Pretreatment with KB-R7943 alters thrombin-evoked rises in  $[Ca^{2+}]_{cyt}$  in  $CD34^+$ -cultured human megakaryocytes in a maturation-dependent manner. Megakaryocytic  $CD34^+$  cell cultures were initiated in which the cells were exposed to either  $30\text{ ng.mL}^{-1}$  TPO and  $7.5\text{ ng.mL}^{-1}$  IL-6 (A,B) or  $50\text{ ng.mL}^{-1}$  TPO and  $20\text{ ng.mL}^{-1}$  IL-6 (C,D). On day 7-9 of the culture cells were loaded with Fura-2. Cells were then washed and resuspended in supplemented HBS. Extracellular  $Ca^{2+}$  was then either raised to  $1\text{ mmol.L}^{-1}$  (A,C) or chelated by addition of  $1\text{ mmol.L}^{-1}$  EGTA (B,D). Cells were then stimulated with  $0.5\text{ U.mL}^{-1}$  thrombin

consistent effect of KB-R7943 on the cells treated in the presence of extracellular  $\text{Ca}^{2+}$ . Initial experiments to assess this possibility therefore examined the effect of KB-R7943 when the concentration of TPO and IL-6 cells were cultured in was increased to  $50 \text{ ng.mL}^{-1}$  and  $20 \text{ ng.mL}^{-1}$  respectively to try to better standardise maturation of the megakaryocytes across cultures. Under these conditions a significant potentiation of the thrombin-evoked rise in  $[\text{Ca}^{2+}]_{\text{cyt}}$  to  $142.7 \pm 18.2$  % of control ( $n = 6$ ;  $P < 0.05$ ; Fig 5.2C) was observed in cells treated in the presence of extracellular  $\text{Ca}^{2+}$ . In contrast, KB-R7943 pre-treatment in the absence of extracellular  $\text{Ca}^{2+}$  did not cause any consistent effect in thrombin evoked rise in  $[\text{Ca}^{2+}]_{\text{cyt}}$  ( $123.8 \pm 29.1$  % of control respectively;  $n = 6$ ;  $P > 0.05$ ; Fig 5.2D). These results suggest the possibility that greater maturation favours greater forward mode NCX activity as inhibition of the NCX removes the consistent inhibition in the absence of extracellular  $\text{Ca}^{2+}$ , and triggers a consistent potentiation in the presence of this cation. How this increased NCX activity is brought about is unclear, but may be due to a change in expression of the receptor or a molecule which regulates its activity. Further work will be needed to examine this further.

### **5.3 KB-R7943 inhibits thrombin-evoked rises in $[\text{Na}^+]_{\text{cyt}}$ in $\text{CD34}^+$ -derived megakaryocytic cells.**

Interference with NCX function should impact on both thrombin-evoked rises in  $[\text{Ca}^{2+}]_{\text{cyt}}$  and  $[\text{Na}^+]_{\text{cyt}}$ . If KB-R7943 is blocking forward mode exchange then it should reduce thrombin-evoked rises in  $[\text{Na}^+]_{\text{cyt}}$ , whereas if reverse mode exchange is being inhibited then it should potentiate this parameter. To confirm the previous findings of an effect of forward-mode activity, experiments were also performed to examine the effect of KB-R7943 pre-treatment on thrombin-evoked rises in  $[\text{Na}^+]_{\text{cyt}}$  in megakaryocytes treated with the higher doses of cytokines. Pre-treatment of

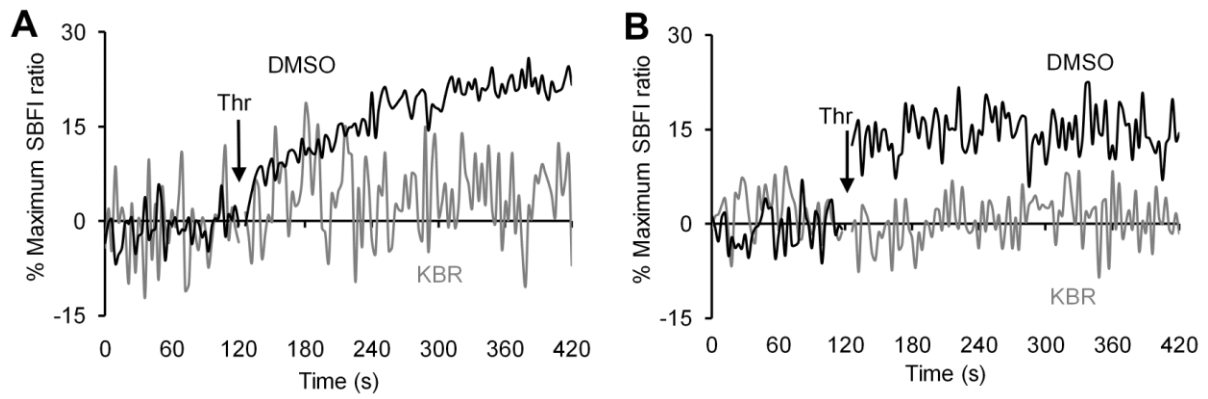


**Figure 5.3 Pre-treatment with KB-R7943 inhibits thrombin-evoked rises in  $[Na^+]_{cyt}$  in CD34<sup>+</sup>-cultured human megakaryocytes.** Megakaryocytic CD34<sup>+</sup> cell cultures were loaded with SBFI on day 7-9 of the culture. Cells were then washed and resuspended in supplemented HBS. Extracellular Ca<sup>2+</sup> was then either raised to 1 mmol.L<sup>-1</sup> (A) or chelated by addition of 1 mmol.L<sup>-1</sup> EGTA (B). Cells were then stimulated with 0.5 U.mL<sup>-1</sup> thrombin

megakaryocytes with KB-R7943 in the presence and absence of extracellular  $\text{Ca}^{2+}$  appeared to almost abolish the thrombin evoked rise in  $[\text{Na}^+]_{\text{cyt}}$  in four out of the five experiments, and significantly inhibit in the other. These data would appear to indicate that KB-R7943 is inhibiting forward mode exchange as KB-R7943 prevents  $\text{Na}^+$  entry into the cell, thus indicating that  $\text{Ca}^{2+}$  must be moving out in the opposite direction. These data also indicate that the forward mode NCX activity is the only significant  $\text{Na}^+$  entry triggered into the megakaryocyte under these conditions.

The abolishment of the  $\text{Na}^+$  rise in KB-R7943-treated cells is surprising as it would be likely that other  $\text{Na}^+$ -permeable channels such as TRPC6 would also be activated by thrombin stimulation (Tolhurst, Carter et al. 2008). These results may suggest the possibility that this NCX inhibitor may be having off-target effects on other cells (Kraft 2007). However the previous data on rises in  $[\text{Ca}^{2+}]_{\text{cyt}}$  showed that  $\text{Ca}^{2+}$  was not significantly blocked in all occasions by pre-treatment with KB-R7943, suggest that  $\text{Ca}^{2+}$ -permeable ion channels are not significantly affected by treatment with this drug. (Fig 5.3A,B). These data suggest that an off-target effect on TRPC channels is unlikely to account for all the data, and that the drugs are inhibiting forward mode activity of the NCX. The most likely reason for being unable to pick up any rises in KB-R7943-treated cells is that this microplate-based assay only has a limited dynamic range and so is not sufficiently sensitive enough to pick up the small residual  $\text{Na}^+$  entry which remains after blockade of the NCX. Repeating these experiments with higher cell number may help us better identify the  $\text{Na}^+$ -permeable pathways in cultured megakaryocytes.

#### 5.4 Replacement of extracellular sodium with NMDG alters thrombin-evoked $\text{Ca}^{2+}$ signalling in megakaryocytes

As NCX inhibitors are known to have non-specific effects on other targets, experiments were also performed to examine the effect of inhibiting NCX function elicited by replacement of  $\text{Na}^+$  in the extracellular medium with an equimolar amount of the non-permeant organic cation, NMDG (Harper & Sage, 2007). Replacement of extracellular  $\text{Na}^+$  with NMDG was shown in initial experiments to significantly reduce thrombin-evoked  $\text{Na}^+$  rises, in line with the loss of the transmembrane sodium gradient ( $25.3 \pm 16.1\%$  and  $7.4 \pm 5.0\%$  of control when stimulated in the presence and absence of  $\text{Ca}^{2+}$  respectively,  $n = 7$ ;  $P < 0.05$ ; Fig 5.4 A,B). Replacement of extracellular  $\text{Na}^+$  with NMDG potentiated thrombin-evoked  $\text{Ca}^{2+}$  signals elicited in the absence of extracellular  $\text{Ca}^{2+}$  to  $162.3\% \pm 38.4\%$  of control ( $n = 8$ ;  $P < 0.05$ ; Fig 5.4C). However there was no consistent effect of  $\text{Na}^+$  replacement on thrombin-evoked rises in  $[\text{Ca}^{2+}]_{\text{cyt}}$  when the megakaryocytic cells were stimulated in the presence of extracellular  $\text{Ca}^{2+}$  ( $118.4\% \pm 19.1\%$  of control when stimulated in the presence and absence of  $\text{Ca}^{2+}$  respectively,  $n = 8$ ;  $P > 0.05$ ; ; Fig 5.4D). Both KB-R7943 and NMDG appear to elicit a tendency towards potentiating the thrombin-evoked  $\text{Ca}^{2+}$  signals observed in cells treated with the higher cytokine concentrations. This would also be consistent with the observed inhibitor effect of KB-R7943 on thrombin-evoked rises in  $[\text{Na}^+]_{\text{cyt}}$ . However, the pattern of inhibition is not consistent when observed in the presence and absence of extracellular  $\text{Ca}^{2+}$ . This inconsistency may be due to the limitations of the use of a single wavelength microplate-based assay. Alternatively it may indicate that megakaryocytes have a mixture of both forward and reverse mode activity in response to stimulation, as KB-R7943 preferentially inhibits reverse mode (Watano *et al.*, 1996) variable blocking of forward mode activity may allow this effect to predominate in some

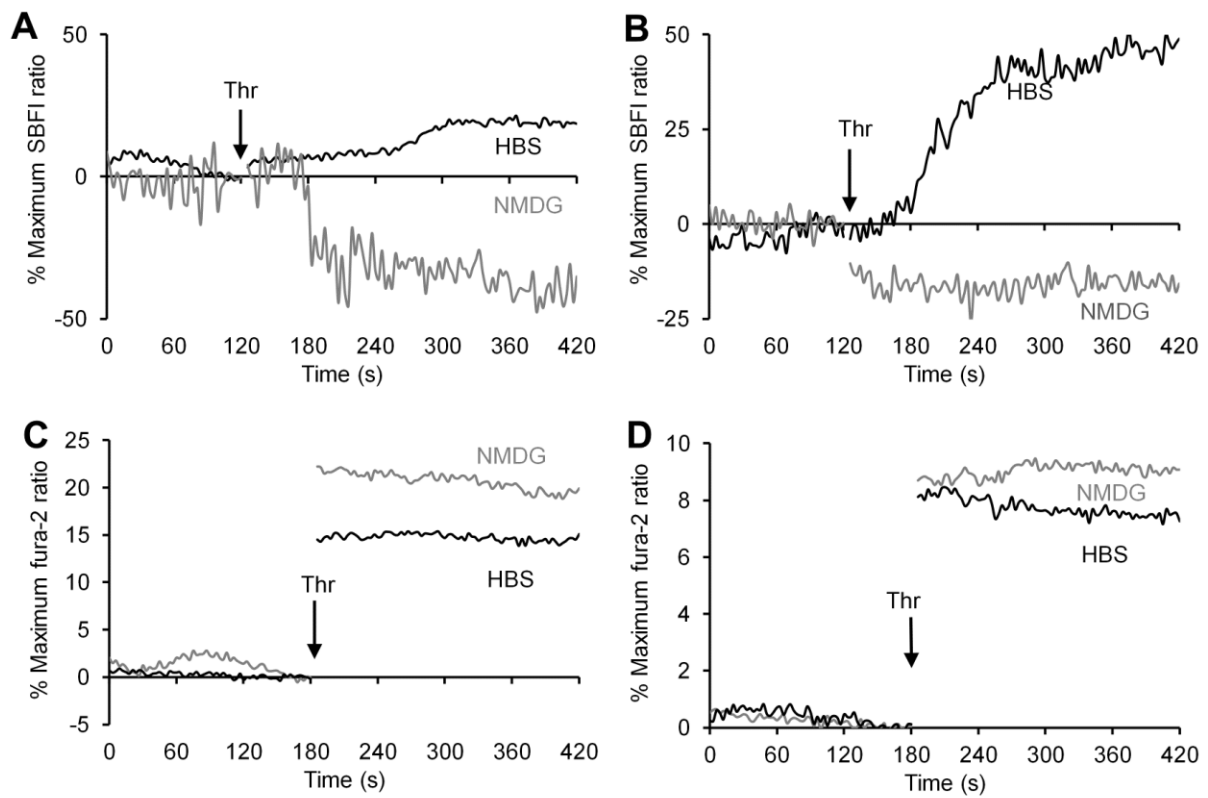


**Figure 5.4 Na<sup>+</sup> replacement affects thrombin-evoked Ca<sup>2+</sup> signalling in CD34<sup>+</sup>-cultured megakaryocytes.** Megakaryocytic CD34<sup>+</sup> cell cultures were loaded with either SBFI (A,B) or Fura-2 (C,D) on day 7-9 of the culture. Cells were then washed and resuspended in either supplemented HBS or an HBS in which Na<sup>+</sup> was replaced with an equimolar amount of NMDG. Extracellular Ca<sup>2+</sup> was then either chelated by addition of 1 mmol.L<sup>-1</sup> EGTA (A,C) or raised to 1 mmol.L<sup>-1</sup> (B,D). Cells were then stimulated with 0.5 U.mL<sup>-1</sup> thrombin

runs leading to the inconsistent effects. Further work will be required to examine these possibilities more closely.

### **5.5 Calcitriol differentially affects thrombin-evoked $\text{Ca}^{2+}$ signalling elicited in the presence and absence of extracellular $\text{Ca}^{2+}$ in $\text{CD34}^+$ -derived megakaryocytic cells.**

Previous studies demonstrated that genetic knock-out of the klotho protein can lead to an upregulation of NCX-mediated activity in megakaryocytes from these mice (Schmid *et al.*, 2015). Klotho is a type 1 transmembrane protein highly expressed in kidney parathyroid glands, and epithelial cells of choroid plexus of brain but not expressed in platelets or megakaryocytes (Kuro-o *et al.*, 1997; Okada *et al.*, 2000; Yoshida *et al.*, 2002; Kurosu *et al.*, 2005; John *et al.*, 2011). Klotho is a negative regulator of the endogenous formation of Calcitriol, and therefore its remove leads to excessive production of this compound. Calcitriol has been shown to be a negative regulator of agonist-evoked rises in  $[\text{Ca}^{2+}]_{\text{cyt}}$  in both platelets and megakaryocytes (Kuro-o *et al.*, 1997; Tsujikawa *et al.*, 2003; Borst *et al.*, 2014). This effect on megakaryocytes appears to be due to an up-regulation of NCX activity which is capable of downregulating the net  $\text{Ca}^{2+}$  signal seen from store-operated  $\text{Ca}^{2+}$  entry (Schmid *et al.*, 2015).

Experiments were performed to investigate whether supplementation of the megakaryocyte liquid culture with calcitriol for the last 72 hours of the culture can alter the thrombin-evoked  $\text{Ca}^{2+}$  signals. Calcitriol elicited a significant reduction in the thrombin-evoked  $[\text{Ca}^{2+}]_{\text{cyt}}$  rises seen in the absence of extracellular  $\text{Ca}^{2+}$  to  $76.6 \pm 6.4$  % of control ( $n = 6$ ;  $P < 0.05$ ; Fig 5.5A). In contrast, initial studies performed with  $\text{Ca}^{2+}$

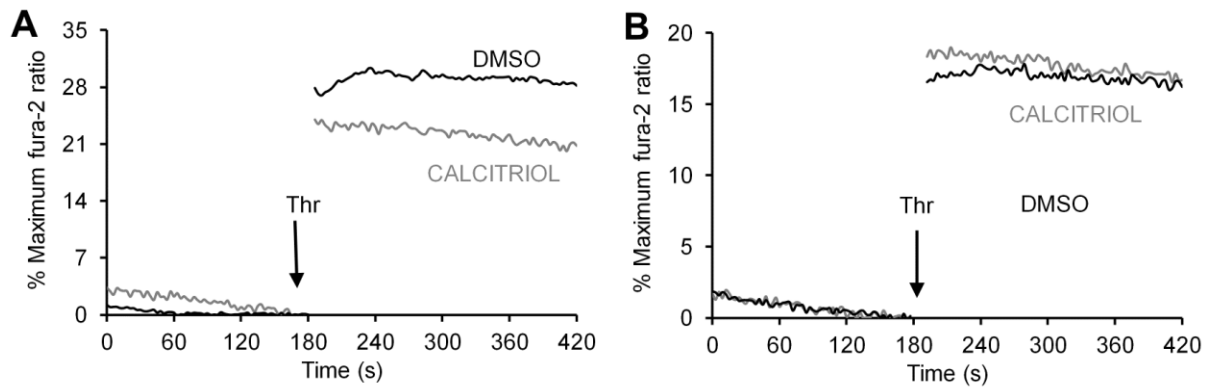


**Figure 5.5 Calcitriol alters thrombin-evoked  $\text{Ca}^{2+}$  signals both in the presence and absence of extracellular  $\text{Ca}^{2+}$  in  $\text{CD34}^+$ -derived megakaryocytic cells.** Megakaryocytic  $\text{CD34}^+$  cell cultures were supplemented on day 4 with either  $100 \text{ nmol.L}^{-1}$  calcitriol, or an equivalent volume of sterile DMSO. On Day 7 cells were loaded with Fura-2, washed and resuspended in supplemented HBS in which extracellular  $\text{Ca}^{2+}$  was either chelated by addition of  $1 \text{ mmol.L}^{-1}$  EGTA (A) or raised to  $1 \text{ mmol.L}^{-1}$  (B). Cells were then stimulated with  $0.5 \text{ U.mL}^{-1}$  thrombin

in the extracellular medium showed that calcitriol treatment tended to increase thrombin-evoked  $\text{Ca}^{2+}$  signals to  $117.1 \pm 35.0$  % of control ( $n = 4$ ;  $P = 0.73$ ; Fig 5.5B), although further repetitions of this work will be required to confirm this preliminary finding.

These results suggest that up regulation of NCX activity leads to a net increase in forward mode NCX activity in the absence of extracellular  $\text{Ca}^{2+}$ , as would be expected in line with previous studies of the effects of calcitriol in platelets (Borst *et al.*, 2014). In contrast, our preliminary studies in the presence of extracellular  $\text{Ca}^{2+}$  suggests that in physiological conditions calcitriol may potentiate thrombin-evoked signalling, possibly via encouraging reverse mode activity. However additional experiments would be needed to confirm that appropriate changes in localised  $[\text{Na}^+]_{\text{cyt}}$  or the membrane potential occur to make this thermodynamically possible.

## **5.6 Calcitriol has no significant effect on NCX3 expression and localisation in megakaryocytes.**

Experiments were performed to investigate whether pre-treatment with Calcitriol increases the basal expression or subcellular distribution of NCX3 in the  $\text{CD34}^+$ -cultured megakaryocytes. To examine this cells were fixed from cultures pre-treated with either Calcitriol or DMSO and stained using the immunolabelling approaches defined for platelets in chapter 4.

Fluorescent imaging of NCX3-labelled megakaryocytes found fluorescence predominantly found associated within bright puncta within the inner regions of the cell. This labelling was not due to non-specific binding of the secondary antibody as primary free control samples taken from each of the cultures did not show any significant staining (Fig 5.6). As the samples were not permeabilised prior to antibody,

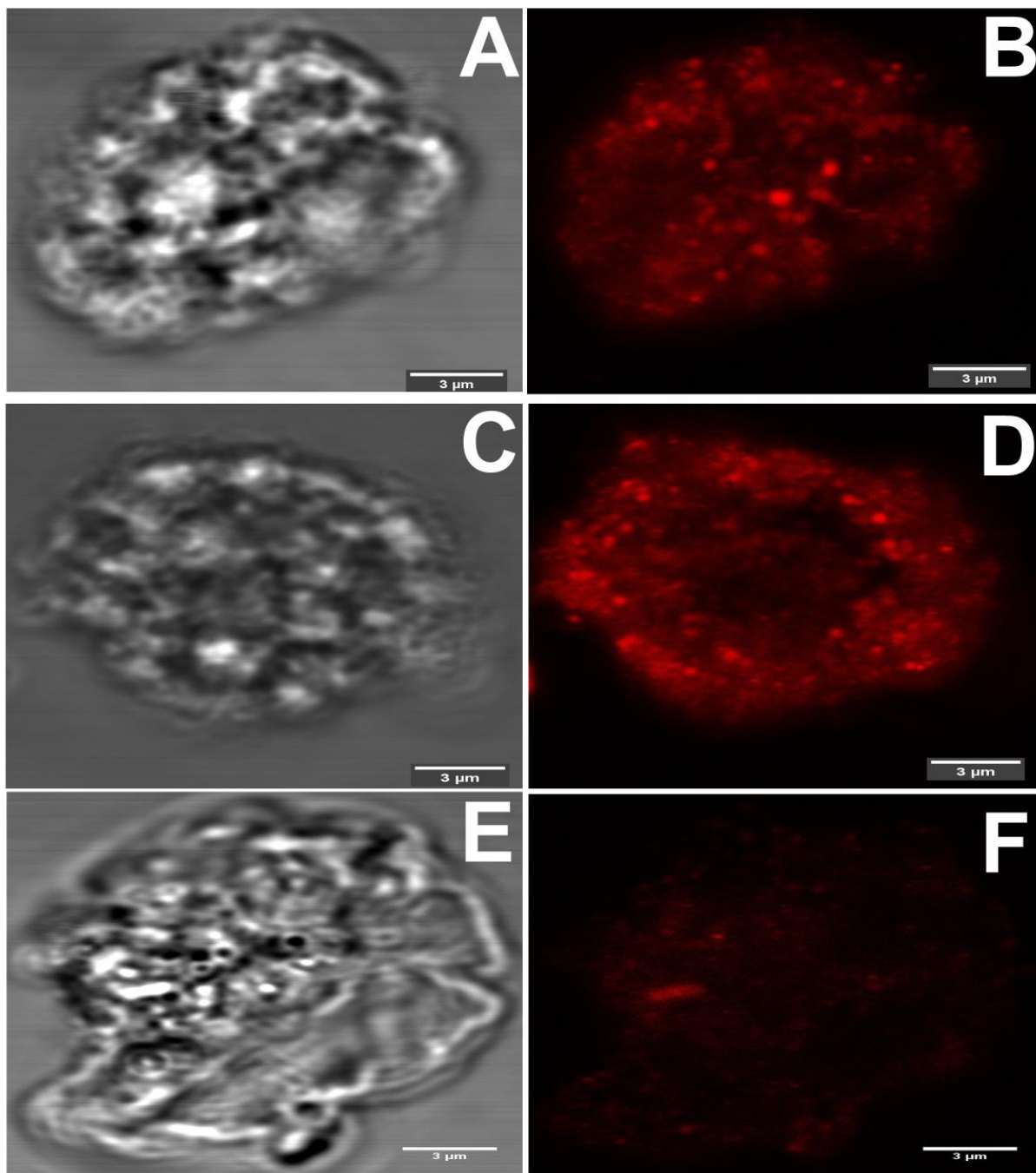


**Figure 5.6 NCX3 appears to be localised within the demarcation membrane system of CD34<sup>+</sup> derived megakaryocytes.** (A-D) Day 4 cells were treated with DMSO (A, B) or 100 nmol.L<sup>-1</sup> calcitriol (C, D) or no antibody (E,F). On Day 7 cells were fixed and incubated with NCX 3 antibody followed by a fluorophore-conjugated secondary antibody. Cells were washed and resuspended in supplemented HBS. The labelled cells were allowed to settle for 10 min on poly-L-lysine –coated chambered slide. Fluorescent images were captured using a Fluoview FV 1200 laser scanning confocal microscope (Olympus, UK) with a PLAPON 100x oil immersion objective. Images for fluorescence alone (left) or overlaid over the transmitted light image (right) are shown. The results presented are representative of 3 experiments respectively.

these results suggest that the NCX3 is likely to be found within the demarcation membrane system. However, Calcitriol treatment did not affect the mean fluorescence found within the cell ( $668.7 \pm 45.4$  vs  $673. \pm 45.4$  for DMSO- and Calcitriol-treated cells respectively  $n = 5$ ;  $P > 0.05$ ). These results demonstrate that Calcitriol-treatment has no effect on the basal expression of NCX3 in the cultured megakaryocytes.

There was however some indication that the intensity of individual puncta may be brighter in calcitriol-treated cells suggesting that while NCX3 expression is unchanged there may be a greater concentration of these exchangers in some sub regions of the cell. To examine this, the skew of the pixel fluorescence distribution was measured for all cells, as a higher skew would indicate more outliers in the distribution indicative of an accumulation in a specific subcellular location. Although there was a tendency to more outliers in the pixel fluorescence distribution of cells, this effect was not significantly different overall (Skew =  $1.7 \pm 0.2$  for DMSO-treated cells and  $1.9 \pm 0.2$  for Calcitriol-treated cells;  $n = 5$ ;  $P > 0.05$ ).

Previous studies have demonstrated that Calcitriol upregulates  $\text{Na}^+/\text{Ca}^{2+}$  exchanger activity in megakaryocytes (Schmid *et al.*, 2015). Our data here suggests that this change may not be due to an increased expression of the NCX3 isoform in the cultured megakaryocytes. Instead this effect may be due to either changed expression of other NCX-regulating proteins or upregulation of expression of a distinct NCX isoform such as NCX1, which has previously been reported to have a low level of expression in human platelets (Roberts *et al.*, 2012). Further work will be required to define this effect more closely.

## 6. Discussion

### 6.1 Human platelets contain a functionally-isolated cytosolic nanodomain which links intracellular $\text{Ca}^{2+}$ release with the $\text{Na}^+/\text{Ca}^{2+}$ exchanger

Previous work in our lab has demonstrated that human platelet  $\text{Ca}^{2+}$  signalling utilises a pericellular  $\text{Ca}^{2+}$  recycling system. This model hypothesises that  $\text{Ca}^{2+}$  release from intracellular  $\text{Ca}^{2+}$  stores occurs initially into a cytosolic nanodomain enclosed within the membrane complex. This hypothesis arose from a previous quantitative analysis of recorded  $\text{Na}^+$  and  $\text{Ca}^{2+}$  fluxes observed out of platelets, which suggested that NCX removal must be intimately associated with  $\text{Ca}^{2+}$  release from intracellular stores (Sage *et al.*, 2013). However, despite the data providing circumstantial evidence for such a nanodomain being present in human platelets, no direct data thus far exists for it.

The work in this thesis has provided the first evidence for the presence of a cytosolic  $\text{Ca}^{2+}$  nanodomain in human platelets. Experiments consistently demonstrated that stimulating DM-BAPTA-loaded platelet with thrombin in the absence of extracellular  $\text{Ca}^{2+}$  prevents any notable rises in cytosolic  $\text{Ca}^{2+}$  concentration. Despite there being no notable  $\text{Ca}^{2+}$  rises in these cells, it was still possible to observe an NCX-mediated  $\text{Ca}^{2+}$  removal from these cells. This is possible as Dimethyl BAPTA buffers  $\text{Ca}^{2+}$  rapidly and thus spatially restricts the spread of free  $\text{Ca}^{2+}$  from its point of entry into the cytosol, however it does not bind it instantly allowing  $\text{Ca}^{2+}$  signals within the nanodomain of cytosol surround the  $\text{Ca}^{2+}$ -permeable channel (Neher & Almers, 1986; Stern, 1992; Deisseroth *et al.*, 1996; Neher, 1998; Parekh, 2008). This therefore suggests that  $\text{Ca}^{2+}$  release from the intracellular stores must be intimately associated with the NCX to prevent it from being buffered by BAPTA before it reaches this exchanger. Previous

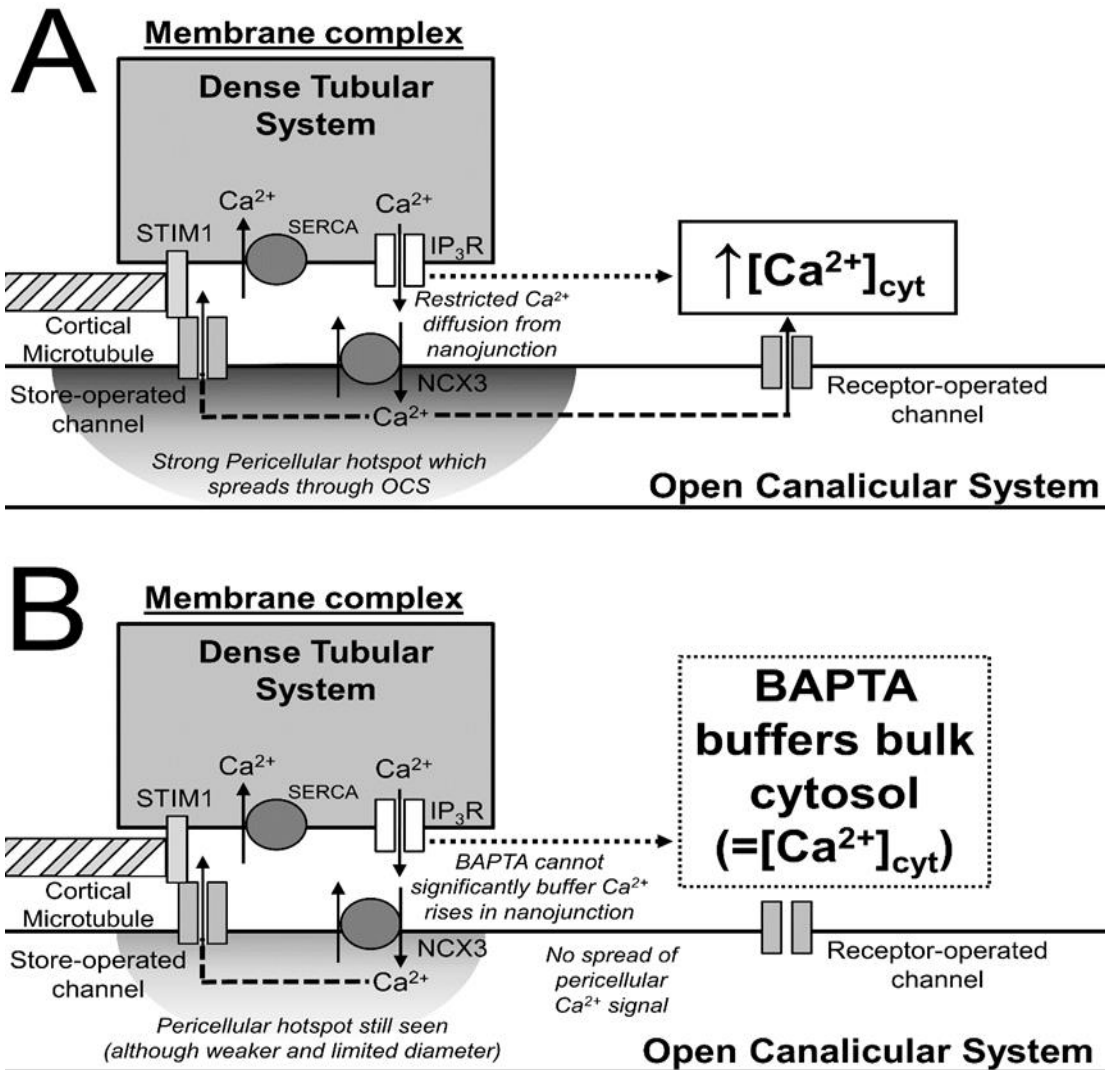


**Fig 6.1 A model of how DM-BAPTA-loading affects human platelet Ca<sup>2+</sup> signalling** (A) In untreated platelets, Ca<sup>2+</sup> release from the dense tubular system occurs into cytosolic nanodomain enclosed within the membrane complex. The NCX present in this cytosolic nanodomain functions in forward mode direction to remove the Ca<sup>2+</sup> into open canalicular system. Ca<sup>2+</sup> accumulated in the open canalicular system then recycles back into the cytosol through Ca<sup>2+</sup> permeable ion channels. This recycled Ca<sup>2+</sup> helps maintain an elevated [Ca<sup>2+</sup>]<sub>cyt</sub> as well as facilitate triggering of dense granule secretion (B) DM-BAPTA is a fast Ca<sup>2+</sup> chelator efficiently buffers Ca<sup>2+</sup> in the bulk cytosol but will not affect Ca<sup>2+</sup> signals within about 20 nm of its point of entry into the cytosol. In DM-BAPTA-loaded cells, the thrombin-evoked rise in bulk [Ca<sup>2+</sup>]<sub>cyt</sub> is prevented. However Ca<sup>2+</sup> entry or release into enclosed areas of the cytosol, such as those in the MC, could occur relatively unaffected. This allows the NCX to continue to remove Ca<sup>2+</sup> released from the DTS into the pericellular region in DM-BAPTA-loaded cells creating a pericellular Ca<sup>2+</sup> hotspot.

work by other investigators have suggested that this apposition of the IP<sub>3</sub>R and NCX must be within 10-20 nm (Neher & Almers, 1986; Stern, 1992; Deisseroth *et al.*, 1996; Neher, 1998; Parekh, 2008) to allow Ca<sup>2+</sup> transport to be unaffected by the presence of DM-BAPTA. As the MC is the only location in which the DTS and plasma membrane come into close enough contact. This provides a clear indication that the transporters must be localised to the MC (White, 1972; van Nispen tot Pannerden *et al.*, 2010). Disorganisation of the DTS structure in platelets by pre-treating with nicergoline, significantly reduced the thrombin-evoked rise in [Ca<sup>2+</sup>]<sub>cyt</sub>, in line with a destabilisation of the normal close relationship between the intracellular stores and the plasma membrane creating the cytosolic nanodomain that has been identified here.

The punctate localisation of the NCX3 antibody inside the boundaries of the platelet suggests that NCX3 is found predominantly in specific sites within the OCS. From our previous data this would be consistent with NCX3 antibody being found at the membrane complex. An interesting finding was that pretreatment of platelets with nicergoline disrupts this distribution leading to a more homogenous distribution of fluorescence throughout the inner reaches of the cell. This suggests that the microtubule-dependent localisation of the DTS also has a knock-on effect on the distribution of the OCS-localised NCX3. These results would therefore suggest the presence of a multimolecular complex that helps bind NCX3 into this localisation within the cell. Further work will be required to identify the identity of this scaffold of proteins that hold this protein in place.

Examination of single cell images of the pericellular Ca<sup>2+</sup> signal showed that DM-BAPTA-loaded platelets could still generate Ca<sup>2+</sup> hotspots, although they were often weaker and smaller than signals seen previously. In addition, pericellular Ca<sup>2+</sup> signals very rarely spread through the platelets. These results therefore suggest that BAPTA-

loading also prevents calcium-induced calcium release (CICR) which is likely responsible for augmenting thrombin-evoked  $\text{Ca}^{2+}$  release (Somasundaram *et al.*, 1997; van Gorp *et al.*, 2002; Sage *et al.*, 2013) and this prevents the platelet from creating stronger pericellular signals which are then able to spread effectively down their concentration gradient. This therefore creates a situation in which we can study the functional properties of the  $\text{Ca}^{2+}$  rise in this nanodomain in isolation.

## **6.2 A role for the cytosolic nanodomain in controlling platelet shape change**

Many platelet functional responses are inhibited by DM-BAPTA-loading thereby demonstrating that  $\text{Ca}^{2+}$  rises in the cytosolic nanodomain alone are not sufficient to elicit functions such as granule secretion or platelet aggregation (Paul *et al.*, 1999). However previous studies have found that one of the platelet shape change is insensitive to buffering with this intracellular  $\text{Ca}^{2+}$  chelator, therefore we examined the effect of manipulations of the  $\text{Ca}^{2+}$  concentration within the microdomain. By utilising pharmacological inhibitors of  $\text{IP}_3\text{R}$  and the NCX, we have found that both of these transporters are likely to be responsible for controlling  $\text{Ca}^{2+}$  in this cytosolic through their ability to modulate the shape change responses seen in these cell types. Further work will be required to see if other channels and transporter might also be able to contribute to this effect.

Our experiments utilising ROCK and MLCK inhibitors have demonstrated a selective role for the  $\text{Ca}^{2+}$ -dependent MLCK response in mediating the thrombin-evoked shape change in our cells. These results therefore confirm that modulation in the  $\text{Ca}^{2+}$  concentration within this nanodomain is responsible for the functional effects we see. It will also be interesting to examine whether other  $\text{Ca}^{2+}$  effectors could be selectively localised at this nanodomain

### **6.3 To what extent are culture-derived megakaryocytes a model for human platelet Ca<sup>2+</sup> signalling?**

The pilot studies examining the role of NCX in human megakaryocytic function suggest that like platelets, agonist-evoked rises in [Ca<sup>2+</sup>]<sub>cyt</sub> in human megakaryocytes are closely regulated by the action of the NCX. This appears to be principally due to inhibition of forward mode activity facilitating Ca<sup>2+</sup> removal, which is similar to what was previously observed in human platelets (Harper *et al.*, 2009; Sage *et al.*, 2013). However, unlike human platelets, the overall effect of blocking this Ca<sup>2+</sup> removal is to potentiate the elicited Ca<sup>2+</sup> signal rather than the inhibition observed in platelets (Harper *et al.*, 2009; Sage *et al.*, 2013). This suggests that Ca<sup>2+</sup> removal could be linked to Ca<sup>2+</sup> release in these cells, but that Ca<sup>2+</sup> recycling back into the cell is not required to help maintain Ca<sup>2+</sup> signals or trigger autocrine stimulation of these cells as seen in platelets (Sage *et al.*, 2013)

Our labelling data indicates that NCX3 may be localised in numerous puncta deep within the demarcation membrane system. Given the recent demonstration that the demarcation membrane system closely couples with portions of the smooth endoplasmic reticulum, this binding would leave open the possibility that the NCX3 is similarly localised within the megakaryocyte equivalent of the platelet membrane complex (Eckly *et al.*, 2014). Therefore, further studies examining Ca<sup>2+</sup> removal from DM-BAPTA-loaded megakaryocytes may be useful as it may be possible to use the cultured megakaryocyte model in which to study the development of the platelet membrane complex and the Ca<sup>2+</sup> signalling systems localised within it. Such a system may be valuable for helping to further our understanding of this poorly understood feature of platelet morphology.

The effect of calcitriol and higher cytokine concentration on megakaryocyte sensitivity to NCX inhibitors, suggests that NCX regulation changes significantly during development of the megakaryocyte. These effects may be brought about by a number of different ways including altering expression of NCX3 or other NCX isoforms, altering expression of regulators of  $[Na^+]_{cyt}$  such as the  $Na^+/K^+$ -ATPase and TRPC channels, or altering expression of other molecules known to affect NCX function (e.g. ATP, PKC and PKA activity). Further work will be required to distinguish these affects.

#### **6.4 Future Plans**

Here we have provided evidence for the presence of an NCX-associated cytosolic nanodomain involved in regulating  $Ca^{2+}$  signalling in human platelets. We have demonstrated that this nanodomain is probably enclosed within the membrane complex of the platelet. Although these results indicate the possibility that NCX3 could be localised at the MC, electron microscopy studies will be needed to confirm this.

As nicergoline can disrupt the distribution of NCX3, it appears that the distribution of this exchanger is determined by its connection with the cortical microtubules and/or the DTS as part of a larger complex. Therefore, further experiments will also be needed to identify the mechanisms that help create the punctate distribution within platelets. These may be due to chaperone proteins holding the NCX3 at the MC, or could be due to its recruitment to specific domains within the plasma membrane. Our early results suggested the possibility of the NCX3 being localised within lipid rafts, but the effects of MBCD on the  $Na^+$  gradient makes this difficult to identify. Western blotting of isolated lipid raft sub fractions of platelets may allow us to better examine this hypothesis.

This and previous work has suggested some interesting avenues for further investigation. For instance, the sensitivity of platelets to 2-APB pre-treatment of the KB-R7943- induced shape change suggests that IP<sub>3</sub>R1 is likely the principle mediator of Ca<sup>2+</sup> release into this nanodomain. It will also be interesting to find whether IP<sub>3</sub>R2 is potentially localised at the membrane complex. Since this and previous data has suggested the close apposition of the IP<sub>3</sub>R and NCX, Fluorescence resonance energy transfer imaging could be used to confirm this close co-localisation of IP<sub>3</sub>R coupled with NCX in human platelets. Our work on the platelet shape change has indicated the possibility that certain subgroups of platelet effector proteins such as calmodulin may be found localised with the cytosolic nanodomain contained within the MC. Further work will be required to examine whether there is a preferential localisation of calmodulin and/or its downstream effector, MLCK in the same sub region as we have found for NCX3. It would also be useful to examine whether other effectors such as CalDAG-GEFI are also localised here, as this may provide a basis for characterising the potential effect of MC-disrupting drugs on human platelet function.

The initial work in culture-derived megakaryocytes has indicated that it could provide a good model for studying human platelet Ca<sup>2+</sup> signalling. However, a wider characterisation of the NCX system in these cells is required. For instance, experiments exploring the expression of NCX1, and whether calcitriol is able to upregulate its function may be useful to allow us to reconcile some of the inconsistencies of the data presented here. In addition, examining whether other indirect modulators of NCX function, such as Na<sup>+</sup>/K<sup>+</sup>-ATPase, are involved in mediating the effect of calcitriol on megakaryocyte Ca<sup>2+</sup> signalling.

## 6.5 Conclusion

This work has provided evidence to support the hypothesis that platelets possess a cytosolic nanodomain made up by the close association of the dense tubular system with the platelet plasma membrane. This work therefore has shown that platelets possess at least 2 distinct cytosolic sub regions – a cytosolic nanodomain probably contained within the membrane complex and the bulk cytosol surrounding this. This could potentially have important consequences for how  $\text{Ca}^{2+}$  coupling to the effector systems may occur in these cells. The work presented on the shape change has supported the hypothesis that specific  $\text{Ca}^{2+}$ -dependent functions may be localised within the cytosolic nanodomain. These therefore suggest that preferential localisation of effectors in either the cytosolic nanodomain or in the bulk cytosol could affect their ability to respond to agonist-evoked  $\text{Ca}^{2+}$  signalling. This work suggests that disrupting the membrane complex could alter the normal  $\text{Ca}^{2+}$  signalling of platelets as well as disrupting the coupling of this signal to its downstream pathways necessary for activating the platelets. These data therefore support the idea that a MC-disrupting drug could present a new method for creating anti-platelet drugs.

## 7. References

- Adelstein RS (1982). Calmodulin and the regulation of the actin-myosin interaction in smooth muscle and non-muscle cells. *Cell* **30**: 349-350.
- Adelstein RS, Conti MA & Anderson W Jr (1973). Phosphorylation of human platelet myosin. *Proc Natl Acad Sci U S A* **70**: 3115-3119
- Ambrosio AL, Boyle JA & Di Pietro SM (2015). TPC2 mediates new mechanisms of platelet dense granule membrane dynamics through regulation of Ca<sup>2+</sup> release. *Mol Biol Cell* **26**: 3263-3274.
- Ariyoshi H & Salzman EW (1996). Association of localized Ca<sup>2+</sup> gradients with redistribution of glycoprotein IIb-IIIa and F-actin in activated human blood platelets. *Arterioscler Thromb Vasc Biol* **16**: 230-235.
- Bauer MM, Retzer JI, Wilde P, Maschberger M, Essler M, Aepfelbacher, Watson SP & Siess W (1999). Dichotomous regulation of myosin phosphorylation and shape change by Rho-kinase and calcium in intact human platelets. *Blood* **94**: 1665-1672.
- Behnke O (1968). An electron microscope study of the megacaryocyte of the rat bone marrow. I. The development of the demarcation membrane system and the platelet surface coat. *J Ultrastruct Res* **24**: 412-433.
- Behnke O (1970). The morphology of blood platelet membrane systems. *Sem Haematol* **3**: 3-16.
- Blankenship K, Dawson ACB, Aronoff GR & Dean WL (2000). Tyrosine phosphorylation of human platelet plasma membrane (Ca<sup>2+</sup>)-ATPase in hypertension. *Hypertension* **35**: 103-107.
- Blaustein MP & Lederer WJ (1999). Sodium/calcium exchange: its physiological implications. *Physiol Rev* **79**: 763-854.
- Bodin SH, Tronchere & Payrastre B (2003). Lipid rafts are critical membrane domains in blood platelet activation processes. *Biochim Biophys Acta* **1610**: 247-57.
- Born GV (1972). Current ideas on the mechanism of platelet aggregation. *Ann N Y Acad Sci* **20**: 4-12.
- Borsch-Haubold AG, Kramer RM & Watson SP (1995). Cytosolic phospholipase A2 is phosphorylated in collagen- and thrombin-stimulated human platelets independent of protein kinase C and mitogen-activated protein kinase. *J Biol Chem* **270**: 25885-25892.
- Borst OP, Munzer E, Schmid EM, Schmidt A Russo B, Walker W, Yang C, Leibrock K, Sztejn S, Schmidt M, Elvers C, Faggio E, Shumilina M, Kuro-o M, Gawaz & Lang F (2014). 1,25(OH)<sub>2</sub> vitamin D<sub>3</sub>-dependent inhibition of platelet Ca<sup>2+</sup> signaling and thrombus formation in klotho-deficient mice. *FASEB J* **28**: 2108-2119.

Boswell KL, James DJ, Esquibel JM, Bruinsma S, Shirakawa R, Horiuchi H & Martin TF (2012). Munc13-4 reconstitutes calcium-dependent SNARE-mediated membrane fusion. *J Cell Biol* **197**: 301-312.

Bourguignon LY, Iida N & Jin H (1993). The involvement of the cytoskeleton in regulating IP3 receptor-mediated internal Ca<sup>2+</sup> release in human blood platelets. *Cell Biol Int* **17**: 751-758.

Brandt P, Neve R L, Kammesheidt A (1992). Analysis of the tissue-specific distribution of mRNAs encoding the plasma membrane calcium-pumping ATPases and characterization of an alternately spliced form of PMCA4 at the cDNA and genomic levels. *J Biol Chem*, **267**: 4376–4385

Brass LF (2003). Thrombin and platelet activation. *Chest* **124**: 18S-25S.

Braun AD, Varga-Szabo C, Kleinschnitz I, Pleines M, Bender M, Austinat M, Bosl G, Stoll & Nieswandt B (2009). Orai1 (CRACM1) is the platelet SOC channel and essential for pathological thrombus formation. *Blood* **113**: 2056-2063.

Broos KH, Feys B, De Meyer SF, Vanhoorelbeke K & Deckmyn H (2011). Platelets at work in primary hemostasis. *Blood Reviews* **25**:155-167.

Brownlow SL, Harper AGS, Harper MT & Sage SO (2004). A role for hTRPC1 and lipid raft domains in store-mediated calcium entry in human platelets. *Cell Calcium* **35**: 107-113.

Burkhart JM, Vaudel M, Gambaryan S, Radau S, Walter U, Martens L, Geiger J, Sickmann A & Zahedi RP (2012). The first comprehensive and quantitative analysis of human platelet protein composition allows the comparative analysis of structural and functional pathways. *Blood* **120**: e73-82.

Carey F, Menashi S & Crawford N (1982). Localization of cyclo-oxygenase and thromboxane synthetase in human platelet intracellular membranes. *Biochem J* **204**: 847-851.

Coller BS (1983). Biochemical and electrostatic considerations in primary platelet aggregation. *Ann N Y Acad Sci* **416**: 693-708.

Coxon CH, Lewis AM, Sadler AJ, Vasudevan SR, Thomas A, Dundas AK, Taylor L, Campbell RD, Gibbins JM, Churchill GC & Tucker KL (2012). NAADP regulates human platelet function. *Biochem J* **441**: 435-442.

Cramer TJ, Griffin JH & AJ Gale (2010). Factor V is an anticoagulant cofactor for activated protein C during inactivation of factor Va. *Pathophysiol Haemost Thromb* **37**: 17-23.

Crawford NSM (1994). Biochemistry of the blood platelet in Haemostasis and Thrombosis. England, Churchill Livingstone.

Croce KR, Flaumenhaft M, Rivers B, Furie BC, Furie IM, Herman & Potter DA (1999). Inhibition of calpain blocks platelet secretion, aggregation, and spreading. *J Biol Chem* **274**: 36321-36327.

- Cutler LS, Feinstein MB, Rodan GA & Christian CP (1981). Cytochemical evidence for the segregation of adenylate cyclase, Ca<sup>2+</sup>-, Mg<sup>2+</sup>-ATPase, K<sup>+</sup>-dependent p-nitrophenyl phosphatase in separate membrane compartments in human platelets. *Histochem J* **13**: 547-554.
- Dandona PK, Thusu U, Khurana U, Love J, Aljada A & Mousa S (1996). Calcium, calmodulin and protein kinase C dependence of platelet shape change. *Thromb Res* **81**: 163-175.
- Daniel JL, Molish IR & Holmsen H (1981). Myosin phosphorylation in intact platelets. *J Biol Chem* **256**: 7510-7514.
- Daniel JL, Molish IR, Rigmaiden M & Stewart G (1984). Evidence for a role of myosin phosphorylation in the initiation of the platelet shape change response. *J Biol Chem* **259**: 9826-9831.
- Davies TA, Drotts DL, Weil GJ & Simons ER (1989). Cytoplasmic Ca<sup>2+</sup> is necessary for thrombin-induced platelet activation. *J Biol Chem* **264**: 19600-19606.
- Dean WL (2010). Role of platelet plasma membrane Ca-ATPase in health and disease. *World J Biol Chem* **1**: 265-270.
- Dean WL, Chen D, Brandt PC & Vanaman TC (1997). Regulation of platelet plasma membrane Ca<sup>2+</sup>-ATPase by cAMP-dependent and tyrosine phosphorylation. *J Biol Chem* **272**: 15113-15119.
- Dean WL, & Whiteheart SW (2004). Plasma membrane Ca(2+)-ATPase (PMCA) translocates to filopodia during platelet activation. *Thromb Haemost* **91**: 325-333.
- Deisseroth KH, Bito & Tsien RW (1996). Signaling from synapse to nucleus: postsynaptic CREB phosphorylation during multiple forms of hippocampal synaptic plasticity. *Neuron* **16**: 89-101.
- den Dekker EG, Gorter H, van der Vuurst JW, Heemskerk & Akkerman JW (2001). Biogenesis of G-protein mediated calcium signaling in human megakaryocytes. *Thromb Haemost* **86**: 1106-1113.
- Devine CE, Somlyo AV & Somlyo AP (1972). Sarcoplasmic reticulum and excitation-contraction coupling in mammalian smooth muscles. *J Cell Biol* **52**: 690-718.
- Diagouraga BA, Grichine A, Fertin J, Wang S, Khochbin S & Sadoul K (2014). Motor-driven marginal band coiling promotes cell shape change during platelet activation. *J Cell Biol* **204**: 177-185.
- Di Buduo CA, Moccia F, Battiston M, De Marco L, Mazzucato M, Moratti R, Tanzi F & Balduini A (2014). The importance of calcium in the regulation of megakaryocyte function. *Haematologica* **99**: 769-778.
- Driver JM, Sage SO & Rosado JA (2001). The inositol trisphosphate receptor antagonist 2-aminoethoxydiphenylborate (2-APB) blocks Ca<sup>2+</sup> entry channels in human platelets: cautions for its use in studying Ca<sup>2+</sup> influx. *Cell Calcium* **30**: 323-329.
- Ebbeling L, Robertson C, McNicol A & Gerrard JM (1992). Rapid ultrastructural changes in the dense tubular system following platelet activation. *Blood* **80**: 718-723.

Eckly A, Heijnen H, Pertuy F, Geerts W, Proamer F, Rinckel JY, Leon C, Lanza F & Gachet C (2014). Biogenesis of the demarcation membrane system (DMS) in megakaryocytes. *Blood* **123**: 921-930.

El-Daher S, Patel SY, Siddiqua A, Hassock S, Edmunds S, Maddison B, Patel G, Goulding D, Lupu F, Wojcikiewicz RJ & Authi KS (2000). Distinct localization and function of (1,4,5)IP(3) receptor subtypes and the (1,3,4,5)IP(4) receptor GAP1(IP4BP) in highly purified human platelet membranes. *Blood* **95**: 3412-3422.

Esmon CT & Owen WG (1981). Identification of an endothelial cell cofactor for thrombin-catalyzed activation of protein C. *Proc Natl Acad Sci U S A* **78**: 2249-2252.

Ezerman EB, & Ishikawa H (1967). Differentiation of the sarcoplasmic reticulum and T system in developing chick skeletal muscle in vitro. *J Cell Biol* **35**: 405-420.

Farndale RW, Siljander PR, Onley DJ, Sundaresan P, Knight CG & Barnes MJ (2003). Collagen-platelet interactions: recognition and signalling. *Biochem Soc Symp* **70**: 81-94.

Fogelson AL & Wang NT (1996). Platelet dense-granule centralization and the persistence of ADP secretion. *Am J Physiol* **270**: H1131-H1140.

Fujii T, Sakata A, Nishimura S, Eto K & Nagata S (2015). TMEM16F is required for phosphatidylserine exposure and microparticle release in activated mouse platelets. *Proc Natl Acad Sci U S A* **112**: 12800-12805.

Fulcher CA, Gardiner JE, Griffin GH & Zimmerman ZS (1984). Proteolytic inactivation of human factor VIII procoagulant protein by activated human protein C and its analogy with factor V. *Blood* **63**: 486-489.

Furie B & Furie BC (2008). Mechanisms of thrombus formation. *NEJM* **359**: 938-949.

Gabella G (1971). Caveolae intracellulares and sarcoplasmic reticulum in smooth muscle. *J Cell Sci* **8**: 601-609.

Gale AJ (2011). Current Understanding of Hemostasis. *Toxicol Pathol* **39**: 273-280.

George JN, Pickett EB, Saucerman S, McEver RP, Kunicki TJ, Kieffer N & Newman PJ (1986). Platelet surface glycoproteins. Studies on resting and activated platelets and platelet membrane microparticles in normal subjects, and observations in patients during adult respiratory distress syndrome and cardiac surgery. *J Clin Invest* **78**: 340-348.

Gerrard JM, White JG, Rao GH & Townsend D (1976). Localization of platelet prostaglandin production in the platelet dense tubular system. *Am J Pathol* **83**: 283-298.

Gilio KR van Kruchten R, Braun A, Berna-Erro A, Feijge MA, Stegner D, van der Meijden PE, Kuijpers MJ, Varga-Szabo D, Heemskerk JW & Nieswandt B (2010). Roles of platelet STIM1 and Orai1 in glycoprotein VI- and thrombin-dependent procoagulant activity and thrombus formation. *J Biol Chem* **285**: 23629-23638.

Ginsberg MH, Taylor L & Painter RG (1980). The mechanism of thrombin-induced platelet factor 4 secretion. *Blood* **55**: 661-668.

Golebiewska EM, and Poole AW (2014). Secrets of platelet exocytosis - what do we really know about platelet secretion mechanisms? *Br J Haematol*. **165**: 204–216.

Goshima M, Kariya K, Yamawaki-Kataoka Y, Okada T, Shibatohe M, Shima F, Fujimoto E & Kataoka T (1999). Characterization of a novel Ras-binding protein Ce-FLI-1 comprising leucine-rich repeats and gelsolin-like domains. *Biochem Biophys Res Commun* **257**: 111-116.

Gousset K, Wolkers WF, Tsvetkova NM, Oliver AE, Field CL, Walker NJ, Crowe JH & Tablin F (2002). Evidence for a physiological role for membrane rafts in human platelets. *J Cell Physiol* **190**: 117-128.

Grette K (1962). Studies on the mechanism of thrombin-catalyzed hemostatic reactions in blood platelets. *Acta Physiol Scand Suppl* **195**: 1-93.

Grgurevich S, Krishnan R, White MM & Jennings LK (2003). Role of in vitro cholesterol depletion in mediating human platelet aggregation. *J Thromb Haemost* **1**: 576-586.

Guinto ER, & Esmon CT (1984). Loss of prothrombin and of factor Xa-factor Va interactions upon inactivation of factor Va by activated protein C. *J Biol Chem* **259**: 13986-13992.

Gunay-Aygun M, Huizing M & Gahl WA (2004). Molecular defects that affect platelet dense granules. *Semin Thromb Hemost* **30**: 537-547.

Hagopian M, & Spiro D (1967). The sarcoplasmic reticulum and its association with the T system in an insect. *J Cell Biol* **32**: 535-545.

Harper AGS, Mason MJ & Sage SO (2009). A key role for dense granule secretion in potentiation of the Ca<sup>2+</sup> signal arising from store-operated calcium entry in human platelets. *Cell Calcium* **45**: 413-420.

Harper AGS & Sage SO (2007). A key role for reverse Na<sup>+</sup>/Ca<sup>2+</sup> exchange influenced by the actin cytoskeleton in store-operated Ca<sup>2+</sup> entry in human platelets: evidence against the de novo conformational coupling hypothesis. *Cell Calcium* **42**: 606-617.

Harper MT, Londono JE, Quick K, Londono JC, Flockerzi V, Philipp SE, Birnbaumer L, Freichel M & Poole AW (2013). Transient receptor potential channels function as a coincidence signal detector mediating phosphatidylserine exposure. *Sci Signal* **6**: ra50.

Harper MT, Mason MJ, Sage SO & Harper AGS (2010). Phorbol ester-evoked Ca<sup>2+</sup> signaling in human platelets is via autocrine activation of P(2X1) receptors, not a novel non-capacitative Ca<sup>2+</sup> entry. *J Thromb Haemost* **8**: 1604-1613.

Harper MT, & Sage SO (2006). Actin polymerisation regulates thrombin-evoked Ca(2+) signalling after activation of PAR-4 but not PAR-1 in human platelets. *Platelets* **17**: 134-142.

Harrison P & Cramer EM (1993). Platelet alpha-granules. *Blood Rev* **7**: 52-62.

Hartwig JH & DeSisto M (1991). The cytoskeleton of the resting human blood platelet: structure of the membrane skeleton and its attachment to actin filaments. *J Cell Biol* **112**: 407-425.

Hassock SR, Zhu MX, Trost C, Flockerzi V & Authi KS (2002). Expression and role of TRPC proteins in human platelets: evidence that TRPC6 forms the store-independent calcium entry channel. *Blood* **100**: 2801-2811.

Hathaway DR & Adelstein RS (1979). Human platelet myosin light chain kinase requires the calcium-binding protein calmodulin for activity. *Proc Natl Acad Sci U S A* **76**: 1653-1657.

Hathaway DR, Eaton CR & Adelstein RS (1981). Regulation of human platelet myosin light chain kinase by the catalytic subunit of cyclic AMP-dependent protein kinase. *Nature* **291**: 252-256.

Heemskerk JW & Sage SO (1994). Calcium signalling in platelets and other cells. *Platelets* **5**: 295-316.

Heptinstall S. (1976). The use of a chelating ion-exchange resin to evaluate the effects of the extracellular calcium concentration on adenosine diphosphate induced aggregation of human blood platelets. *Thromb Haemost* **36**: 208-220.

Heptinstall S, Johnson A, Glenn JR & White AE (2005). Adenine nucleotide metabolism in human blood--important roles for leukocytes and erythrocytes. *J Thromb Haemost* **3**: 2331-2339.

Howard A, Legon S, Walters J R (1993). Human and rat intestinal plasma membrane calcium pump isoforms. *Am J Physiol* **265**: G917- 925

Hussain JF & Mahaut-Smith MP (1999). Reversible and irreversible intracellular Ca<sup>2+</sup> spiking in single isolated human platelets. *J Physiol* **514**: 713-718.

Ignarro LJ, Buga GM, Wood KS, Byrns RE & Chaudhuri G (1987). Endothelium-derived relaxing factor produced and released from artery and vein is nitric oxide. *Proc Natl Acad Sci U S A* **84**: 9265-9269.

Italiano JE Jr, Lecine P, Shivdasani RA & Hartwig JH (1999). Blood platelets are assembled principally at the ends of proplatelet processes produced by differentiated megakaryocytes. *J Cell Biol* **147**: 1299-1312.

Italiano JE Jr, Richardson JL, Patel-Hett S, Battinelli E, Zaslavsky A, Short S, Ryeom S, Folkman J & Klement GL (2008). Angiogenesis is regulated by a novel mechanism: pro- and antiangiogenic proteins are organized into separate platelet alpha granules and differentially released. *Blood* **111**: 1227-1233.

Itoh K, Hara T, Yamada F & Shibata N (1992). Diphosphorylation of platelet myosin ex vivo in the initial phase of activation by thrombin. *Biochim Biophys Acta* **1136**: 52-56.

Jackson SP & Schoenwaelder SM (2010). Procoagulant platelets: are they necrotic? *Blood* **116**: 2011-2018.

Jedlitschky GK, Tirschmann LE, Lubenow H, Nieuwenhuis K, Akkerman JW, Greinacher A & Kroemer HK (2004). The nucleotide transporter MRP4 (ABCC4) is highly expressed in human platelets and present in dense granules, indicating a role in mediator storage. *Blood* **104**: 3603-3610.

Jennings LK (2009). Mechanisms of platelet activation: need for new strategies to protect against platelet-mediated atherothrombosis. *Thromb Haemost* **102**: 248-257.

Hartwig JH. (2007). Platelet structure in platelets. *Sandiego, Academic Press Elsevier*.

Italiano JE Jr & Hartwig JH (2007). Megakaryocyte development and platelet formation, in Platelets. *Heamatology Division, Brigham and Womens Hospital, Harvard Medical School, Boston, Massachusetts*. p27-49.

Johansson JS & Haynes DH (1988). Deliberate quin2 overload as a method for in situ characterization of active calcium extrusion systems and cytoplasmic calcium binding: application to the human platelet. *J Membr Biol* **104**: 147-163.

Johansson JS, Nied LE & Haynes DH (1992). Cyclic AMP stimulates Ca<sup>(2+)</sup>-ATPase-mediated Ca<sup>2+</sup> extrusion from human platelets. *Biochim Biophys Acta* **1105**: 19-28.

John GB, Cheng CY & Kuro-o M (2011). Role of Klotho in aging, phosphate metabolism, and CKD. *Am J Kidney Dis* **58**: 127-134.

Jones S, Solomon A, Sanz-Rosa D (2010). The plasma membrane calcium ATPase (PMCA) modulates calcium homeostasis, intracellular signalling events and function in platelets. *J Thromb Haemost* **8**: 2766–2774

Jones SR, Evans J & Mahaut-Smith MP (2014). Ca<sup>2+</sup> influx through P2X1 receptors amplifies P2Y1 receptor-evoked Ca<sup>2+</sup> signaling and ADP-evoked platelet aggregation. *Mol Pharmacol* **86**: 243-251.

Kang YL, Saleem MA, Chan KW, Yung BY & Law HK (2014). The cytoprotective role of autophagy in puromycin aminonucleoside treated human podocytes. *Biochem Biophys Res Commun* **443**: 628-634.

Kasirer-Friede AM, Cozzi R, Mazzucato M, De Marco L, Ruggeri ZM & Shattil SJ (2004). Signaling through GP Ib-IX-V activates alpha IIb beta 3 independently of other receptors. *Blood* **103**: 3403-3411.

Kaushansky K, Lichtman MA, Beutler E, Kipps TJ, Seligsohn U, Prchal JT (2010). *Williams Hematology*. New York, McGraw Hill 1737-1738.

Kimura M, Aviv A & Reeves JP (1993). K(+)-dependent Na<sup>+</sup>/Ca<sup>2+</sup> exchange in human platelets. *J Biol Chem* **268**: 6874-6877.

Kraft R (2007). The Na<sup>+</sup>/Ca<sup>2+</sup> exchange inhibitor KB-R7943 potently blocks TRPC channels. *Biochem Biophys Res Commun* **361**: 230-236.

Kulkarni S & Jackson SP (2004). Platelet factor XIII and calpain negatively regulate integrin alphallbbeta3 adhesive function and thrombus growth. *J Biol Chem* **279**: 30697-30706.

Kumar V & Abbas AK (2015). *Pathologic Basis of Disease*, Elsevier

Kuro-o M, Matsumura Y, Aizawa H, Kawaguchi H, Suga T, Utsugi T, Ohyama Y, Kurabayashi M, Kaname T, Kume E, Iwasaki H, Iida A, Shiraki-Iida T, Nishikawa S, Nagai R & Nabeshima YI (1997). Mutation of the mouse klotho gene leads to a syndrome resembling ageing. *Nature* **390**: 45-51.

Kurosu H, Yamamoto M, Clark JD, Pastor JV, Nandi A, Gurnani P, McGuinness OP, Chikuda H, Yamaguchi M, Kawaguchi H, Shimomura I, Takayama Y, Herz J, Kahn CR, Rosenblatt KP & Kuro-o M (2005). Suppression of aging in mice by the hormone Klotho. *Science* **309**: 1829-1833.

Lei L, Lu S, Wang Y, Kim T, Mehta D & Wang Y (2014). The role of mechanical tension on lipid raft dependent PDGF-induced TRPC6 activation. *Biomaterials* **35**: 2868-2877.

Le Menn R, Migne J & Probst-Dvojakovic RJ (1979). Ultrastructural study on the effect of an inhibitor of platelet aggregation. *Arzneimittelforschung* **29**: 1278-1282.

Lewandrowski U, Wortelkamp S, Lohrig K, Zahedi RP, Wolters DA, Walter U & Sickmann A (2009). Platelet membrane proteomics: a novel repository for functional research. *Blood* **114**: e10-19.

Lopez E, N. Bermejo A, Berna-Erro N, Alonso G, Salido M, Redondo PC & Rosado JA (2015). Relationship between calcium mobilization and platelet alpha- and delta-granule secretion. A role for TRPC6 in thrombin-evoked delta-granule exocytosis. *Arch Biochem Biophys* **585**: 75-81.

Lopez JJ, Camello-Almaraz C, Pariente JA, Salido GM & Rosado JA (2005). Ca<sup>2+</sup> accumulation into acidic organelles mediated by Ca<sup>2+</sup>- and vacuolar H<sup>+</sup>-ATPases in human platelets. *Biochem J* **390**: 243-252.

Lopez JJ, Redondo PC, Salido GM, Pariente JA & Rosado JA (2006). Two distinct Ca<sup>2+</sup> compartments show differential sensitivity to thrombin, ADP and vasopressin in human platelets. *Cell Signal* **18**: 373-381.

MacKenzie AB, Mahaut-Smith MP & Sage SO (1996). Activation of receptor-operated cation channels via P2X1 not P2T purinoceptors in human platelets. *J Biol Chem* **271**: 2879-2881.

Mahaut-Smith MP, Jones PS & Evans RJ (2011). The P2X1 receptor and platelet function. *Purinergic Signal* **7**: 341-356.

Mahaut-Smith MP, Tolhurst G & Evans RJ (2004). Emerging roles for P2X1 receptors in platelet activation. *Platelets* **15**: 131-144.

Mangin P, Yuan Y, Goncalves I, Eckly A, Freund M, Cazenave JP, Gachet C, Jackson SP & Lanza F (2003). Signaling role for phospholipase C gamma 2 in platelet glycoprotein Ib alpha calcium flux and cytoskeletal reorganization. Involvement of a pathway distinct from FcR gamma chain and Fc gamma RIIA. *J Biol Chem* **278**: 32880-32891.

Mann KG, Nesheim ME, Church WR, Haley P & Krishnaswamy S (1990). Surface-dependent reactions of the vitamin K-dependent enzyme complexes. *Blood* **76**: 1-16.

Markello T, Chen D, Kwan JY, Horkayne-Szakaly I, Morrison A, Simakova O, Maric I, Lozier J, Cullinane AR, Kilo T, Meister L, Pakzad K, Bone W, Chainani S, Lee E, Links A, Boerkoel C, Fischer R, Toro C, White JG, Gahl WA & Gunay-Aygun M (2015). York platelet syndrome is a CRAC channelopathy due to gain-of-function mutations in STIM1. *Mol Genet* **114**: 474-482.

Marshall SJ, Senis YA, Auger JM, Feil R, Hofmann F, Salmon G, Peterson JT, Burslem F & Watson SP (2004). GPIIb-dependent platelet activation is dependent on Src kinases but not MAP kinase or cGMP-dependent kinase. *Blood* **103**: 2601-2609.

Mazzucato M, Pradella P, Cozzi MR, De Marco L & Ruggeri ZM (2002). Sequential cytoplasmic calcium signals in a 2-stage platelet activation process induced by the glycoprotein Ibalph mechanoreceptor. *Blood* **100**: 2793-2800.

McCarl CA, Picard C, Khalil S, Kawasaki T, Rother J, Papolos A, Kutok J, Hivroz C, Ledeist F, Plogmann K, Ehl S, Notheis G, Albert MH, Belohradsky BH, Kirschner J, Rao A, Fischer A & Feske S (2009). ORAI1 deficiency and lack of store-operated Ca<sup>2+</sup> entry cause immunodeficiency, myopathy, and ectodermal dysplasia. *J Allergy Clin Immunol* **124**: 1311-1318 .

Mc Nicol A & Israels SJ (1999). Platelet dense granules: structure, function and implications for haemostasis. *Thromb Res.* **95** :1-18.

Michelson AD. (1992). Thrombin-induced down-regulation of the platelet membrane glycoprotein Ib-IX complex. *Semin Thromb Hemost* **18**: 18-27.

Misceo D, Holmgren A, Louch WE, Holme PA, Mizobuchi M, Morales RJ , De Paula AM, Stray-Pedersen A, Lyle R, Dalhus B, Christensen G, Stormorken H, Tjonnfjord GE & Frengen E (2014). A dominant STIM1 mutation causes Stormorken syndrome. *Hum Mutat.* **35**: 556-564.

Mohammad MA, Oceandy D, Min Zi, Prehar S, Alatwi N, Wang Y, Shaheen MA, Riham Abou- Leisa, Schelcher C, Hegab Z, Baudoin F, Michael Emerson, Mamas Mamas, Giulietta Di Benedetto, Manuela Zaccolo, Ming Lei, Cartwright EJ, & Ludwig Neyses (2011). Plasma Membrane Calcium Pump (PMCA4)-Neuronal Nitric-oxide Synthase Complex Regulates Cardiac Contractility through Modulation of a Compartmentalized Cyclic Nucleotide Microdomain. *J. Biol. Chem* **286**: 41520

Munnix IC, Kuijpers MJ, Auger J, Thomassen CM, Panizzi P, van Zandvoort MA, Rosing J, Bock PE, Watson SP & Heemskerk JW (2007). Segregation of platelet aggregatory and procoagulant microdomains in thrombus formation: regulation by transient integrin activation. *Arterioscler Thromb Vasc Biol* **27**: 2484-2490.

Nachmias VT & Yoshida K. (2008). The Cytoskeleton of the Blood Platelet: *A Dynamic Structure. Advances in Molecular and cell Biology* **2**: 181-211.

Naik M, Nigam UA, Manrai P, Millili P, Czymmek K, Sullivan M & Naik UP (2009). CIB1 deficiency results in impaired thrombosis: the potential role of CIB1 in outside-in signaling through integrin alpha IIb beta 3. *J Thromb Haemost* **7**: 1906-1914.

Nakai KY, Suzuki H, Kihira H, Wada M, Fujioka M, Ito T, Nakano K, Kaibuchi H, Shiku & Nishikawa M (1997). Regulation of myosin phosphatase through phosphorylation of the myosin-binding subunit in platelet activation. *Blood* **90**: 3936-3942.

Nakao K & Angrist AA (1968). Membrane surface specialization of blood platelet and megakaryocyte. *Nature* **217**: 960-961.

Neher E. (1998). Usefulness and limitations of linear approximations to the understanding of Ca<sup>++</sup> signals. *Cell Calcium* **24**: 345-357.

- Neher E. & Almers W (1986). Fast calcium transients in rat peritoneal mast cells are not sufficient to trigger exocytosis. *EMBO J* **5**: 51-53.
- Nesbitt WS, Giuliano S, Kulkarni S, Dopheide SM, Harper IS & Jackson SP (2003). Intercellular calcium communication regulates platelet aggregation and thrombus growth. *J Cell Biol* **160**: 1151-1161.
- Nesbitt WS, Kulkarni S, Giuliano S, Goncalves I, S. M. Dopheide SM, Yap CL, Harper IS, Salem HH & Jackson SP. (2002). Distinct glycoprotein Ib/V/IX and integrin alpha IIb beta 3-dependent calcium signals cooperatively regulate platelet adhesion under flow. *J Biol Chem* **277**: 2965-2972.
- Nieswandt B, & Watson SP (2003). Platelet-collagen interaction: is GPVI the central receptor? *Blood* **102**: 449-461.
- Niggli E & Shirokova N (2007). A guide to sparkology: the taxonomy of elementary cellular Ca<sup>2+</sup> signaling events. *Cell Calcium* **42**: 379-387.
- Nurden AT & Nurden P (2015). Inherited disorders of platelet function: selected updates. *J Thromb Haemost* **13 Suppl 1**: S2-S9.
- Nurden P, Heilmann E, Paponneau A & Nurden A (1994). Two-way trafficking of membrane glycoproteins on thrombin-activated human platelets. *Semin Hematol* **31**: 240-250.
- Nurden P, Poujol C, Winckler J, Combrie R, Pousseau N, Conley PB, Levy-Toledano S, Habib A & Nurden AT (2003). Immunolocalization of P2Y1 and TPalpha receptors in platelets showed a major pool associated with the membranes of alpha -granules and the open canalicular system. *Blood* **101**: 1400-1408.
- Oceandy D, Cartwright EJ, Emerson M (2007). Neuronal nitric oxide synthase signaling in the heart is regulated by the sarcolemmal calcium pump 4b. *Circulation* **115**: 483-492
- Okada S, Yoshida T, Hong Z, Ishii G, Hatano M, Kuro OM, Nabeshima Y & Tokuhsa T (2000). Impairment of B lymphopoiesis in precocious aging (klotho) mice. *Int Immunol* **12**: 861-871.
- Okunade G W, Miller M L, Pyne G J. (2004) Targeted ablation of plasma membrane Ca<sup>2+</sup>-ATPase (PMCA) 1 and 4 indicates a major housekeeping function for PMCA1 and a critical role in hyperactivated sperm motility and male fertility for PMCA4. *J Biol Chem*, **279**: 33742-33750
- Paez Espinosa EV, Murad JP, Ting HJ & Khasawneh FT (2012). Mouse transient receptor potential channel 6: role in hemostasis and thrombogenesis. *Biochem Biophys Res Commun* **417**: 853-856.
- Palmer RM, Ferrige AG & Moncada S (1987). Nitric oxide release accounts for the biological activity of endothelium-derived relaxing factor. *Nature* **327**: 524-526.
- Pande J, Mallhi K K, Sawh A (2006). Aortic smooth muscle and endothelial plasma membrane Ca<sup>2+</sup> pump isoforms are inhibited differently by the extracellular inhibitor caloxin 1b1. *Am J Physiol Cell Physiol* **290**: C1341-1349

- Papp B, Enyedi A, Kovacs T, Sarkadi B, Wuytack F, Thastrup O, Gardos G, Bredoux R, Levy-Toledano S & Enouf J (1991). Demonstration of two forms of calcium pumps by thapsigargin inhibition and radioimmunoblotting in platelet membrane vesicles. *J Biol Chem* **266**: 14593-14596.
- Papp B, Enyedi A, Paszty K, Kovacs T, Sarkadi B, Gardos G, Magnier C, Wuytack F & Enouf J (1992). Simultaneous presence of two distinct endoplasmic-reticulum-type calcium-pump isoforms in human cells. Characterization by radio-immunoblotting and inhibition by 2,5-di-(t-butyl)-1,4-benzohydroquinone. *Biochem J* **288**: 297-302.
- Parekh AB (2008). Ca<sup>2+</sup> microdomains near plasma membrane Ca<sup>2+</sup> channels: impact on cell function. *J Physiol* **586**: 3043-3054.
- Paul BZ, Daniel JL & Kunapuli SP (1999). Platelet shape change is mediated by both calcium-dependent and -independent signaling pathways. Role of p160 Rho-associated coiled-coil-containing protein kinase in platelet shape change. *J Biol Chem* **274**: 28293-28300.
- Peters CG, Michelson AD & Flaumenhaft R (2012). Granule exocytosis is required for platelet spreading: differential sorting of alpha-granules expressing VAMP-7. *Blood* **120**: 199-206.
- Picard C, McCarl CA, Papolos A, Khalil S, Luthy K, Hivroz C, LeDeist F, Rieux-Laucat F, Rechavi G, Rao A, Fischer A & Feske S (2009). STIM1 mutation associated with a syndrome of immunodeficiency and autoimmunity. *N Engl J Med* **360**: 1971-1980.
- Pineault N, Robert A, Cortin V & Boyer L (2013). Ex vivo differentiation of cord blood stem cells into megakaryocytes and platelets. *Methods Mol Biol* **946**: 205-224.
- Quinton TM & Dean WL (1996). Multiple inositol 1,4,5-trisphosphate receptor isoforms are present in platelets. *Biochem Biophys Res Commun* **223**: 740-746.
- Ramanathan G, Gupta S, Thielmann I, Pleines I, Varga-Szabo D, May F, Mannhalter C, Dietrich A, Nieswandt B, Braun A (2012). Defective diacylglycerol-induced Ca<sup>2+</sup> entry but normal agonist-induced activation responses in TRPC6-deficient mouse platelets. *J Thromb Haemost* **10**: 419-429.
- Ramanathan G & Mannhalter C (2015). Increased expression of transient receptor potential canonical 6 (TRPC6) in differentiating human megakaryocytes. *Cell Biol Int.* **40**: 223-31
- Reed GL (2007). Platelet Secretion. In Michelson AD (ed). *Platelets*. San Diego: Elsevier Science. pp. 181–195.
- Ren Q, Wimmer C, Chicka MC, Ye S, Ren Y, Hughson FM & Whiteheart SW (2010). Munc13-4 is a limiting factor in the pathway required for platelet granule release and hemostasis. *Blood* **116**: 869-877.
- Rink TJ & Sage SO (1990). Calcium signaling in human platelets. *Annu Rev Physiol* **52**: 431-449.
- Rink TJ, Smith SW & Tsien RY (1982). Cytoplasmic free Ca<sup>2+</sup> in human platelets: Ca<sup>2+</sup> thresholds and Ca-independent activation for shape-change and secretion. *FEBS Lett* **148**: 21-26.

- Roberts DE, Matsuda T & Bose R (2012). Molecular and functional characterization of the human platelet Na<sup>(+)</sup> /Ca<sup>(2+)</sup> exchangers. *Br J Pharmacol* **165**: 922-936.
- Robson SC (2001). Thromboregulation by endothelial cells: significance for occlusive vascular diseases. *Arterioscler Thromb Vasc Biol* **21**: 1251-1252.
- Rodriguez Del Castillo A, Vitale ML, Tchakarov L & Trifaro JM (1992). Human platelets contain scinderin, a Ca<sup>(2+)</sup>-dependent actin filament-severing protein. *Thromb Haemost* **67**: 248-251.
- Rolf MG, Brearley CA & Mahaut-Smith MP (2001). Platelet shape change evoked by selective activation of P2X1 purinoceptors with alpha,beta-methylene ATP. *Thromb Haemost* **85**: 303-308.
- Rosado JA (2011). Acidic Ca<sup>(2+)</sup> stores in platelets. *Cell Calcium* **50**: 168-174.
- Rosado JA, Graves D & Sage SO (2000). Tyrosine kinases activate store-mediated Ca<sup>2+</sup> entry in human platelets through the reorganization of the actin cytoskeleton. *Biochem J* **351 Pt 2**: 429-437.
- Rosado JA, Saavedra FR, Redondo PC, Hernandez-Cruz JM, Salido GM & Pariente JA (2004). Reduced plasma membrane Ca<sup>2+</sup>-ATPase function in platelets from patients with non-insulin-dependent diabetes mellitus. *Haematologica* **89**: 1142-1144.
- Rosado JA & Sage SO (2000a). Coupling between inositol 1,4,5-trisphosphate receptors and human transient receptor potential channel 1 when intracellular Ca<sup>2+</sup> stores are depleted. *Biochem J* **350**: 631-635.
- Rosado JA & Sage SO (2000b). Regulation of plasma membrane Ca<sup>2+</sup>-ATPase by small GTPases and phosphoinositides in human platelets. *J Biol Chem* **275**: 19529-19535.
- Ruggeri ZM (2002). Platelets in atherothrombosis. *Nat Med* **8**: 1227-1234.
- Ruiz FA, Lea CR, Oldfield E & Docampo R (2004). Human platelet dense granules contain polyphosphate and are similar to acidocalcisomes of bacteria and unicellular eukaryotes. *J Biol Chem* **279**: 44250-44257.
- Safer D & Nachmias VT (1994). Beta thymosins as actin binding peptides. *Bioessays* **16**: 473-479.
- Sage SO, Pugh N, Farndale RW & Harper AGS (2013). Pericellular Ca<sup>(2+)</sup> recycling potentiates thrombin-evoked Ca<sup>(2+)</sup> signals in human platelets. *Physiol Rep* **1**: e00085.
- Sage SO, Pugh N, Mason MJ & Harper AGS (2011). Monitoring the intracellular store Ca<sup>2+</sup> concentration in agonist-stimulated, intact human platelets by using Fluo-5N. *J Thromb Haemost* **9**: 540-551.
- Saleem H, Tovey SC, Molinski TF & Taylor CW (2014). Interactions of antagonists with subtypes of inositol 1,4,5-trisphosphate (IP3) receptor. *Br J Pharmacol* **171**: 3298-3312.

Savage B, Almus-Jacobs F & Ruggeri ZM (1998). Specific synergy of multiple substrate-receptor interactions in platelet thrombus formation under flow. *Cell* **94**: 657-666.

Schmid E, Yan J, Hosseinzadeh Z, Almilaji A, Shumilina E, Kuro-o M, Borst O, Gawaz M & Lang F (2015). Up-regulation of megakaryocytic Na(+)/Ca(2+) exchange in klotho-deficient mice. *Biochem Biophys Res Commun* **460**: 177-182.

Schuh K, Cartwright E J, Jankevics E (2004). Plasma membrane Ca<sup>2+</sup> ATPase 4 is required for sperm motility and male fertility. *J Biol Chem* **279**: 28220–28226

Senis YA, Mazharian A & Mori J (2014). Src family kinases: at the forefront of platelet activation. *Blood* **124**: 2013-2024.

Shen L & Dahlback B (1994). Factor V and protein S as synergistic cofactors to activated protein C in degradation of factor VIIIa. *J Biol Chem* **269**: 18735-18738.

Shi J, Takahashi S, Jin XH, Li YQ, Ito Y, Mori Y & Inoue R (2007). Myosin light chain kinase-independent inhibition by ML-9 of murine TRPC6 channels expressed in HEK293 cells." *Br J Pharmacol* **152**: 122-131.

Somasundaram B, Mason MJ & Mahaut-Smith MP (1997). Thrombin-dependent calcium signalling in single human erythroleukaemia cells. *J Physiol* **501**: 485-495.

Stalker TJ, Traxler EA, Wu J, Wannemacher KM, Cermignano SL, Voronov R, Diamond SL & Brass LF (2013). Hierarchical organization in the hemostatic response and its relationship to the platelet-signaling network. *Blood* **121**: 1875-1885.

Stefanini L, Roden RC & Bergmeier W (2009). CalDAG-GEFI is at the nexus of calcium-dependent platelet activation. *Blood* **114**: 2506-2514.

Stern MD. (1992). Buffering of calcium in the vicinity of a channel pore. *Cell Calcium* **13**: 183-192.

Strehl A, Munnix IC, Kuijpers MJ, van der Meijden PE, Cossemans JM, Feijge MA, Nieswandt B & Heemskerk JW (2007). Dual role of platelet protein kinase C in thrombus formation: stimulation of pro-aggregatory and suppression of procoagulant activity in platelets. *J Biol Chem* **282**: 7046-7055.

Stauffer T P, Guerini D, Carafoli E (1995). Tissue distribution of the four gene products of the plasma membrane Ca<sup>2+</sup> pump. A study using specific antibodies. *J Biol Chem* **270**: 12184–12190

Suzuki H, Murasaki K, Kodama K & Takayama H (2003). Intracellular localization of glycoprotein VI in human platelets and its surface expression upon activation. *Br J Haematol* **121**: 904-912.

Suzuki H, Nakamura S, Itoh Y, Yamazaki H, & Tanoue K (1992). Immunocytochemical evidence for the translocation of  $\alpha$ -granule membrane glycoprotein IIb/IIIa (integrin  $\alpha$ IIb $\beta$ 3) of human platelets to the surface membrane during the release reaction. *Histochemistry* **97**:381-388.

Suzuki J, Umeda M, Sims PJ & Nagata S (2010). Calcium-dependent phospholipid scrambling by TMEM16F. *Nature* **468**: 834-838.

Mohamed TM, Oceandy D, Zi M, Prehar S, Alatwi N, Wang Y, Shaheen MA, Abou-Leisa R, Schelcher C, Hegab Z, Baudoin F, Emerson M, Mamas M, Di Benedetto G, Zaccolo M, Lei M, Cartwright EJ, Neyses L (2011). Plasma Membrane Calcium Pump (PMCA4)-Neuronal Nitric-oxide Synthase Complex Regulates Cardiac Contractility through Modulation of a Compartmentalized Cyclic Nucleotide Microdomain. *J Biol Chem* **48**: 41520-41529.

Tao J, Johansson JS & Haynes DH (1992a). Protein kinase C stimulates dense tubular  $Ca^{2+}$  uptake in the intact human platelet by increasing the  $V_m$  of the  $Ca^{2+}$ -ATPase pump: stimulation by phorbol ester, inhibition by calphostin C. *Biochim Biophys Acta* **1107**: 213-222.

Tao J, Johansson JS & Haynes DH (1992b). Stimulation of dense tubular  $Ca^{2+}$  uptake in human platelets by cAMP. *Biochim Biophys Acta* **1105**: 29-39.

Tolhurst G, Carter RN, Amisten S, Holdich JP, Erlinge D & Mahaut-Smith MP (2008). Expression profiling and electrophysiological studies suggest a major role for Orai1 in the store-operated  $Ca^{2+}$  influx pathway of platelets and megakaryocytes. *Platelets* **19**: 308-313.

Tolhurst G, Vial C, Leon C, Gachet C, Evans RJ & Mahaut-Smith MP (2005). Interplay between P2Y(1), P2Y(12), and P2X(1) receptors in the activation of megakaryocyte cation influx currents by ADP: evidence that the primary megakaryocyte represents a fully functional model of platelet P2 receptor signaling. *Blood* **106**: 1644-1651.

Trepakova ES, Cohen RA & Bolotina VM (1999). Nitric oxide inhibits capacitative cation influx in human platelets by promoting sarcoplasmic/endoplasmic reticulum  $Ca^{2+}$ -ATPase-dependent refilling of  $Ca^{2+}$  stores. *Circ Res* **84**: 201-209.

Tsujikawa H, Kurotaki Y, Fujimori T, Fukuda K & Nabeshima Y (2003). Klotho, a gene related to a syndrome resembling human premature aging, functions in a negative regulatory circuit of vitamin D endocrine system. *Mol Endocrinol* **17**: 2393-2403.

Tsunoda Y, Matsuno K & Tashiro Y (1988). Spatial distribution and temporal change of cytoplasmic free calcium in human platelets. *Biochem Biophys Res Commun* **156**: 1152-1159.

Valant PA, Adjei PN & Haynes DH (1992). Rapid  $Ca^{2+}$  extrusion via the  $Na^{+}/Ca^{2+}$  exchanger of the human platelet. *J Membr Biol* **130**: 63-82.

van Breemen C, Fameli N & Evans AM (2013). Pan-junctional sarcoplasmic reticulum in vascular smooth muscle: nanospace  $Ca^{2+}$  transport for site- and function-specific  $Ca^{2+}$  signalling. *J Physiol* **591**: 2043-2054.

van Gestel MA, Heemskerk JW, Slaaf DW, Heijnen VV, Sage SO, Reneman RS & Oude Egbrink MG (2002). Real-time detection of activation patterns in individual platelets during thromboembolism in vivo: differences between thrombus growth and embolus formation. *J Vasc Res* **39**: 534-543.

van Gorp RM, Feijge MA, Vuist WM, Rook MB & Heemskerk JW (2002). Irregular spiking in free calcium concentration in single, human platelets. Regulation by modulation of the inositol trisphosphate receptors. *Eur J Biochem* **269**: 1543-1552.

- van Gorp RM, van Dam-Mieras MC, Hornstra G & Heemskerk JW (1997). Effect of membrane-permeable sulfhydryl reagents and depletion of glutathione on calcium mobilisation in human platelets. *Biochem Pharmacol* **53**: 1533-1542.
- van Joost T, van Ulsen J, Vuzevski VD, Naafs B & Tank B (1990). Purpuric contact dermatitis to benzoyl peroxide. *J Am Acad Dermatol* **22**: 359-361.
- van Kruchten R, Braun A, Feijge MA, Kuijpers MJ, Rivera-Galdos R, Kraft P, Stoll G, Kleinschnitz C, Bevers EM, Nieswandt B & Heemskerk JW (2012). Antithrombotic potential of blockers of store-operated calcium channels in platelets. *Arterioscler Thromb Vasc Biol* **32**: 1717-1723.
- van Kruchten R, Mattheij NJ, Saunders C, Feijge MA, Swieringa F, Wolfs JL, Collins PW, Heemskerk JW & Bevers EM (2013). Both TMEM16F-dependent and TMEM16F-independent pathways contribute to phosphatidylserine exposure in platelet apoptosis and platelet activation. *Blood* **121**: 1850-1857.
- van Nispen tot Pannerden H, de Haas F, Geerts W, Posthuma G, van Dijk S & Heijnen HF (2010). The platelet interior revisited: electron tomography reveals tubular alpha-granule subtypes. *Blood* **116**: 1147-1156.
- Varga-Szabo D, Braun A, Kleinschnitz C, Bender M, Pleines I, Pham M, Renne T, Stoll G & Nieswandt B (2008). The calcium sensor STIM1 is an essential mediator of arterial thrombosis and ischemic brain infarction. *J Exp Med* **205**: 1583-1591.
- Varga-Szabo D, Pleines I & Nieswandt B (2008). Cell adhesion mechanisms in platelets. *Arterioscler Thromb Vasc Biol* **28**: 403-412.
- Verboomen H, Wuytack F, De Smedt H, Himpens B & Casteels R (1992). Functional difference between SERCA2a and SERCA2b Ca<sup>2+</sup> pumps and their modulation by phospholamban. *Biochem J* **286**: 591-595.
- Vemana HP, Karim ZA, Conlon C & Khasawneh FT (2015). A critical role for the transient receptor potential channel type 6 in human platelet activation. *PLoS One* **10**: e0125764.
- Walford T, Musa FI & Harper AGS (2015). Nicergoline inhibits human platelet Ca signalling through triggering a microtubule-dependent reorganisation of the platelet ultrastructure. *Br J Pharmacol*. **173**: 234-247.
- Walker FJ (1980). Regulation of activated protein C by a new protein. A possible function for bovine protein S. *J Biol Chem* **255**: 5521-5524.
- Wan TC, Zabe M & Dean WL (2003). Plasma membrane Ca<sup>2+</sup>-ATPase isoform 4b is phosphorylated on tyrosine 1176 in activated human platelets. *Thromb Haemost* **89**: 122-131.
- Watano T, Kimura J, Morita T & Nakanishi H (1996). A novel antagonist, No. 7943, of the Na<sup>+</sup>/Ca<sup>2+</sup> exchange current in guinea-pig cardiac ventricular cells. *Br J Pharmacol* **119**: 555-563.
- Weisel JW, Nagaswami C, Vilaire G & Bennett JS (1992). Examination of the platelet membrane glycoprotein IIb-IIIa complex and its interaction with fibrinogen and other ligands by electron microscopy. *J Biol Chem* **267**: 16637-16643.

- White JG (1968). The substructure of human platelet microtubules. *Blood* **32**: 638-648.
- White JG (1972). Interaction of membrane systems in blood platelets. *Am J Pathol* **66**: 295-312.
- White JG (1974). Electron microscopic studies of platelet secretion. *Prog Hemost Thromb* **2**: 49-98.
- White JG (1987). Anatomy and structural organization of the platelet. In Hemostasis and Thrombosis: Basic Principles and Clinical Practice. Philadelphia, *J. B. Lippincott Company*. 537-554.
- White JG & Rao GH (1998). Microtubule coils versus the surface membrane cytoskeleton in maintenance and restoration of platelet discoid shape. *Am J Pathol* **152**: 597-609.
- Witke WA, Sharpe AH, Hartwig JH, Azuma T, Stossel TP & Kwiatkowski DJ (1995). Hemostatic, inflammatory, and fibroblast responses are blunted in mice lacking gelsolin. *Cell* **81**: 41-51.
- World Health Organization (2002). The ten leading causes of death by broad income group. *Fact Sheet*. 1-5.
- Yang H, Kim A, David T, Palmer D, Jin T, Tien J, Huang F, Cheng T, Coughlin SR, Jan YN & Jan LY (2012). TMEM16F forms a Ca<sup>2+</sup>-activated cation channel required for lipid scrambling in platelets during blood coagulation. *Cell* **151**: 111-122.
- Yoshida T, Fujimori T & Nabeshima Y (2002). Mediation of unusually high concentrations of 1,25-dihydroxyvitamin D in homozygous *klotho* mutant mice by increased expression of renal 1 $\alpha$ -hydroxylase gene. *Endocrinology* **143**: 683-689.
- Youssefian T, Masse JM, Rendu F, Guichard J & Cramer EM (1997). Platelet and megakaryocyte dense granules contain glycoproteins Ib and IIb-IIIa. *Blood* **89**: 4047-4057.